4.0 Photochemical Air Quality Model Inputs

4.1 Introduction

Photochemical air quality models require inputs specifying emissions, geography, meteorology, initial air quality and boundary conditions. The quality of model predictions depend on accurately describing the inputs. This chapter reviews the selection and treatment of meteorological variables, air quality parameters and emission inventories.

Before using the air quality models to establish source-air quality relationships, the performance of the model should be evaluated. This includes choosing an historical ozone episode and checking to see that the model can accurately reproduce the observed pollutant concentrations. This is an indication that the model is correctly describing the important processes affecting the evolution of the pollutants in the atmosphere. A part of the evaluation is collecting and processing the meteorological variables, air quality measurements, and emissions data corresponding to the evaluation period. It is beneficial to have as much evaluation data as possible.

It is necessary to look at many possible fuel utilization scenarios for several reasons. First, the modeling periods, the years 2000 and 2010, are 12 and 22 years in the future. Technology advances, or lack thereof, may either enable source emissions to be lower than currently projected, or may not allow levels to reach current projections. This applies to both methanol fueled and conventionally fueled sources. Second, since methanol fueled vehicles have not been built on a commercial scale there is an amount of uncertainty regarding the attainable emission levels of exhaust products, especially formaldehyde. Third, it is easier to convert some sources to methanol fuel than others, and future policies have to take ease of conversion into account.

A majority of the air quality simulations and methanol utilization calculations, including all of the trajectory modeling and many of the airshed simulations, were based on the year 2000 inventory. For this reason, and that the 2010 inventory has the same general structure (though a different spatial and temporal pattern of emissions), the year 2000 inventory will be described in detail, and the 2010 inventory will be summarized. Procedures for manipulating the two base inventories to represent future methanol utilization scenarios are identical, so they will be described for the general case, with details for individual calculations following. Using the same procedures assures reproducibility and consistency between calculations.

This chapter also reviews the technique by which the base case emissions inventories were perturbed to create alternate emissions inventories. Previous studies have been subjected to criticism because they looked at gross changes in the emissions, not on a source by source basis. In this study, emissions from each source are treated in a detailed fashion. Because the emissions inventories are large, a standard methodology for creating alternate inventories is necessary to insure consistency. It is also important to specify the methodology so that the assumptions used in creating the databases are presented clearly. This enables future studies to consider how changes in assumptions will change emissions predictions. The methodology is reviewed in this chapter, along with some example calculations.

4.2 Selection of the Modeling Period

A primary objective of this study is to quantify how photochemical air pollutant concentrations will respond to increased utilization of methanol fuel. In particular, the response of high ozone concentrations is examined. Episodes leading to high ozone levels are usually multiday events, characterized by high temperatures, low inversion, and limited advection of pollutants out of the SoCAB. Such an episode occurred from August 30 to September 1, 1982, and has been chosen to serve as the basis for the current study.

This three day period was chosen because several factors make it ideal for modeling the impact of control strategies on ozone and other photochemical pollutants:

1. The meteorological conditions present during the three day period, high temperatures, sunlight, and relatively stagnant air, are conducive to forming high ozone concentrations. By the third day of the 1982 episode, ozone concentrations built up to second stage alert (0.35 ppm) levels at two measurement sites in the SoCAB.

2. The atmosphere prior to the start of the ozone episode was relatively unpolluted. This, and the use of a three day modeling period make predicted ozone concentrations on the third day relatively independent of initial conditions throughout most of the basin.

3. Extensive pollutant measurements were made over the first and second day of the three day period. In addition to pollutants like ozone and NO_x,which are routinely measured, trace pollutants like peroxyacetyl nitrate (PAN), nitric acid, aerosol nitrate and ammonia were also measured. This gives a large database of information which can be used to test whether the model can represent actual atmospheric processes.

4. During this time period, winds were primarily westerly from over the Pacific Ocean. Pollutant concentrations over the ocean are generally low, and if the boundary is taken far enough out, the concentrations are independent of emissions within the basin. This decreases the effect of boundary specification on model predictions, and decreases the uncertainty in the model predictions.

In a previous study, this modeling period was used to study the formation and control of aerosol nitrate and nitric acid (Russell, et al. 1988ab). Comparison between model predictions and observations was quite good for not only ozone, but also the trace nitrogen containing species measured as part of the special program. Meteorological and air quality inputs are derived from the measurements taken during this three day period.

4.3 Modeling Region

Figure 4.1 shows the modeling regions used in this study, and the underlying 80 x 30 grid system used to develop inputs into the model. Meteorological, topographical and emission inputs were developed over the 400 km x 150 km system of 5 km x 5 km grids. In the vertical direction, the model region extends up to 1500 m. Two modeling regions were used, one for the year 2000 calculations and the evaluation against the measurements in 1982. The region was enlarged for the 2010 simulations because of the increased emissions in the eastern SoCAB.

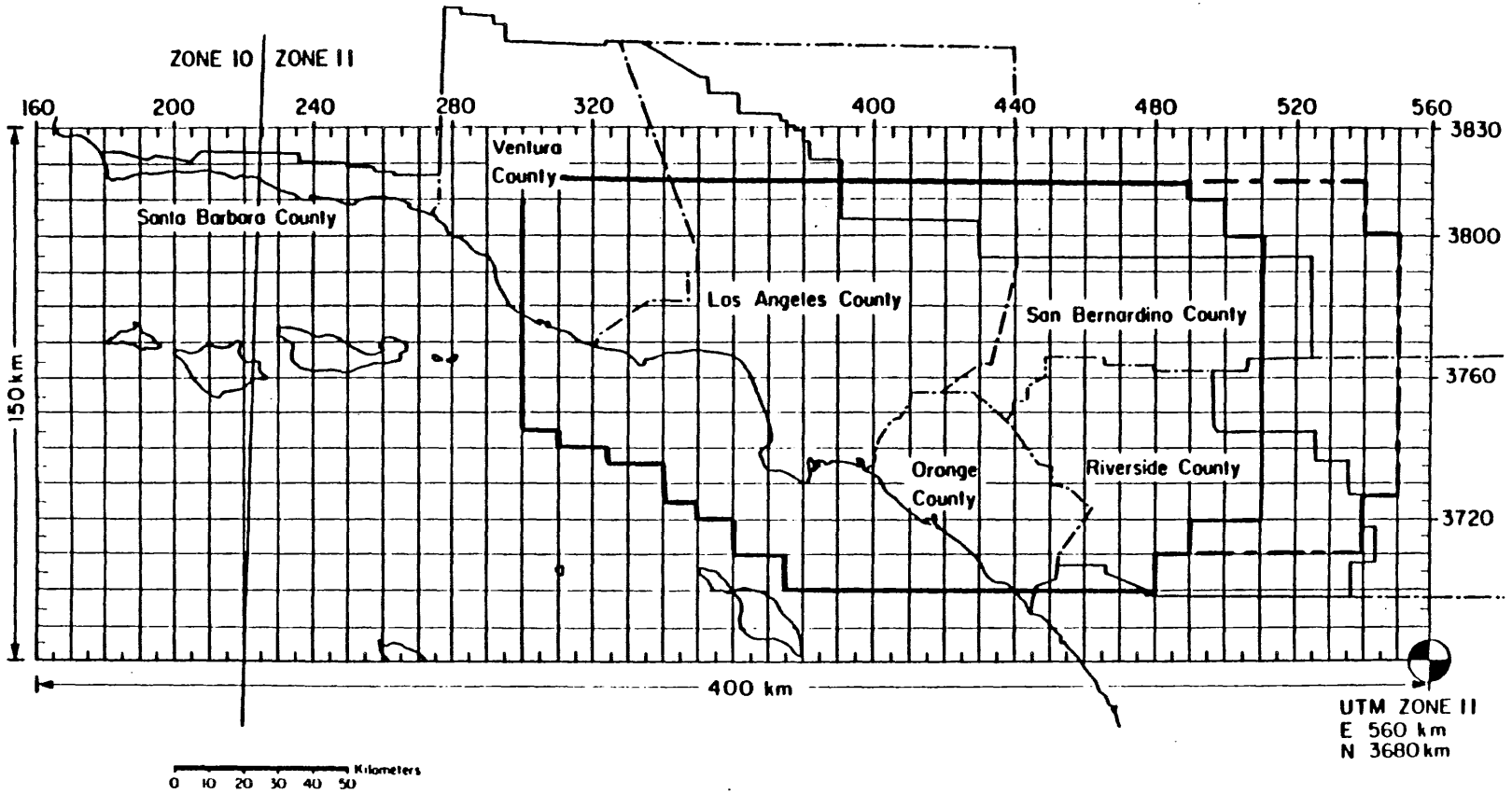

Figure 4.1 Gridded map of California's South Coast Air Basin (SoCAB), showing the regions used for airshed modeling, and the 5 km by 5 km grid system used for developing the spatially resolved emissions, meteorology and geographic fields. The heavy solid line (———) shows the boundary used for year 2000 air quality calculations, and the heavy dashed line (— — —) delineates the region used for year 2010 calculations.

4.4 Meteorological Fields and Air Quality Data

Meteorological fields required for model evaluation were obtained as prescribed in Russell, et al. (1988). The data from that earlier, two day, study was supplemented with information obtained from the same sources for the third day added as part of the current project. Likewise, air quality data used to determine initial and boundary conditions were collected to extend the fields calculated for the previous two day period to include the third day used here. Organic gas boundary conditions over the Pacific Ocean were derived from Killus (1984) and Blumenthal (1984). More detailed discussion about the techniques used to develop the model inputs can be found in Russell, et al. (1988) and Goodin, et al. (1979).

4.5 Selection of Future Modeling Years

Two future years were chosen for studying the air quality impact of converting sources to methanol. The year 2000 was selected as the first modeling period because it is felt that this is the earliest date by which methanol fueled vehicles would make up a significant portion of the total vehicle fleet within the basin. Less than 10% of the vehicle fleet is replaced in a typical year, so if one were to convert to an MFV fleet by requiring all new vehicles to be methanol fueled, a date twelve years in the future would be about the earliest time at which MFVs constituted a significant portion of the fleet. The year 2010 was selected because a significant shift in the emissions contributions of various source groups between 2000 and 2010 result in a redistribution of emissions. Also the spatial distribution of sources is expected to shift emissions towards the east. The South Coast Air Quality Management District and the Southern California Association of Governments (SCAQMD and SCAG,1988) are using 2010 for the Air Quality Management Plan (AQMP).

4.6 Base Emission Inventories

Emission inventories for the SoCAB and surrounding areas in the modeling region, corresponding to three different years, 1982, 2000 and 2010, were used in the course of this study (Ranzierri, 1982; Avlani, 1986; Mahoney, 1988). The 1982 inventory was used in the model performance evaluation (See Chapter 6), and is described in detail elsewhere (Russell, et al., 1988). A summary of those emissions is shown in Table 4.1.[1]

A forecast emissions inventory for summer conditions in the year 2000 was provided by CARB (Avlani, 1986). The structure of the inventory includes the temporal and spatial emissions of total organic gases (TOG), nitrogen oxides (NO_x), carbon monoxide (CO), particulate matter (PM), and sulfur oxides (SO_x) by source class category (SCC). Separate files are used to speciate the total organic gas emissions into emissions by individual compound (e.g. methane, ethane, propane, toluene, etc...) and NO_x is split into NO and NO_2, according to the source category. After speciation, the emitted organic

---

[1] CARB's revised estimate indicates that the forecast NO_x emissions used in this study may be slightly underestimated (K. Wagner, personal communication, 1989). Comparison to the AQMP projections (SCAQMD, 1988) for the years 2000 and 2010 indicate that the NO_x emissions may be 13% to 18% low. Higher NO_x emissions would increase the benefits of methanol use. Also, recent tests indicate that evaporative emissions from on-road vehicles may be significantly greater than is accounted for in the current ROG estimates and the EMFAC motor vehicle emission factor procedures. The magnitude of the excess emissions is not yet known. If they are found to be significant, it would increase the relative benefits of conversion to methanol.

compounds are lumped into the classes used by the chemical mechanism, extended to include methanol chemistry (Falls, et al., 1979; McRae, et al., 1982; Russell, 1985).

The structure and the detail of the base inventory is necessary for control strategy studies looking at changing the composition of the ROG emissions. Methanol utilization in mobile sources has an impact on air quality more because it changes the reactivity and chemistry of the organic gases emitted than it changes the mass emission rate of TOGs. Thus, having the detailed chemical structure is necessary. Secondly, converting to methanol will be used to control specific sources, which are neither spatially uniform nor have the same general composition of the aggregate inventory. By using the SCC classification, emissions can be altered in a source specific fashion, as discussed below. From this, source impact relationships can be developed, and the effectiveness of controls can be tested.

The forecast emissions inventory for the year 2000, within the modeling region, is summarized in Table 4.2[1]. This includes emissions in the SoCAB and adjoining inventory regions, such as part of the South Central Coast region. The total organic gas emissions rate, which includes methane and methanol, was 1855 metric tons day^{-1}. Because methane is generally non-reactive over the residence time of emittants in the basin, it is often subtracted from the total. Also, methanol is significantly less reactive than other organics, and for other studies has often not been included for modeling purposes. In this study, methanol is treated separately from the more reactive organics. The total non-methane, non-methanol organic gas (NMOG) emissions are also tabulated. The large difference between TOG and NMOG is due, in part, to methane emissions from waste disposal operation. Total forecast NMOG emissions in the region are 1130 metric tons day^{-1}, or 67% of the TOG. NO_x emissions, roughly split 5% NO_2, 95% NO, total 744 metric tons day^{-1} and CO was emitted at 3915 metric tons day^{-1}.

Concern has arisen over to what degree utilizing methanol will impact ambient HCHO concentrations. In part, this will depend on the current, direct HCHO vehicle emission rate compared to the future if methanol is employed. In the base 2000 inventory, all sources combined emit 19216 kgs HCHO day^{-1}, of which 4727 kgs day^{-1} are due to on-road motor vehicles. The forecast emission rate of methanol (without significant utilization of methanol) is only 13,000 kgs/day.

An interesting aspect of the 2000 inventory is that on-road mobile sources comprise a relatively small fraction of the forecast NMOG emissions - 28% (the modified base inventory, described later, has only 23%). This is important because methanol utilization in motor vehicles is perceived to be an organic gas control (reducing the reactivity, not emission rate), as opposed to a NO_x control (though NO_x from diesel cycle vehicles is expected to be reduced significantly if methanol is used.) Thus, the impact of switching to methanol is limited by the relatively small fraction of the ROG being from automobiles. If control programs are not as effective as now forecast, a larger fraction of the ROG emissions will be due to mobile sources. In this case, the effect of switching to methanol will be greater than is predicted in this study.

Table 4.1
Summary of 1982 Emissions
(1000's kg day^{-1})

	TOG	NO_x	CO
Mobile Sources	652	763	5353
Stationary Sources	1763	357	498
Total	2415	1120	5851

Table 4.2
Summary of Year 2000 Emissions
(1000's kg day^{-1})

	TOG	NO_x	CO	NMOG[1]
Mobile Sources	338	394	2929	323
Stationary Sources	1517	350	986	812
Total	1855	744	3915	1135

[1] NMOG stands for non-methane, non-methanol organic gases

Table 4.3
Summary of Year 2010 Emissions
(1000's kg day^{-1})

	TOG	NO_x	CO	NMOG[1]
Mobile Sources	405	430	4274	389
Stationary Sources	1607	436	1836	1107
Total	2012	866	6110	1496

[1] NMOG stands for non-methane, non-methanol organic gases

General basin wide activity is expected to increase substantially from 2000 to 2010, but emissions from individual sources (e. g. a single automobile) will generally decrease due to further control (Table 4.3[1]). This results in a shift in source emissions contribution between these dates. For example, in 2000, on-road vehicles emit 28% of basin wide ROG, while in 2010 this decreases to 25% of the total. On-road NO_x emissions increase slightly, from 46% to 50% of total NO_x emissions. These emission inventories are based on current projections of basin wide activity for these later dates, and provide a base from which emissions in other scenarios are derived.

4.7 Creation of Alternate Emissions Databases

Three steps were followed to generate the emission inputs for control strategy testing. First, the base inventories were divided into individual categories according to the SCC number and the applicability of potential controls. Those sources that would not be altered under any of the control scenarios were left intact. Next the sources were altered to reflect the presumed effect of the control techniques being examined (e.g. the use of very clean conventionally fueled vehicles, M100, or M85[2] , vehicles or stationary source control). Lastly, the altered emissions were re-assembled into the inventory as used for the particular simulations. The control techniques used in each simulation are specified in the following two chapters. The same inventory is used all three days of a simulation.

4.7.1 Inventory De-aggregation and Construction

The inventories, as supplied by CARB (year 2000) and SCAQMD (year 2010), identifies the location and source type of emissions. Using the source codes, the inventory is split into lower level databases corresponding to specific source types. The process is outlined in Figure 4.2. The sub-databases used in this study are on-road mobile sources, off-road mobile sources, petroleum refining operations, utility boilers and power plants, petroleum retail marketing, stationary internal combustion engines, and other sources. In a specific scenario, any of these source types can have their emissions modified. One then has a new set of modified databases for the source types. These are resumed to get a new basin wide emissions database which applies to a specific scenario. The original basin wide databases are as supplied by CARB and SCAQMD, and the source type databases come directly from this main database without modification. The database for other sources represents all the source types which are not altered in this study, and are grouped together for convenience. Each source group is revised in a different way, so the specific techniques for changing source emissions are presented below.

---

[2] M100 and M85 refer to the type of methanol fuel used. M100, also referred to as neat or nearly-neat methanol fuel, is a blend consisting of methanol with some added agents to help cold startability, luminosity or improve other fuel characteristics. M85 is a blend of 85% methanol and 15% other organics, such as gasoline, by volume. The added organics help cold start and luminosity. Neither fuel has a standard composition, and in the case of M100, study is required to develop the engine technology to readily use the fuel in standard applications. The uncertainty in fuel compositions, and that its composition may change as methanol-burning engine technology advances, leads to uncertainties as to what the composition of the emissions from methanol vehicles will be in the future. For example, European methanol fuel has a different composition than American M85 fuel. Hence, both evaporative and exhaust emissions will be different.

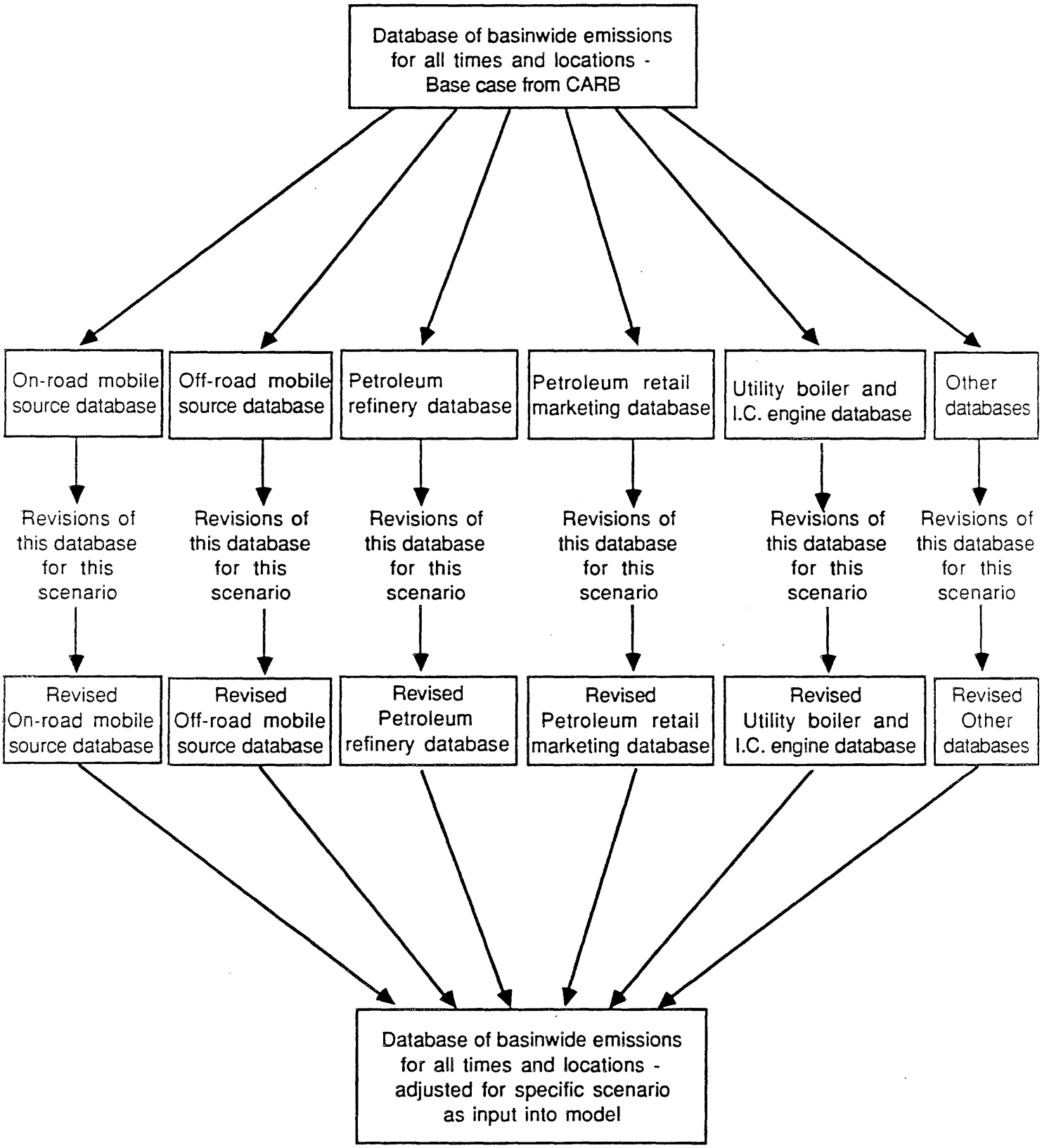

Figure 4.2 Methodology used to disaggregate, manipulate and recompile the emissions inventory for use in photochemical modeling.

4.7.2 On-Road Mobile Sources Database

The majority of methanol conversion scenarios consider changes in motor vehicle emissions. Because of this a detailed methodology for calculating motor vehicle emissions is used. This study uses the methodology and emission factors specified as part of EMFAC7C (California Air Resources Board, 1986a), for the year 2000, and in EMFAC7D (California Air Resources Board, 1988a) for the year 2010. EMFAC7 methodologies and the output of BURDEN are used to determine running and evaporative emissions within the modeling region (California Air Resources Board; 1986b, 1988b). Spatial and temporal emission patterns are derived from the output of the Direct Traffic Impact Model (DTIM). A detailed description of the calculations follows.

First, the on-road mobile sources are split into five categories: light duty automobiles (LDA), light duty trucks (LDT), medium duty trucks (MDT), heavy duty trucks (HDT) and motorcycles (MCY). These five categories are then further split into groups according to fuel types: gasoline fueled, catalyst equipped (CAT); gasoline fueled, non-catalyst equipped (NCAT); diesel fueled (DSL); and methanol fueled, catalyst equipped (METH). All categories have all groups except MCY which only has NCAT, and MDT which does not have DSL. Thus, there are a total of 16 on-road, mobile source categories.

The categories and sources are then broken down by year. In the 2000 scenarios there are a total of 26 vehicle model years (vehicles from 1976 to 2001) and in the 2010 scenarios there are a total of 25 model years (2010 to 1986) considered. Classification by category, group, and year is the most detailed breakdown used in this study, and will be called a unit, for clarity. The EMFAC7C and EMFAC7D specify the emission factors for TOG, CO, and NO_x for the CAT, NCAT, and DSL units. Included in the data base are new car emission factors, deterioration rates, speed correction factors and temperature correction factors. CARB has updated these tables and also determined emissions tables for METH units, which have emissions of TOG (when M85 fuel is used), CH4O, HCHO, NO_x, and CO. These Tables are presented in Appendices 4.A, 4.A1, 4.B, 4.C, 4.D, and 4.E (Drachand, 1988).

In simulations involving M85 fuel, approximately half of the ROG emitted is estimated to be methanol and the other half is estimated to be organic gases similar in composition to gasoline fueled vehicles. Very little data is available for speciating the species composition of the organic emitted, or for the relative emission rates of the vehicles. Less is known about the emissions from M100 vehicles, and there is considerable uncertainty in the emissions from future vehicles. An issue is how much of the measured non-methanol organic emissions in the exhaust of MFVs is from the fuel oil, and how reactive are those compounds. It is very possible that the non-methanol, non-formaldehyde ROG emitted from M85 fueled MFVs is less reactive than the assumed mix corresponding to typical gasoline fueled vehicles. Conversely, the emissions from M100 fueled vehicles may be more reactive than the almost pure methanol vapor assumed here. These two calculations are meant to bracket the likely range. The paucity of data in this area is a major contributor to the uncertainties in the conclusions of this study. The current measurement programs will add greatly to determining the running and evaporative emissions from MFVs, and the ability to forecast the air quality impact of switching to methanol.

Running emissions for each category (e.g. LDA) are determined by completing the operations specified in the EMFAC reports. Vehicle emissions are determined by vehicle category, group, age, and accumulated mileage, then adjusted for differences between the Federal Test Procedure (FTP) test and forecast traffic operation. In particular, speed and

bag corrections are used to adjust the emissions factors to account for vehicle operation specific to the SoCAB in the years 2000 and 2010. Data used in these calculations come from the Tables of Appendices 4.A-E, and the two EMFAC reports (CARB 1986a, 1988a). Evaporative emissions are calculated using the spatial distribution of the hot soak and diurnal emissions from the base case inventories and the EMFAC reports. The mass emission rates are corrected for vapor pressure differences as described below in section 4.7.6. In the specified scenarios, for both the year 2000 and the year 2010, MFVs are introduced starting in 1990[3] (see appendix 4.C). Simulations involving advanced technology[4] MFVs have no light or medium duty CFVs.

Total emissions for all on-road mobile sources are obtained by combining the emissions from each category. This is done by weighting the emissions of each category, exhaust and evaporative, by the fraction of total on-road mobile source mileage driven by that category. These weighted emissions are then summed to calculate final mass emissions of TOG, NO_x, CH_4O and HCHO for each scenario. The final species emissions for all on-road sources is then converted into a percentage reduction from the baseline. Methanol and HCHO are distributed using the same pattern as TOG emissions from the appropriate vehicle type. Air quality models use a mole basis for emissions, so the mass emissions are converted to moles. Reduction of NO_x and CO emissions are the same on a mass basis as they are on a mole basis, though the organics in the TOG have differing molecular weights. All the various species which make up TOG are each reduced by the percentage that TOG was reduced, and then the mole emissions are calculated. When MFV usage is being simulated, HCHO emissions are affected by two processes. First HCHO emissions are reduced in the database by any reduction of TOG from CFVs, because HCHO is one of the species that makes up TOG. Second HCHO emissions are increased in the database because MFVs emit HCHO. Thus mole emissions of HCHO are determined by the addition of these two factors.

This methodology assumes a specific control will affect all vehicles in a certain class uniformly throughout the basin. Thus, if MFVs make up 50% of the light duty vehicle fleet, they make up 50% independent of geographical location. At present, the data bases do not allow for any greater dissection to account for spatial difference in the penetration of MFVs into the vehicle fleet.

As an example of how the emissions were treated for specific calculations, in one simulation the effect of varying the deterioration rate of the motor vehicle fleet was tested. CARB (1986a) specified that the assumed deterioration rate of exhaust organics from a

---

[3] Significant penetration of MFVs into the vehicle fleet is not possible by 1990. This start date was chosen to simulate the probable air quality impacts after a ten and twenty year period of full MFV penetration. Use of a later starting date would not allow the use of the year 2000 and 2010 inventories that were constructed and checked for modeling purposes. Extrapolating inventories further into the future would add uncertainty.

[4] Advanced technology refers to simulations where the motor vehicle fleet uniformly meets the regulations set for year 2000 vehicles. This does not mean that the vehicles are assumed to involve a technology beyond that for the standard cases. Advanced technology vehicles are assumed to meet the year 2000 standards, so that emissions from the older, dirtier vehicles do not overwhelm the emissions from the newer vehicles. It was found that the inherently dirtier, pre-1990 vehicles (which were all conventionally fueled) emitted a disproportionately large amount of the emissions in the simulations of fleet conversion starting in 1990. This decreased the apparent effectiveness of converting to methanol fuel. The advanced technology simulations can be used to view the effect if all of the vehicles met the emission regulations for the year modeled, i.e. the year 2000 or 2010, that is the long term impact of conversion. The cases involving roll in of MFVs or CFVs at correspondingly more stringent emission levels shows the impact in the shorter term.

1990 LDA was 0.091 (g mi^{-1})/10,000 mi, on top of new car emissions of 0.26 g mi^{-1}. Thus, the 50,000 mile emission rate is 0.72 g mi^{-1}. If the deterioration rate is doubled, the emission factor at 50,000 miles is 1.17 g mi^{-1}, which is not double the base rate because the new car emission rate is not changed. When the varying deterioration rates between years and vehicle models, and the different vehicle mileage fractions are considered, the relationship between emission factor and deterioration rate is seen to be non-proportional. As a second example, to calculate the emissions from a 1990 M85 vehicle, Appendix 4.E is used to find that the in-use (50,000 mi) emission rate of methanol is 0.295 g mi^{-1} (on a carbon basis, or 0.68 g mi^{-1} methanol), and 0.295 g mi^{-1} NMOG. However, in 2000, the average 1990 vehicle has 90,000 miles on it, with a deterioration rate of 0.041 g mi^{-1}. Thus the emissions from a 1990 vehicle, in the year 2000, are:

0.295 g mi^{-1} + (90,000 mi - 50,000) x (0.041 g mi^{-1} per 10,000 mi) = 0.459 g mi^{-1} CH_4O

on a carbon basis (or 1.059 g mi^{-1} methanol), and

0.295 g mi^{-1} + (90,000 mi - 50,000) x (0.041 g mi^{-1} per 10,000 mi) = 0.459 g mi^{-1} NMOG

A similar calculation is done for each model year, and the emissions from each year are summed up to get the total on-road vehicle emissions for each species.

4.7.3 Altering Off-Road Mobile Source Databases

Because vehicle emissions information for off-road mobile sources has not been compiled using the same detail with which it has for on-road mobile sources, a less data intensive technique for modifying the off-road emissions database is used. First, all the source types that are potentially convertible to methanol fuel are identified. These include farm equipment, construction equipment, agricultural equipment, off-road recreational vehicles (excluding motorcycles), utility vehicles, and locomotives. Within these categories, diesel fueled and gasoline fueled vehicles are separated. Scenarios affecting off-road vehicles consider total conversion of appropriate vehicles from conventional to methanol fuel. CO emissions were kept the same for either vehicle type. NO_x emissions remain the same for gas-fueled vehicles and are reduced 50% when the vehicle was diesel-fueled before conversion. TOG emissions are replaced on an equivalent carbon mass basis by methanol and formaldehyde emissions. The MFV exhaust composition from off-road vehicles is assumed to be 96% methanol and 4% formaldehyde.

4.7.4 Altering Petroleum Refinery Databases

Scenarios in this study consider either currently projected refinery operation, or no operation at all. In the first case, refinery emissions are unchanged. In the second case they are removed, as are emissions from wholesale petroleum distribution, for example, from tanker operations. A few calculations in the year 2000 looked at removing refinery emissions if 100% of the vehicle fleet was converted to methanol. Year 2010 simulations did not alter refinery emissions.

4.7.5 Altering Utility Boiler and Power Plant Databases

Calculations have been designed to test the effectiveness of utilizing methanol as a NO_x control in stationary sources, such as utility boilers. In this case, a fraction of the large boilers are "converted", lowering the NO_x emissions from this category of sources by 50%. CO and TOG emissions, which are comparatively small, are not changed. Appendix 4.G outlines the reductions expected from stationary source conversion to methanol.

4.7.6 Altering Petroleum Retail Marketing Databases

Included in petroleum retail marketing, are spillage and tank vapor displacement from retail facilities. These sources emit only ROGs. Non-methane, non-methanol organic gas (NMOG) emissions are reduced by the amount that on-road and off-road mobile sources are converted to methanol. Methanol emissions replace the NMOG removed, accounting for vapor pressure differences, increased consumption of methanol due to a lower energy content, and whether the emissions are due to spillage or vapor displacement. Methanol is about half as energy dense as gasoline, and diesel is more energy dense than gasoline. Therefor, methanol fueled vehicles will require more fuel on a volumetric basis than a comparable CFV. On the other hand, methanol-fueled engines are expected to be thermodynamically more efficient, slightly compensating for the lower energy content of the fuel. Estimates of the relative fuel requirements range from 1.4 gals. methanol to replace 1 gal. of gasoline, to a ratio of about 2.0(see, for example, Gray and Tomlinson, 1985; Murrell and Piotrowski, 1987; Schieler, et al. 1985, Katoh, et al. 1986). In this study 1.75 gal methanol/gal gasoline is used. Both spillage and vapor displacement calculations account for the increased volumetric fuel consumption.

To convert service station gasoline spillage emissions to account for methanol displacement, it was assumed that the amount of methanol spilled, per fill-up, was the same as for gasoline. However, because of the expected need for increased refueling due to the lower energy density of methanol, the total mass emissions of methanol was set to be 1.75 times as great for an M100 vehicle fleet. For an M85 fleet, spillage emissions were increased by a factor of 1.64, of which 85% was methanol. The remaining 15% used the gasoline vapor profile.

If the emissions were originally due to vapor displacement from a fixed volume (such as an underground tank or gas tank during refueling), it is necessary to account for the very different vapor pressures and evaporative composition of methanol, gasoline and methanol-gasoline mixtures. Methanol has a lower vapor pressure than gasoline. The Reid Vapor Pressure (RVP) of methanol is 4 psi, compared to gasoline having an RVP of about 9. (The RVP of gasoline can be highly variable, but regulations in the SoCAB set an RVP limit at 9 psi.) The saturated vapor above a tank of methanol would contain less fuel, on a mole or mass basis, than would the atmosphere above gasoline. Vapor displacement emissions of methanol can be found by using the RVP, the relative molecular weights and the base case emissions of gasoline:

[Mass of Methanol] = [Mass of Gasoline] x (Molecular Wt. Methanol / Molecular Wt. Gasoline)

x (RVP Methanol / RVP Gasoline)

Because the day in question recorded temperatures about 100° F, no adjustment was made for temperature.

The calculation for M85 fuel is somewhat more involved, and requires use of solution theory and Raoult's Law from thermodynamics. The vapor pressure of M85 is not a linear interpolation between gasoline and methanol. The JPL study (O'Toole, et al. 1983), citing Volkswagen of America, used an RVP of 10 psia for M95 fuel. In this study it was assumed that the RVP of the fuel would be subject to the same limitations of gasoline, and an RVP of 9 psia was used. However, the gasoline fraction of the fuel evaporates preferentially compared to the methanol.

Methanol is not an ideal solution, so to determine the vapor pressure of a methanol blend, Raoult's Law is used. Let γ^1 be the solution activity of the solute (in this case the gasoline type component) and γ^0 be the activity of the solvent (methanol), then the vapor pressure of the solvent , P_0, is:

$$P_0 = f_0 \gamma^0 P_0^0$$

where f_0 is the molar fraction of the solvent, and P_0^0 is the vapor pressure of the pure solvent. Likewise, using Henry's Law (Denbigh, 1971), the vapor pressure of the solute, P_1, is:

$$P_1 = f_1 \gamma^1 K_1$$

where K_1 is the Henry's Law constant and f_1 is the molar fraction of the solute. f_0 and f_1 sum up to one. Following the method in O'Toole, et al. (1983), at 72°F (taken as the solution temperature of an underground storage tank) the vapor displaced is 19% methanol and 81% gasoline components, by mass. A more detailed calculation requires the exact composition of M85 fuel, which has not yet been established.[5]

4.7.7 Stationary Internal Combustion Engines

Stationary internal combustion engines can be converted to run on methanol or a methanol blend. This would change the ROG composition of their emissions, and can lower their NO_x emissions. In calculations testing the effects of stationary source utilization of methanol, mass emissions of ROG from stationary I.C. engines were converted on an equal mass basis to 96% methanol and 4% HCHO, and NO_x emissions were reduced by 50% (Appendix 4.G).

4.8 Summary

Air quality models require inputs specifying the modeling domain topography, emissions, air quality and meteorology. In this case the modeling domain includes the SoCAB and outlying regions, and the inputs correspond to that area. A three day period, August 30 - September 1, 1982, was chosen as the base time period for model evaluation, and as the base for control strategy testing. This three day period is well suited to determining the effect of control strategies on reducing high ozone concentrations. The meteorology led to a rapid build up of ozone up to second stage levels, though the period

---

[5] Recent tests indicate that the diurnal, evaporative emissions from M100 fueled vehicles were 24% methanol, agreeing with the calculation (Snow, et al. 1989). Hot soak, evaporative emissions were 82% methanol. Thus, the calculation should slightly over estimate the percentage of gasoline vapors, and the procedure used provides a conservative (high) estimate of the reactivity of the evaporative emissions. These recent tests, and similar future tests, provide critical data to accurately assess the impact from switching to methanol fuel. See also footnote 1.

started with relatively clean air. A second aspect of this period was that extra measurements taken during this period were available for very detailed evaluation of the model.

Testing of source specific control techniques requires a detailed treatment of emissions. This was facilitated by de-aggregating the inventory into source types, and operating on each individual source that would be impacted by adoption of specific controls. The inventory is then reconstructed, and used in the air quality models. As described above, individual sources were treated in detail. For example, on-road motor vehicle emissions are calculated by model year, size of vehicle, and engine type, explicitly, using EMFAC methodologies, corrected for temperature and vehicle speeds. Spillage and vapor displacement losses from service stations are also treated separately, accounting for vapor pressure differences. Stationary source controls and emissions were accounted for on a source by source basis.

The method used to treat emissions has three major benefits. First, it results in a detailed inventory to be used in testing the control strategies, minimizing uncertainty and providing for a more solid foundation on which to base policy decisions. Second, it provides the information needed to interpret the findings of this study as future information becomes available. The procedures used have been conservative, so as not to overestimate the potential benefits of methanol use. Finally, it has helped identify uncertainties, and requirements for future studies. For example, the composition of exhaust and evaporative emissions from methanol fueled vehicles have not been well characterized. They will depend on the advances in MFV engine technology and fuel composition. Other uncertainties derive from using a forecast inventory. The data processed as described here, serve as inputs to the trajectory and grid-based airshed models.

Appendix 4.A. Conventionally Fueled Vehicle Emissions

This appendix contains the "expected" emission rates resulting from implementation of the likely technological and regulatory advances. These emissions are used in all scenarios which have conventionally fueled vehicles, namely Scenarios BASE1, STD M100, BASE-ROG, BASE-NO_x, METH 50, STD M85 and HIGH FORM.

Emissions (g/mi) at 50K mi

Pollutant Species	Year	Vehicle Type LDA	LDT	MDT	HDG	HDD
NMHC	1991-	N/C	N/C	N/C	N/C	N/C
	1992-94	0.36[a]	0.37	0.44[g]	N/C	N/C
	1995+	0.25[b]	0.26	0.32	N/C	N/C
NO_x	1989-	N/C	N/C	N/C	N/C	N/C
	1990-93	0.71[c]	0.74	N/C	N/C	N/C
	1994	0.65[c]	0.69	0.7	N/C	N/C
	1995-96	0.40	0.42	0.7	N/C	N/C
	1997+	0.20[d]	0.21	0.7	N/C	10.32[i]
CO	1991-	N/C	N/C	N/C	N/C	N/C
	1992-94	4.06[e]	4.40	6.0[g]	N/C	N/C
	1995+	3.5	3.5	5.8[h]	N/C	N/C
HCHO	All	f	f	f	f	f

N/C - No change = value from EMFAC7C.

a. 0.36 g/mi NMHC at 50K mi for LDA for model years 1992-1994 is obtained according to the following calculation approach:

Applicable Standard	In-Use Emission Factor (from Attachment A)	Emission at 50K mi
0.41	0.179 + 0.082 M	0.589
0.25	0.109 + 0.05 M	0.359

b. Excess emissions from LDAs, LDTs, and MDTs are expected to be eliminated by the 1995 model year.

c. Obtained from the "Exhaust Emission Factors" table for passenger cars in Attachment A. The rate reflects the partial or full implementation of the 0.4 g/mi NO_x emission standard.

d. The probable NO_X emission standard for LDAs to be implemented in 1997.

e. It is projected that passenger cars will emit CO emissions at half the current in-use emission rate (8.12 g/mi at 50K miles) as a result of a 0.25 NMHC standard.

f. Formaldehyde emissions, expressed as a percentage of total hydrocarbons, for various vehicle classes are given below. These emission rates were excerpted from an EPA report entitled "Air Toxics Emissions From Motor Vehicles" (September, 1987).

Vehicle Class	% of Total Exhaust HC
LDGV	1.0
LDGT	1.1
LDDV	4.1
LDDT	4.1
HDGV	3.1
HDDV-Truck	3.0
HDDV-Bus	10.0

g. The emission rate is for model year 1994 only. Notice that 0.32 NMHC is the probable MDGT standard (for trucks with 3,751 - 5,750 lbs. EIW) to be implemented in 1994. 0.44 NMHC is the corresponding in-use rate.

h. As a result of a more stringent 0.32 NMHC standard (for MDTs with 3,751 - 5,750 EIW), CO emission rates are expected to decrease accordingly. The corresponding CO emission rate of 5.8 g/mi is obtained by adjusting the current CO standard of 9.0 g/mi for MDTs by the ratio of 0.32 and 0.50 (the current NMHC standard for MDTs).

i. 4.0 g/bhp-hr NO_X is the probable emission standard for HDDVs to be implemented in 1997. 10.32 g/mi NO_X at 50K miles is obtained by multiplying the NO_X emission factor of 12.898 g/mi (from Attachment A) for HDDVs meeting the 5.0 g/bhp-hr standard by the ratio of 4.0 and 5.0.

Appendix 4.A1. Conventionally Fueled Vehicle Emissions From EMFAC7C

These emissions are used in BASE1A for the Year 2000 Base Case.

Emissions (g/mi) at 50K mi

Pollutant Species	Year	Vehicle Type LDA	LDT	MDT	HDG	HDD
NMHC	1989-	N/C	N/C	N/C	N/C	N/C
	1990+	0.59	0.61	0.68	N/C	N/C
NO_X	1989-	N/C	N/C	N/C	N/C	N/C
	1990-93	0.71	0.74	0.975	N/C	N/C
	1994+	0.65	0.69	0.975	N/C	N/C
CO	1989-	N/C	N/C	N/C	N/C	N/C
	1990+	8.12	8.80	9.38	N/C	N/C
HCHO	All	N/C	N/C	N/C	N/C	N/C

N/C - No change (Values shown are from EMFAC7C, and are included for ease of comparison with other tables instead of just showing N/C for all entries.)

Appendix 4.B. Methanol Fueled Vehicle Emissions Using M100 Fuel

These emissions are used in Scenarios STD M100, METH 50 and HIGH FORM. The HCHO emissions tables at the bottom indicate which HCHO emissions are used in the particular scenario.

Emissions at 50K mi - for CH_4O emissions are (g C/mi)
- for other species emissions are (g/mi)

Pollutant Species	Year	Vehicle Type LDA	LDT	MDT	HDG	HDD
Methanol	1990-91	0.59[a]	0.61	0.68[c]	e	e
	1992-94	0.36[b]	0.37	0.44[d]	e	e
	1995+	0.25	0.26	0.32	e	e
NO_x	1990-93	0.71	0.74	0.975	e	e
	1994	0.65	0.69	0.7	e	e
	1995-96	0.40	0.42	0.7	e	e
	1997+	0.20	0.21	0.7	e	e
CO	1990-91	8.12	8.80	9.38[c]	e	e
	1992-94	4.06	4.40	6.0[d]	e	e
	1995+	3.5	3.5	5.8	e	e

Use the following emissions for HCHO (g/mi) at 50K mi for scenarios with HCHO emissions of 15 mg/mi for LDV. Used in Scenarios STD M100 and METH 50.

		LDA	LDT under 3750#	LDT over 3751#	MDT 3751-5750#	MDT over 5751#	HDG[g]	HDD[h]
HCHO[f]	1990-93	0.023	0.023	0.027	0.027	0.033	0.095	0.234
	1994+	0.015	0.015	0.018	0.018	0.022	0.046	0.116

Use the following emissions for HCHO (g/mi) at 50K mi for scenarios with HCHO emissions of 55 mg/mi for LDV and MDV. Used in Scenario HIGH FORM.

HCHO	All	0.055	0.055	0.055	0.055	0.055	0.095	0.234

a. This value is obtained from the corresponding entry in Appendix 4.A1. It should be noted that 0.59 g/mi NMHC from conventionally fueled vehicles does not account for formaldehyde emissions since the FID does not respond to formaldehyde.

b. Obtained from the corresponding entry in Appendix 4.A.

c. This emission rate is for model years 1990-93.

d. This emission rate is for the model year 1994 only.

e.

		HDG	HDD
Methanol	1990	1.58	2.99
	91-93	1.51	2.99
	94-96	1.49	2.97
	97-2000	1.47	2.94
NO_X	1990	5.10	7.20
	91-93	4.95	6.56
	94-96	4.83	6.50
	97-2000	4.75	5.16
CO	1990	21.07	8.67
	91-93	20.77	8.62
	94-96	20.36	8.53
	97-2000	20.09	8.41

These values are obtained from the corresponding "Exhaust Emission Factors" tables in Attachment A. Notice that NO_X emissions from methanol-fueled HD diesel-cycle engines are half of those from diesel-fueled counterparts.

f. Formaldehyde emissions for various vehicle types are obtained from ARB's proposed formaldehyde emission standards for methanol-fueled vehicles. These values are contained in ARB's response to EPA's NPRM concerning emission standards and test procedures for methanol-fueled vehicles.

g. The conversion factors of 0.95 bhp-hr/mi and 0.92 bhp-hr/mi (from MOBILE3) for years 1990-1993 and 1994+ were used to convert g/bhp-hr formalydehyde standards to an equivalent unit of g/mi. It is assumed that the conversion factors for methanol-fueled HD Otto-cycle vehicles are equivalent to those for gasoline-fueled HDVs. In addition, these formaldehyde emission rates are applicable to the useful life of methanol-fueled HDGTs, which is assumed to be the same as the useful life of 110,000 miles for HDGVs.

h. The conversion factors of 2.34 and 2.31 bhp-hr/mi (from MOBILE3) for HDDVs for years 1990-93 and 1994+ were used. It is assumed that the conversion factors for methanol-fueled HD diesel-cycle vehicles are equivalent to those for HDDVs. The useful life periods for light HDDVs, medium HDDVs, and heavy HDDVs are 110,000, 185,000, and 290,000 miles, respectively. It is assumed, however, that methanol-fueled HDDV catalysts will maintain an overall 50 percent conversion efficiency for formaldehyde emissions only up to 110,000 miles. Beyond 110,000 miles, formaldehyde levels are assumed to increase to uncontrolled levels of 468 mg/mi and 232 mg/mi for the years 1990-93 and 1994+.

Appendix 4.C. Emissions for Advanced Technology CFVs

Pollutant Species	Year	Emissions (g/mi) at 50K mi[a] LDA[b]	LDT under 3750#	LDT over 3751#	MDT 3751- 5750#	MDT over 5751#	HDG[d]	HDD[e]
NMHC	All	0.25	0.25	0.32	0.32	0.41	1.01	3.00
NO_X	All	0.2	0.2	0.4	0.7	1.0	2.0	9.24
CO	All	3.5	3.5	3.5	5.8[c]	5.8	13.25	8.41
HCHO	All	f	f	f	f	f	f	f

a. Emission rates for advanced technology CFVs meeting probable future standards.

b. 0.25 NMHC that is probable future standard for passenger cars; 0.2 NO_X and 3.5 CO are expected emission rates for future advanced LDAs.

c. Obtained from the corresponding entry in Appendix 4.A.

d. The conversion factor of 0.92 bhp-hr/mi (obtained from MOBILE3) for HDGVs was used to convert g/bhp-hr standards to an equivalent g/mi unit. 2.0 g/mi NO_X is considered the possible rate for future advanced HDGVs. Note that the useful life for HDGVs is 110,000 miles.

e. The conversion factor of 2.31 bhp-hr/mi (from MOBILE3) for HDDVs was used. 4.0 g/bhp-hr NO_X is considered the possible rate for future advanced HDDVs. Note that the useful life periods for light HDDVs, medium HDDVs and heavy HDDVs are 110,000, 185,000, and 290,000 miles, respectively. In addition, 8.41 g/mi CO at 50,000 miles is an in-use emission rate (from Attachment A) for HDDVs rather than the emission level meeting the future CO emission standard. This is due to the fact that the in-use rate is lower than the CO standard for HDDVs.

f. Formaldehyde emissions, expressed as a percentage to total hydrocarbons, for various vehicle classes contained in the table of Footnote f in Appendix 4.A are applicable to the current case.

Appendix 4.D. Emissions For Advanced Technology MFVs Using M100 Fuel

These emissions are used in Scenarios ADV METH and FULL METH.

Emissions at 50K mi - for CH_4O emissions are (g C/mi)
- for other species emissions are (g/mi)

Pollutant Species	Year	LDA	LDT under 3750#	LDT over 3751#	MDT 3751- 5750#	MDT over 5751#	HDG	HDD
Methanol	All	0.25	0.25	0.32	0.32	0.41	1.01	3.00
NO_X	All	0.2	0.2	0.4	0.7	1.0	2.0	4.62[a]
CO	All	3.5	3.5	3.5	5.8	5.8	13.25	8.41
HCHO	All	0.003[b]	0.003	0.018	0.018	0.022	0.046[c]	0.116[c]

a. The 4.62 g/mi NO_X rate is half of the 9.24 g/mi NO_X level for advanced technology HDDVs.

b. .003 g/mi or 3 mg/mi formaldehyde is equivalent to that for advanced technology gasoline-fueled LDAs. The 3 mg/mi formaldehyde rate is obtained based on the 0.25 NMHC standard and the 1 percent formaldehyde content in THC (from Footnote f of Appendix 4.A).

c. The conversion factors of 0.92 and 2.31 bhp-hr/mi (from MOBILE3) for HDGVs and HDDVs were used. The useful life for methanol-fueled HDGVs is assumed to be 110,000 miles. The useful life periods for light, medium, and heavy HDDVs are 110,000, 185,000, and 290,000 miles, respectively. It is assumed that advanced methanol-fueled HDDVs will comply with the 116 mg/mi formaldehyde standard over the corresponding useful life periods for different HDDV classes. In contrast, compliance with the applicable formaldehyde standards for "medium" advanced methanol-fueled HDDVs in Appendix 4.B is assumed to be over the period of 110,000 miles only (see Footnote h in Appendix 4.B).

Appendix 4.E. Methanol Fueled Vehicle Emissions Using M85 Fuel

These emissions are used in Scenario STD M85.

Emissions at 50K mi - for CH_4O emissions are (g C/mi)
- for other species emissions are (g/mi)

		Vehicle Type				
Pollutant Species	Year	LDA	LDT	MDT	HDG	HDD
Methanol	1990-91	0.295[a]	0.305	0.34[b]	d	d
	1992-94	0.18	0.185	0.22[c]	d	d
	1995+	0.125	0.13	0.16	d	d
NMHC	1990-91	0.295[a]	0.305	0.34[b]	d	d
	1992-94	0.18	0.185	0.22[c]	d	d
	1995+	0.125	0.13	0.16	d	d
NO_x	1990-93	0.71	0.74	0.975	d	d
	1994	0.65	0.69	0.7	d	d
	1995-96	0.40	0.42	0.7	d	d
	1997+	0.20	0.21	0.7	d	d
CO	1990-91	8.12	8.80	9.38[b]	d	d
	1992-94	4.06	4.40	6.0[c]	d	d
	1995+	3.5	3.5	5.8	d	d

Pollutant			LDT		MDT		HDG[e]	HDD[e]
Species	Year	LDA	under 3750#	over 3751#	3751-5750#	over 5751#		
HCHO	1990-93	0.023	0.023	0.027	0.027	0.033	0.095	0.234
	1994+	0.015	0.015	0.018	0.018	0.022	0.046	0.116

a. 0.295 g C/mi methanol and 0.295 g/mi NMHC are obtained from the following steps:

1) The EPA proposed organic emission rate:

$$\text{NMHC rate} = \text{NMHC} + \frac{13.876}{32.042}\ \text{methanol} + \frac{13.876}{30.026}\ \text{formaldehyde}$$

2) Ignore formaldehyde emissions due to the reason stated in Footnote a of Appendix 4.B.

3) 0.59 NMHC is the emission rate at 50K miles from Appendix 4.B. Thus,

$$0.59 = \text{NMHC} + \frac{13.876}{32.042}\ \text{methanol}$$

4) The emission composition split for M85-fueled vehicles is 70/30 for methanol emissions and NMHC emissions. So,

$$\text{NMHC} = \frac{30}{70}\ \text{methanol}$$

5) Substitute this relationship into the equation in Item 3 and solve the equation to obtain the following results:

Methanol = 0.68 g/mi or 0.295 g C/mi
NMHC = 0.295 g/mi

b. This emission rate is for model years 1990-93.

c. This emission rate is for the model year 1994 only.

d.

		HDG	HDD
Methanol	1990	0.79	1.50
	91-93	0.76	1.50
	94-96	0.75	1.48
	97-2000	0.74	1.47
NMHC	1990	0.79	1.50
	91-93	0.76	1.50
	94-96	0.75	1.48
	97-2000	0.74	1.47

NO_X	1990	5.10	7.20
	91-93	4.95	6.56
	94-96	4.83	6.50
	97-2000	4.75	5.16
CO	1990	21.07	8.67
	91-93	20.77	8.62
	94-96	20.36	8.53
	97-2000	20.09	8.41

e. These values are obtained from the corresponding entries of the HCHO Table in Appendix 4.B.

Appendix 4.F. NO_X Emission Reductions for Stationary Sources Fired with Methanol

Source Category	% Reduction in NO_X From Utilizing Methanol*
Non-Refinery Boilers and Heaters	20%
Utility Boilers	50%
Stationary Industrial I.C. Engines	50%

* From Personal Communication, Manjit Ahuja, February 16, 1988.

5.0 Trajectory Modeling of Ozone, PAN and Formaldehyde

5.1 Introduction

The second tier of the three-tiered modeling program is to use the trajectory model to further test the sensitivity of the air quality model components to inputs, and to develop preliminary methanol use-air quality relationships. The trajectory model is a powerful tool for analyzing the effects of many different parameters on air quality because of its computational speed. Over 50 different scenarios were run along three trajectories to calculate how pollutant concentrations respond to emissions changes. These calculations serve both to test the effectiveness of emission controls, and to test the photochemical model's sensitivity to inputs. Particularly useful calculations then were identified to be studied further with the airshed model.

While the trajectory model is significantly less computationally intensive than the airshed model, there are inherent model limitations. The trajectory model only gives information along the specific path that it travels through the basin, and not the remainder of the basin. Also, the mathematical formulation of the trajectory model equation neglects certain physical processes. The lack of information about other areas of the basin can be compensated by running multiple trajectories through the basin, but the other limitations of the trajectory model make it more suitable for determining the relative effectiveness of changes in emissions and other conditions than for rigorous testing of control strategy effectiveness.

5.2 Trajectory Model Formulation

The trajectory model uses a vertically resolved, Lagrangian formulation of the reaction-diffusion-advection equation:

$$\frac{\partial c_i}{\partial t} = \frac{\partial}{\partial z}\left(K_{zz}\frac{\partial c_i}{\partial z}\right) + R_i\left(c_1, c_2, \ldots . c_n, T\right) - \frac{\partial v_s c_i}{\partial z} + s(c_i) \qquad (5.1)$$

where c_i is the concentration of species i, $K_{zz}(z)$ is the vertical turbulent eddy diffusivity, $R_i(c_1, c_2, \ldots, c_n, T)$ is the rate of chemical production of species i at temperature T, and v_s is the settling velocity. The initial conditions are:

$$c_i(z,0) = c_i^0(z) \quad \text{at} \quad t = 0 \qquad (5.2)$$

and the boundary conditions are:

$$\left(K_{zz}\frac{\partial c_i}{\partial z}\right) = 0 \qquad \text{at} \quad z = H \qquad (5.3)$$

at the top boundary, and at the bottom boundary:

$$\left(v_g^i c_i - K_{zz}\frac{\partial c_i}{\partial z}\right) = E_i \qquad (5.4)$$

where v_g^i is the deposition velocity of species i and E_i is the emissions of species i, a function of time and location. Boundary conditions imply no vertical flux at the top boundary, while at the bottom boundary vertical flux is the difference of emissions and the ground level deposition. Negligible vertical flux from the top of the air parcel is a result of setting the column height significantly above the mixing height. At that height, (1500 m) both the vertical diffusion and pollutant concentrations are small. A graphical representation of the Lagrangian trajectory model formulation appears in Figure 5.1. Within the air parcel the model describes chemical kinetics, turbulent vertical diffusion, horizontal transport, ground level deposition, and emissions. Inputs to the trajectory model include pollutant emissions as a function of time and location, wind speeds, mixing heights, meteorology, and information on surface characteristics such as surface roughness. A more complete description and evaluation of the trajectory model can be found in Russell, et al. (1983) and Russell and Cass (1986). The program was updated to include the Extended Caltech mechanism as discussed in chapter 2.

Because the trajectory formulation follows a one-dimensional vertical air parcel through the basin, it cannot include all physical processes. Two notable processes which the formulation does not include are horizontal diffusion and wind shear (Liu and Seinfeld, 1975). The airshed model does not have these limitations, and is more suited for making absolute determinations of air quality.

5.3 Description of Trajectory Paths

The basic requirements of a photochemical air quality model, either in the Lagrangian trajectory or the Eulerian form, are a description of the meteorology, emissions, and atmospheric chemistry, as was shown in Figure 5.1. The chemistry used is the Extended Caltech mechanism as previously discussed. Chapter 4 discussed the choice of modeling period and treatment of emissions. These inputs are common to the two photochemical models. The major difference in the two models is that the trajectory formulation requires identifying trajectories of individual air parcels, and determining how the pollutants evolve along a particular path.

Trajectory paths were calculated by integrating the equation of motion backwards in time, starting at three different receptor sites. Three paths were chosen for study. Wind fields used for calculating the trajectories were generated using the objective analysis techniques described by Goodin, et al. (1982), beginning with the observations collected around the SoCAB during the three day modeling period. The three paths are shown in Figure 5.2 and were selected because each is affected by different emissions source types and typify how pollutants respond in different regions of the SoCAB. Predictions agreed well with the observed ozone at the three sites. By considering the effects on all three trajectories, the results can be used to develop a more global view of how air quality will respond to emission changes.

The first trajectory selected starts over the ocean, comes ashore on August 31, and ends at Norco at 2 PM (PST) on September 1. This trajectory was selected because Norco recorded the highest measured ozone concentration, 0.35 ppm, in the 1982 ozone episode. The predicted ozone peaked at 0.29 ppm. Also, this trajectory passes through an area with extensive refinery emissions. This trajectory is particularly sensitive to changes in refinery emissions and can be used to determine the effects of reductions in those emissions on air quality.

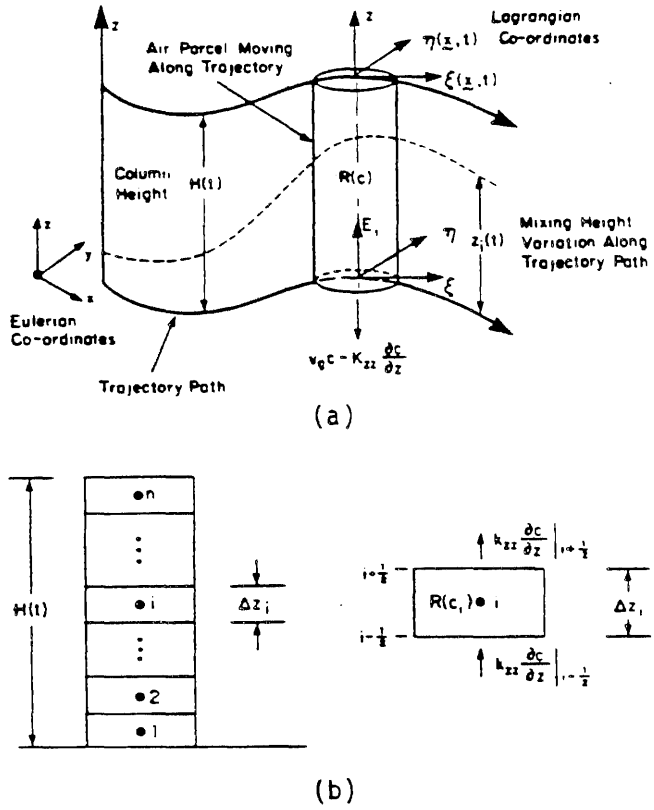

Figure 5.1 Schematic representation of (a) vertically resolved Lagrangian trajectory model and (b) the computational grid cell convention.

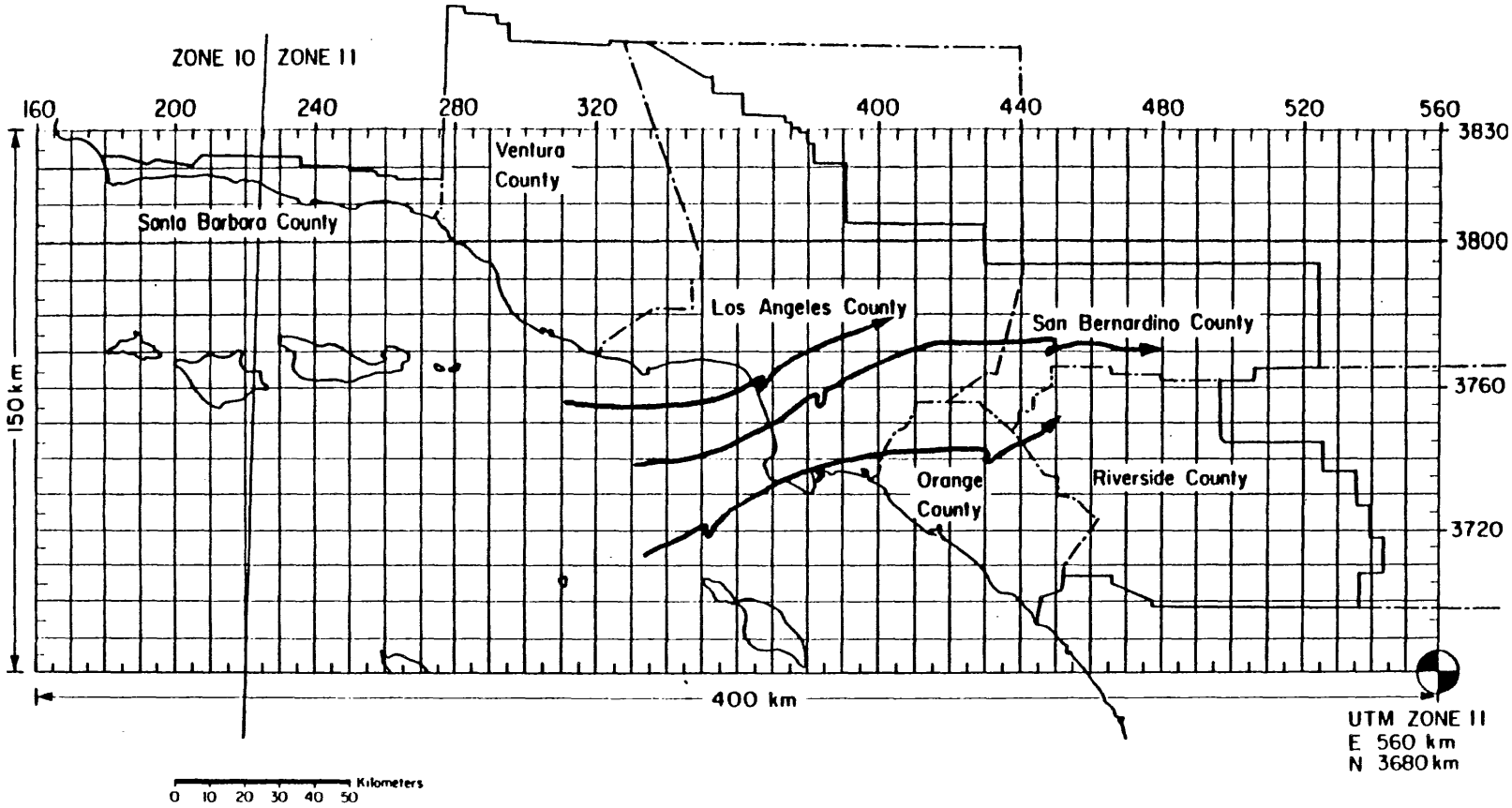

Figure 5.2 Trajectory paths of the air parcels passing over San Bernardino at 1500 (PST), Norco at 1400 (PST), and Pasadena at 1300 (PST) on September 1, 1982. Pasadena is the northern trajectory and Norco is the southern trajectory.

The second trajectory selected also begins over the ocean. It comes ashore on August 30 and ends at 3 PM, September 1 at San Bernardino. The observed ozone maximum was 0.28 ppm, and the predicted ozone at that time was 0.32 ppm. This trajectory has one of the longest residence times in the basin of trajectories that end at receptor sites. Therefore, it is less affected by assumptions in initial conditions than other scenarios. This trajectory is heavily influenced by mobile source emissions. Since these sources are the primary focus of emissions control and alternate fuel use scenarios, this trajectory is particularly useful for determining air quality changes resulting from different mobile source emissions. Also, this trajectory is well suited for testing if methanol buildup over three days diminishes the effectiveness of switching to methanol.

Both these trajectories terminate in the eastern portion of the SoCAB. They are both relatively long trajectories, and the pollutants in the air mass are well aged by the time they reach their respective end points. Many of the reactive organic gases, especially the alkanes, have atmospheric lifetimes of two to five days, as opposed to NO_x, which reacts more rapidly, and is depleted from the atmosphere. As a result, these air parcels become NO_x-limited. Being NO_x-limited means that photochemical oxidant formation is limited by the availability of NO_x, as opposed to reactive organic gases. This is characterized by high ROG/NO_x values, as is found in the eastern SoCAB. It was decided to add a third trajectory which terminates in the central region of the SoCAB that would be more sensitive to ROG controls, such as methanol use.

The third trajectory was selected ending at Pasadena at 12 noon, the time of maximum recorded ozone concentration at that site on September 1. The trajectory comes ashore on August 31, and is over land for less time than the other two trajectories. Air quality at Pasadena is more similar to the air quality experienced in central Los Angeles than the other two sites. This trajectory is used to study the air quality sensitivities in the regions with a lower ROG/NO_x ratio.

Each air parcel trajectory starts over the ocean. In this way, trajectory length is maximized and the initial pollutant concentrations are lowered. Both factors reduce the impact of initial condition specification. For a 50% reduction in initial pollutant concentrations, the predicted O_3 changed 0.5% for the San Bernardino trajectory, to 5% for the Pasadena trajectory. This test shows that the model predictions are primarily a function of the input emissions and meteorology, not assumed initial conditions. This is a necessary condition for determining the role of emissions in a highly nonlinear system.

5.4 Trajectory Scenarios

Over 50 different emission scenarios were analyzed with the trajectory model. Additional calculations tested how other inputs affect predicted air quality. First, a number of scenarios were identified to conduct preliminary tests of how the air quality would change if methanol fuel use were mandated. These included the use of methanol at varying fractions of the total vehicle fleet, and with differing emission levels and compositions. The base year, and the corresponding emissions, for testing methanol use is the year 2000.

Any air quality modeling exercise, especially when using forecast emissions, is subject to uncertainty in the inputs. Examples of uncertainties include the emissions of the different pollutants into the air mass, the timing of the emissions, and the meteorology. A major uncertainty when testing how utilizing methanol will impact air quality is that MFVs are not a standard technology. Emissions from the present generation of methanol fueled vehicles are not well characterized, and emissions from future vehicles will depend on advances in the technology, regulations, fuel composition, local driving conditions,

temperature, and more. A parametric test of how changes in these factors would affect the predicted air quality was conducted to quantify the uncertainties, and hence identify what areas require more study. This also led to the identification of future calculations for study using the airshed model.

There are also uncertainties unrelated to emissions. Two examples are the deposition rates of pollutants, and the description of the atmospheric chemistry. An additional set of calculations were conducted to test how trajectory model predictions respond to changing the chemical mechanism and other parameters. A list of all the scenarios studied, and their descriptions, appears in Table 5.1ab. Results of some of the trajectories tested were supplanted by later calculations, and for brevity are not listed. The **BASE** calculation corresponds to the forecast, year 2000 emissions supplied by CARB (1987), with mobile source emissions corresponding to EMFAC7C (CARB, 1986). Other scenarios are derived from this case, with the changes specified in Table 5.1.

5.5 Results

Results of trajectory model testing show that methanol fuel use can improve air quality to a significantly greater extent than conventional emissions controls alone. However, the air quality changes vary significantly within the basin. This section presents how the predicted concentrations of ozone, formaldehyde and PAN would change as a result of implementing the controls corresponding to each scenario described in Table 5.1. Tables 5.2 - 5.4 present the predicted concentrations of these species at San Bernardino, Norco, and Pasadena for the various scenarios tested.

Ozone concentrations at San Bernardino and Norco do not change markedly in response to replacing CFV-type emissions with those characteristic of MFVs. As explained above, ozone formation at this point is mainly dependent on the availability of NO_x. For this reason it is convenient to test the effectiveness of changing the organic gas emissions relative to having no organic gas emissions at all. This also normalizes the predicted reduction of ozone relative to the magnitude of the source emissions. As an example, mobile sources emit only about a fourth of the ROG, so even removing all the mobile source ROG will not eliminate ozone formation. A relative measure shows the effectiveness compared to removing those emissions. A preferable measure of methanol fuel's effectiveness is to compare the reduction in ozone concentration that occurs with methanol fuel usage to the reduction in ozone concentration that occurs when the emissions, or a component of those emissions, from a source undergoing conversion are removed. Mathematically this can be expressed as:

$$R_i^O = \frac{[O_3]_{base} - [O_3]_i}{[O_3]_{base} - [O_3]_{source\text{-}removed}} \qquad (5.5)$$

where R_i^O is the relative reduction in ozone obtained with the scenario being analyzed, $[O3]_i$ is the ozone level of the scenario, $[O3]_{source\text{-}removed}$ is the ozone level that occurs when the source, or component of that source, is removed and $[O3]_{base}$ is the ozone level in the base year 2000 scenario. The relative reduction calculations for formaldehyde and PAN are similar, except that concentrations of ozone are replaced by the corresponding concentrations of formaldehyde and PAN:

Table 5.1a List of Emissions Scenarios

BASE	Current best estimates of year 2000 emissions
PETRO/AREA	Year 2000 emissions excluding mobile sources
AREA	Year 2000 emissions excluding mobile and petroleum sources
SC01	Full penetration of advanced[1] technology MFVs (0.25 g mi^{-1} ROG, 0.20 g mi^{-1} NO_x, 1% HCHO)
SC02	Base scenario minus mobile source ROG emissions
SC03	Base scenario minus mobile source NOx emissions
SC04	Full penetration of advanced[1] technology CFVs (0.25 g mi^{-1} ROG, 0.20 g mi^{-1} NO_x)
SC05	Same as SC11 but 85% HDG and 45% HDD MFV penetration
SC06	Base scenario with mobile emissions staggered +2 hrs
SC07	Base scenario with mobile emissions staggered -2 hrs
SC08	No emissions
SC11	Full MFV penetration from 1990, current emissions estimates (EMFAC7C rates)
SC12	Same as SC11 but mobile source ROG, NOx emissions deterioration rates up 50%
SC13	Same as SC11 but mobile source ROG, NOx emissions deterioration rates down 50%
SC14	Same as SC11 but using M85 fuel
SC15	Same as SC14 with emissions deterioration rates 50% greater than current projections
SC16	Same as SC14 with emissions deterioration rates 50% less than current projections
SC17	Same as SC14 but with HCHO emissions 10% of ROG emissions by mass
SC18	Same as SC14 but with HCHO emissions 1% of ROG emissions by mass
SC19	Same as SC11 but HCHO emissions 1% by mass
SC20	Same as SC11 but HCHO emissions 10% by mass
SC21	M100 fuel, 50% MFV penetration LDA, LDT;100% penetration MDT,HDT
SC22	M100 fuel, 25% MFV penetration LDA, LDT;100% penetration MDT,HDT
SC23	M100 fuel, 10% MFV penetration LDA, LDT;100% penetration MDT,HDT
SC24	M85 fuel, 10% MFV penetration LDA, LDT;100% penetration MDT, HDT
SC25	M85 fuel, 25% MFV penetration LDA, LDT;100% penetration MDT, HDT
SC26	M85 fuel, 50% MFV penetration LDA, LDT;100% penetration MDT, HDT
SC27	All gasoline - base scenario (test of methodology)
SC31	100% penetration of M100 fueled MFVs with 4% HCHO, ROG emissions 0.41g mi^{-1}, NO_x emissions 0.7 g mi^{-1}
SC32	Same as SC31 but with NO_x emissions 0.4 g mi^{-1}
SC33	Same as SC31 but with NO_x emissions 0.2 g mi^{-1}
SC34	100% penetration of M100 fueled MFVs with 4% HCHO, ROG emissions 0.25 g mi^{-1}, NO_x emissions 0.2 g mi^{-1}
SC35	Same as SC34 but with NO_x emissions 0.4 g mi^{-1}
SC36	Same as SC34 but with NO_x emissions 0.7 g mi^{-1}
SC41	Same as SC01 with no methanol emissions
SC42	Same as SC01 with no formaldehyde emissions
SC43	Same as SC01 without methanol and formaldehyde emissions
SC44	Same as SC01 except HCHO emissions increased by a factor of three
SC52	Base case with mobile ROG emissions increased 100%
SC53	Base case with mobile NO_x emissions increased 30%
SC54	Base case with mobile NO_x emissions decreased 30%
SC70	Same as SC11 without methanol and formaldehyde from MFVs
SC71	ROG emissions same as SC01, NO_x twice that of BASE
SC72	ROG emissions same as SC04, NO_x twice that of BASE
SC73	ROG same as BASE, NO_x twice that of BASE
SC74	ROG same as AREA, NO_x twice that of BASE
SC91	No mobile source ROG, NO_x correspond to advanced CFVs

[1] Advanced Technology vehicles meet the in-use standard proposed for the year 2000 vehicles. It does not mean that a different, newer technology is assumed.

Table 5.1b: Sensitivity Calculations

IC+	Initial conditions increased , uniformly, 50%
IC-	Initial conditions decreased , uniformly, 50%
NOX+	NO_x emissions increased 20%
NOX-	NO_x emissions decreased 20%
ROG+50	ROG emissions increased 50%
ROG+100	ROG emissions increased 100%
DEPO_O3	Ozone deposition set to zero
DEPO_HCHO	HCHO deposition set to zero
ERT	BASE simulation using the SAPRC/ERT chemical mechanism
ERT/NOX+	Similar to NOX+, except that the SAPRC/ERT mechanism is used
ERT/NOX-	Similar to NOX-, except that the SAPRC/ERT mechanism is used
ERT/ROG+50	Similar to ROG+50, except that the SAPRC/ERT mechanism is used
ERT/ROG+100	Similar to ROG+100, except that the SAPRC/ERT mechanism is used
SC01/NOX+	Same as SC01, except that NO_x emissions are increased 20%
SC41/NOX+	Same as SC41, except that NO_x emissions are increased 20%
SC04/NOx+	Same as SC04, except that NO_x emissions are increased 20%
NO_HCHO	No emissions of HCHO in the BASE case
HALF_HCHO	Half the HCHO emissions of the BASE case
1982	1982 Evaluation calculations

Filename	Ozone	HCHO	PAN
BASE	0.2603	0.01497	0.009528
PETRO/AREA	0.1976	0.01192	0.006322
AREA	0.1617	0.01964	0.013090
sc01	0.2442	0.01311	0.007960
sc02	0.2496	0.01217	0.008406
sc03	0.2018	0.01562	0.006383
sc04	0.2468	0.01345	0.008440
sc11	0.2537	0.01447	0.008521
sc12	0.2624	0.01496	0.008961
sc13	0.2434	0.01401	0.008019
sc14	0.2549	0.01474	0.008849
sc15	0.2656	0.01530	0.009455
sc16	0.2444	0.01419	0.008198
sc17	0.2551	0.01478	0.008827
sc18	0.2549	0.01471	0.008860
sc19	0.2515	0.01363	0.008536
sc21	0.2550	0.01471	0.008876
sc22	0.2558	0.01481	0.009013
sc23	0.2558	0.01492	0.009119
sc24	0.2563	0.01501	0.009208
sc25	0.2557	0.01496	0.009143
sc26	0.2557	0.01483	0.008998
sc27	0.2603	0.01496	0.009528
sc31	0.2537	0.01402	0.008604
sc32	0.2459	0.01401	0.008153
sc33	0.2403	0.01405	0.007858
sc34	0.2401	0.01376	0.007884
sc35	0.2451	0.01372	0.008162
sc36	0.2532	0.01372	0.008619
sc71	0.2409	0.01492	0.008785
sc72	0.2681	0.01481	0.010580
sc73	0.2999	0.01575	0.012540
sc74	0.2367	0.01408	0.008656
DEPO_HCHO	0.2630	0.01712	0.009341
DEPO_O3	0.3632	0.01477	0.009548
ERT	0.2232	0.01430	0.004680
ERT ROG+100	0.2376	0.02090	0.004870
ERT ROG+50	0.2393	0.01810	0.005080
ERT NOX+	0.1948	0.01320	0.003260
ERT NOX-	0.2278	0.01520	0.005590
ROG +100	0.2622	0.03214	0.010860
ROG+50	0.2625	0.02343	0.010760
IC+	0.2539	0.01306	0.008787
IC-	0.2614	0.01745	0.009875
NOX+	0.2105	0.01558	0.006615
NOX-	0.2914	0.01670	0.011250
sc01_NOX+	0.2642	0.01340	0.009279
sc01_NOX+_NoCH4O	0.2615	0.01249	0.009241
sc04_NOX+	0.2793	0.01335	0.010310
1982	0.3232	0.02832	0.021250

Table 5.3 Ozone, Formaldehyde, and PAN at Norco, 14:00

Filename	Ozone	HCHO	PAN
BASE	0.1920	0.01562	0.012740
Petro/Area	0.1223	0.01130	0.005993
AREA	0.1194	0.01114	0.005764
sc01	0.1685	0.01305	0.009884
sc02	0.1627	0.01244	0.009591
sc03	0.1302	0.01532	0.006163
sc04	0.1768	0.01364	0.010850
sc11	0.1809	0.01470	0.011060
sc12	0.1835	0.01551	0.011360
sc13	0.1728	0.01399	0.010090
sc14	0.1854	0.01507	0.011610
sc15	0.1700	0.01255	0.008110
sc16	0.1740	0.01423	0.010260
sc17	0.1857	0.01514	0.011600
sc18	0.1853	0.01507	0.011660
sc19	0.1788	0.01389	0.011070
sc20	0.1811	0.01469	0.011030
sc21	0.1855	0.01505	0.011660
sc22	0.1868	0.01524	0.011870
sc23	0.1872	0.01540	0.012020
sc24	0.1875	0.01547	0.012040
sc25	0.1873	0.01544	0.012030
sc26	0.1869	0.01528	0.011860
sc27	0.1920	0.01562	0.012740
sc31	0.1800	0.01431	0.011140
sc32	0.1750	0.01407	0.010390
sc33	0.1695	0.01388	0.009635
sc34	0.1693	0.01366	0.009746
sc35	0.1745	0.01377	0.010400
sc36	0.1794	0.01396	0.011090
sc43	0.1660	0.01208	0.009854
sc91	0.1556	0.01214	0.010300

Filename	Ozone	HCHO	PAN
BASE	0.2368	0.02634	0.02393
Petro/Area	0.1535	0.01777	0.01311
sc01	0.1661	0.02037	0.01158
sc02	0.1461	0.01912	0.00932
sc03	0.1709	0.02485	0.01440
sc04	0.2060	0.02237	0.01817
sc05	0.1904	0.02394	0.01474
sc06	0.2213	0.02484	0.02178
sc07	0.2348	0.02633	0.02355
sc08	0.0395	0.00532	0.00001
sc11	0.1925	0.02372	0.01508
sc12	0.1810	0.02458	0.01317
sc13	0.1990	0.02266	0.01652
sc14	0.2169	0.02500	0.01943
sc15	0.2192	0.02655	0.01936
sc16	0.2108	0.02343	0.01885
sc17	0.2179	0.02519	0.01950
sc18	0.2163	0.02490	0.01938
sc19	0.1882	0.02243	0.01476
sc20	0.1936	0.02383	0.01515
sc21	0.2174	0.02497	0.01959
sc22	0.2261	0.02548	0.02148
sc23	0.2304	0.02578	0.02252
sc24	0.2329	0.02603	0.02318
sc25	0.2310	0.02588	0.02267
sc26	0.2270	0.02559	0.02168
sc27	0.2368	0.23640	0.23930
sc31	0.1887	0.02303	0.01466
sc32	0.1975	0.02279	0.01620
sc33	0.2000	0.02257	0.01679
sc34	0.1990	0.02210	0.01675
sc35	0.1962	0.02232	0.01613
sc36	0.1874	0.02259	0.01458
sc41	0.1624	0.01910	0.01133
sc42	0.1650	0.02012	0.01149
sc43	0.1613	0.01885	0.01124
sc44	0.1684	0.02088	0.01173
sc70	0.1851	0.02140	0.01456
No HCHO	0.2345	0.02561	0.02381
Half HCHO	0.2357	0.02597	0.02387
NOx+	0.1660	0.02020	0.00974
NOx-	0.2160	0.01913	0.01730
ROG+50	0.2670	0.02841	0.02470
ROG+100	0.3110	0.03555	0.03550

$$R_i^P = \frac{[PAN]_{base} - [PAN]_i}{[PAN]_{base} - [PAN]_{source\text{-}removed}} \quad (5.6)$$

$$R_i^F = \frac{[HCHO]_{base} - [HCHO]_i}{[HCHO]_{base} - [HCHO]_{source\text{-}removed}} \quad (5.7)$$

Results from these calculations are presented graphically in Figures 5.3 through 5.9, and are used for comparing the relative effectiveness of methanol strategies.

5.5.1 Ozone Sensitivity to Methanol Fuel Use Levels

A striking characteristic of the results at San Bernardino and, to a lesser extent, Norco is how little change there is as methanol fueled vehicles replace their conventionally fueled counterparts (Table 5.2 and 5.3). This trend was investigated further by removing mobile source ROG emissions (SC02). The predicted ozone at San Bernardino drops from the Base Case value of 0.26 to 0.25 ppm, or a 4% reduction. On the other hand, removing mobile source NO_X reduced ozone to 0.20 ppm, or 23%. This indicates that for the trajectory chosen, ozone formation at San Bernardino is NO_X-limited, and is more sensitive to NO_X than ROG emission changes. In this case, the relative effect of replacing the ROG emissions with MFV exhaust and evaporative components was tested. In this case, $[O_3]_{source\ removed}$ of Equation 5.5 is the predicted ozone if ROG emissions from mobile sources are removed) (SC02). The result is that, as methanol is rolled into the vehicle fleet from 10% to 100%, the relative ozone reduction ranges to 62%. Two aspects of this calculation should be mentioned. First, the heavy- and medium-duty trucks are treated as being converted to methanol. Secondly, the replacement of CFVs with MFVs begins in 1990, so by the Year 2000 a sizable fraction of the emissions is from older, deteriorated CFVs. This limits the degree of improvement realized in a finite time period from switching to methanol.

Switching to M85 fuel, instead of M100, decreases the apparent benefits. For example, comparing the case if M85 cars replace 100% of new cars entering the fleet from 1990 on (SC14) versus M100 cars (SC11), the peak ozone is reduced 0.005 ppm versus 0.006 ppm. The difference in the absolute change is small because of the ROG insensitivity. The relative reduction from introducing M85 MFVs at increasing rates is shown in Figure 5.4.

The insensitivity of ozone formation in the Eastern SoCAB to ROG controls in the Year 2000 is not surprising. The Year 2000 inventory shows only a 9% decrease in organic gas emissions from 1982, and a 34% decrease in NO_X. Ozone isopleths constructed for the 1982 draft AQMP (SCAQMD and SCAG, 1982) indicate that after these reductions peak ozone formation should be more sensitive to NO_X control rather than ROG control. Similarly, the UCR smog chamber experiments show an increased sensitivity to NO_X during multiday experiments. A particularly notable example is experiment ITC-;867 of Carter, et al. (1986[a]), where adding NO_X on the second and third days increased ozone formation.

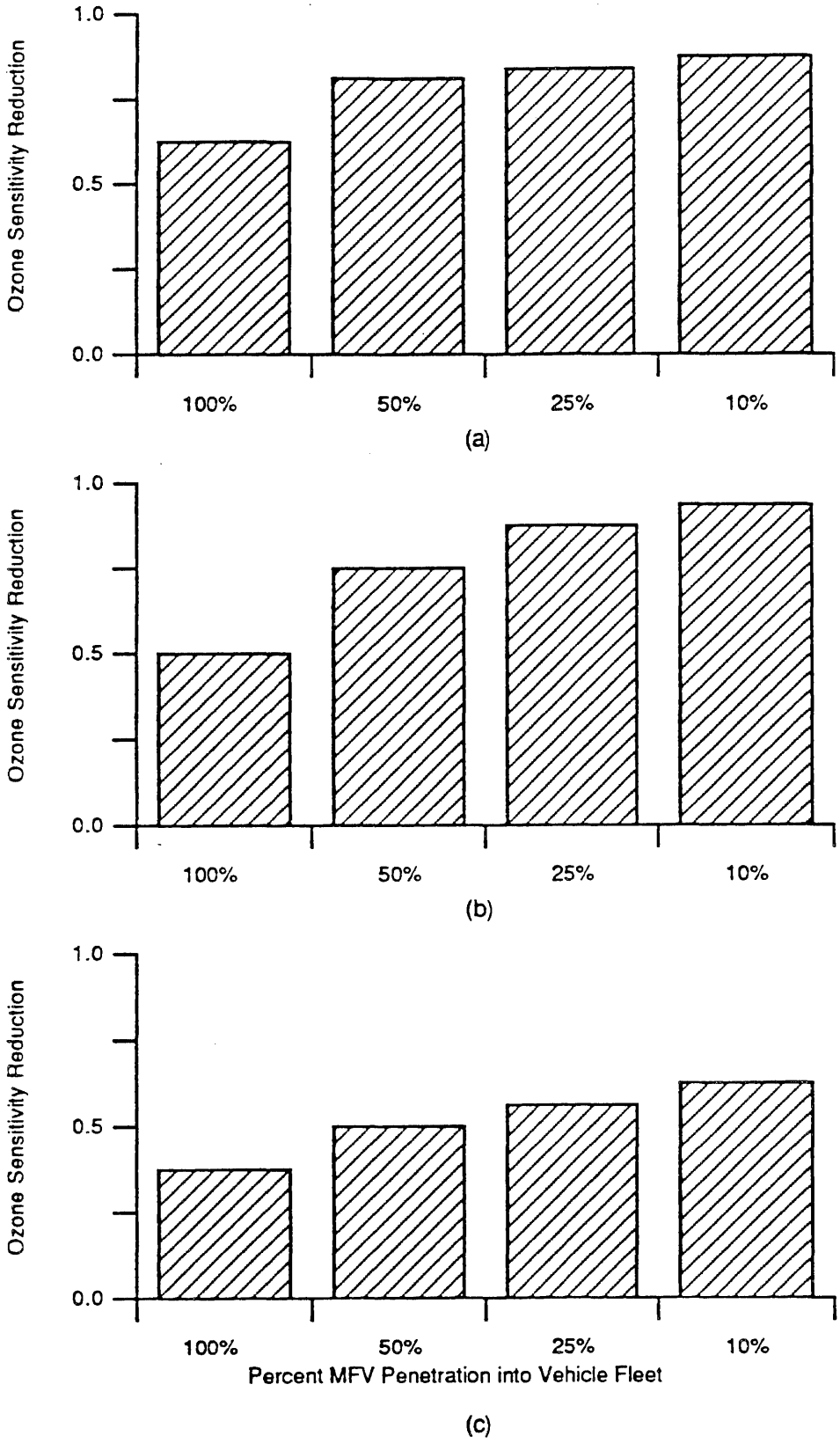

Figure 5.3 Ozone reductions relative to removing mobile source ROG emissions as a function of M100 MFV penetration into the vehicle fleet. A value zero would indicate that it is comparable to removing the ROG from the emissions. a)Norco, b) Pasadena and c) San Bernardino

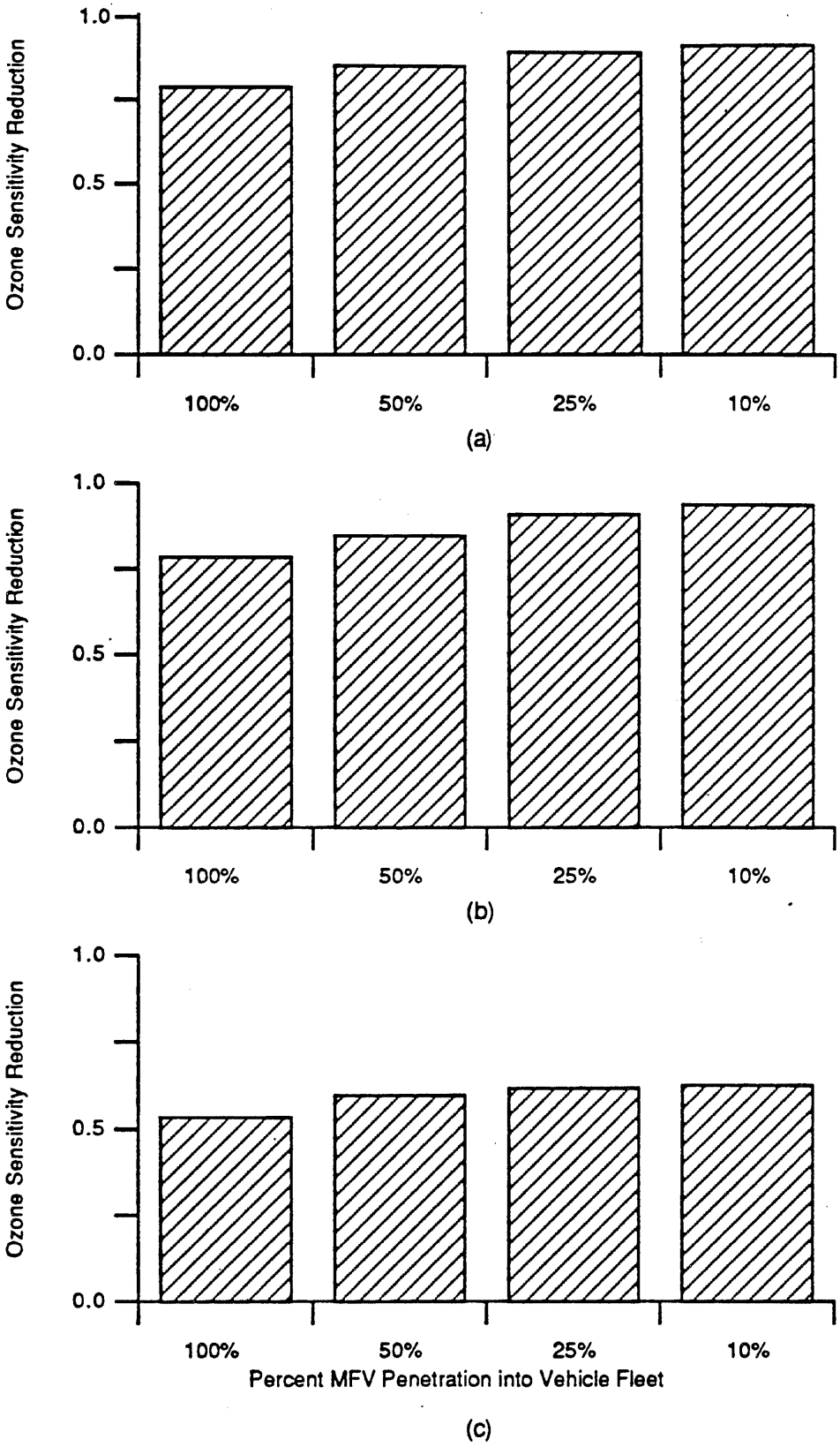

Figure 5.4 Ozone reductions relative to removing mobile source ROG emissions as a function of M85 MFV penetration into the vehicle fleet. A value zero would indicate that it is comparable to removing the ROG from the emissions. a)Norco, b) Pasadena and c) San Bernardino

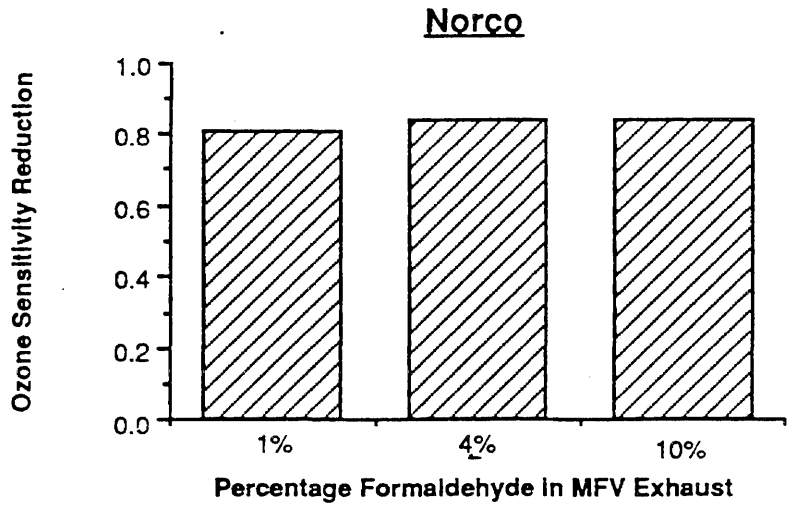

(a)

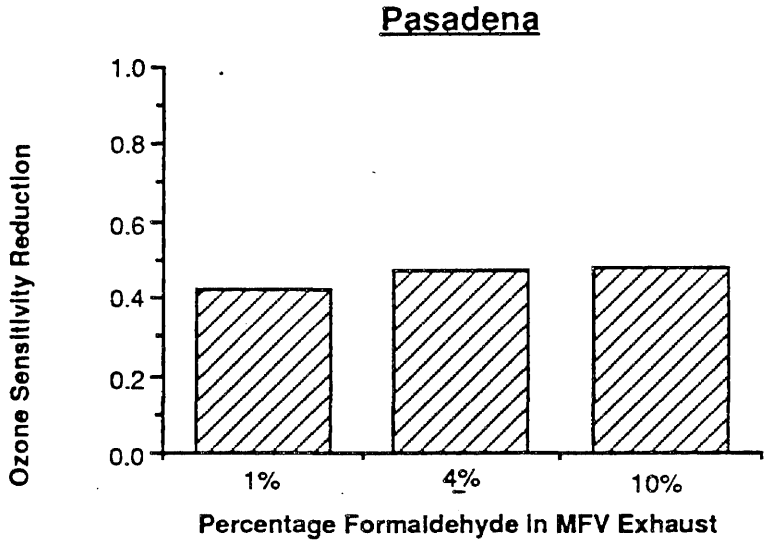

(b)

Figure 5.5 Ozone Sensitivity Reductions with Varying Formaldehyde Fraction of M100 MFV Exhaust. a) Ozone at Norco, b) Ozone at Pasadena

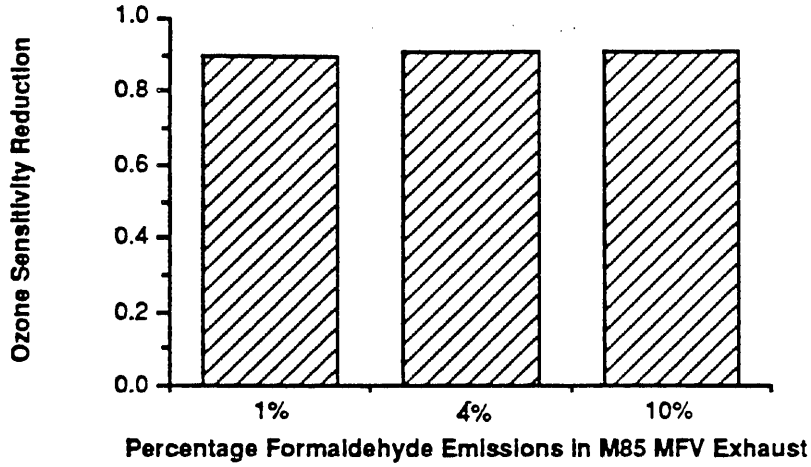

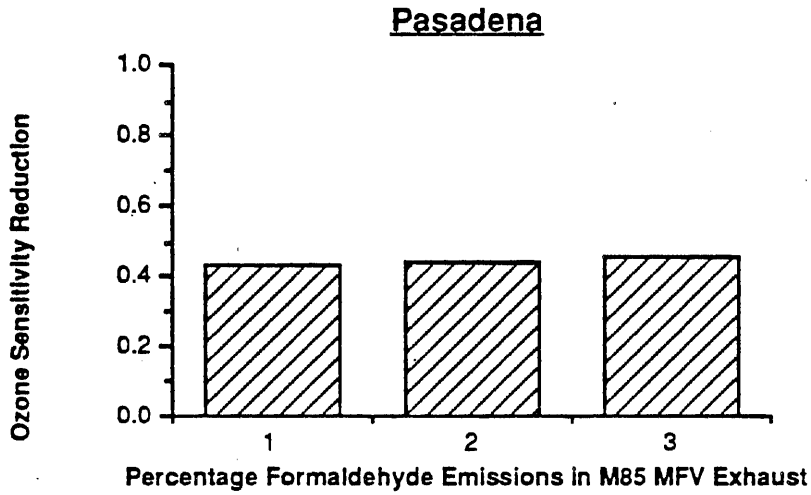

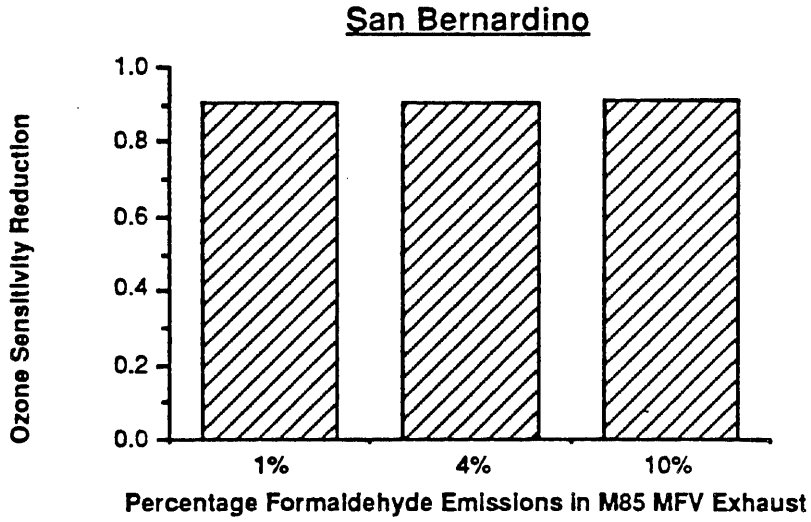

Figure 5.6 Ozone Sensitivity Reductions with Varying Formaldehyde Fraction of M85 MFV Exhaust

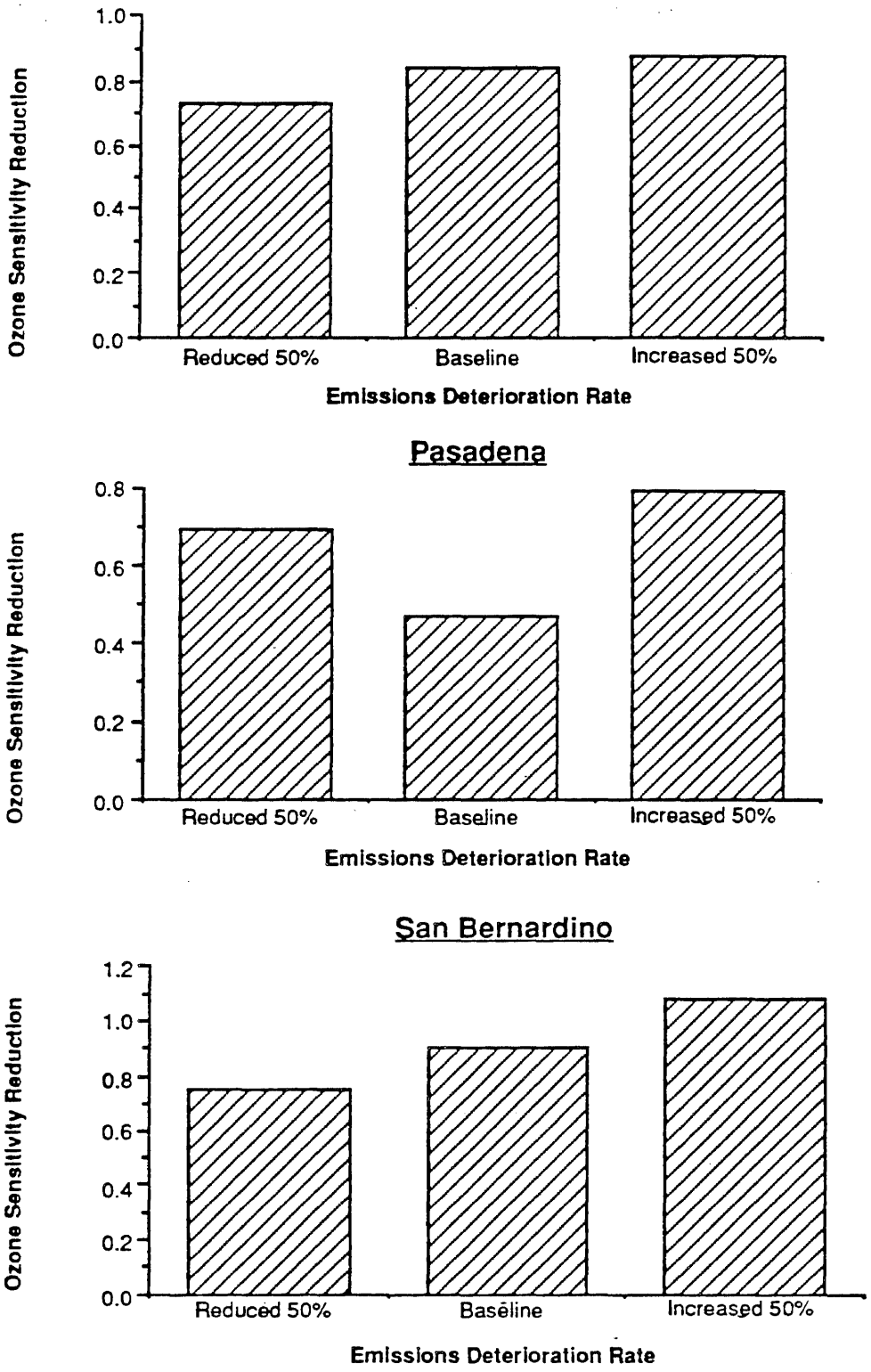

Figure 5.7 Ozone Sensitivity Reductions with Varying Emissions Deterioration Rates

Norco is not as far east, and is found to be more sensitive to the use of methanol. As an example, converting from conventionally fueled vehicles to methanol dropped the ozone 6% (Base vs. SC11). Again, the ozone levels do not change dramatically as methanol is used, though a greater improvement is realized than if CFVs are used. This can be explained, in part, that the ozone at Norco is more sensitive to reducing NO_X, and that a relatively small fraction of the ROG is being affected. For example, removing mobile source ROG reduced ozone by only 15% (Base vs. SC02). The 6% reduction noted for switching to methanol is 40% of what is found for removing all mobile source ROG (Fig. 5.3). Conversely, removing mobile source NO_X reduces ozone 32%. NO_X control would be more effective at reducing ozone at Norco.

Relative reductions in ozone realized by introducing M100 and M85 fueled vehicles are shown in Figures 5.3 and 5.4, respectively. The response is relatively flat to increasing levels of MFV penetration. The benefit to having the less reactive emissions of M100 fueled vehicles is clear.

After finding that the predicted ozone concentrations at San Bernardino and Norco were significantly more sensitive to NO_X control than switching the ROG emissions to those characteristic of methanol, a third trajectory ending at Pasadena was chosen for further analysis. Pasadena is more heavily impacted by fresh traffic-related emissions than the other two, and the atmosphere has higher NO_X levels. This leads to a greater response to motor vehicle ROG controls.

The BASE case, Year 2000 predicted ozone was 0.24 ppm at Pasadena. Switching to methanol vehicles with similar NO_X emissions, and the ROG exhaust component replaced by methanol and formaldehyde (SC11) reduced the ozone by 35%. Totally removing the ROG from the exhaust lowered the predicted ozone to 0.15 ppm, or 38% (SC02). Totally removing on-road emissions reduced ozone to (34%). Thus, conversion to methanol reduced the mobile source "fraction" of the ozone (i.e., the base level ozone minus the ozone with no mobile source emissions) by 55%. The response to increasing methanol use at Pasadena is shown in Figures 5.3 and 5.4 for M100 and M85 fueled vehicles, respectively. Both the absolute changes, and relative changes, are much greater for the Pasadena trajectory.

5.5.2. Sensitivity to Formaldehyde Exhaust Fraction

Formaldehyde is a major contributor to the reactivity of MFV exhaust. The level of HCHO in the exhaust will impact the benefits of using methanol as an automobile fuel. An issue was how important is controlling HCHO emissions in determining the benefits. Six sensitivity runs were conducted for each of the trajectories, altering the HCHO content in the exhaust from 1% to 4% to 10%, by mass, of the organic gas emissions for both M100 and M85 fuel (Scenarios SC11, SC14, and SC17-SC20). The results are shown in Figures 5.5 and 5.6. The relative reductions are shown, using as the basis the ozone predicted with and without automobile emissions (BASE versus SC02). Ozone at Pasadena showed the strongest sensitivity to HCHO exhaust content, and the trend at all stations was that lower HCHO emissions led to correspondingly lower ozone.

5.5.3 Ozone Sensitivity to Varying Deterioration Rates

The deterioration characteristics of MFVs are not well known. Early tests indicated possible increased deterioration rates of MFV exhaust emissions (Austin, 1988). The

impact of varying deterioration rates at plus and minus 50% of the nominal (as given by EMFAC7C methodology) was tested (SC11 vs. SC12 vs. SC13). The results of this calculation are shown in Figure 5.7. In all cases, increased deterioration greatly increased ozone formation. At Pasadena, decreasing the deterioration rate also lead to an increase in O_3 because of the reduction in local NO_x emissions. Further analysis showed that the sensitivity to deterioration was primarily the sensitivity to NO_x emissions, and the ROG impact was secondary because of the low reactivity of methanol.

5.5.4 Use of Advanced Conventional and Methanol Fueled Vehicles

A set of calculations compared the relative benefits of low emitting ("advanced"[1]) conventional and the corresponding M100 fueled vehicles (SC04 vs. SC01). These vehicles emit 0.25 g ROG mi^{-1} (on a carbon basis) and 0.20 g mi^{-1} NO_x. The results of this comparison are shown graphically in Figure 5.8. The most marked difference is at Pasadena where the predicted maximum ozone decreased from 0.21 ppm for the advanced CFVs, to 0.17 ppm for the advanced MFVs. The relative improvement from going to a standard fleet to advanced methanol is over twice that of going to advanced CFVs. The standard M100 case (SC11) has lower ozone than the advanced CFV.

5.5.5 Role of Emission Timing

Observation of air quality during the Olympics in Los Angeles indicated that changing the emission timing could alter ozone formation. This was tested by staggering mobile source emissions by two hours, both forward and backward in time (SC06 and SC07). While moving the emissions earlier by two hours had little effect, delaying the traffic peak reduced ozone in Pasadena by 7%. This is shown in Figure 5.9. A reason for this phenomena is that a certain amount of time is required to react the organics and NO_x to form ozone. Delaying emissions reduces the amount by time for ozone formation before mid day.

5.5.6 Response of Formaldehyde and PAN to Emission Changes

Originally, there was concern that widespread use of methanol may increase ambient HCHO levels to unacceptable levels. Trajectory modeling showed that contrary to that concern formaldehyde levels changed minimally, and might even decrease. (This conclusion is supported by airshed modeling, as described in the next chapter.) Tables 5.2, 5.3 and 5.4, and Figures 5.10 through 5.12, show that HCHO levels are within a few ppb of the Base Case, and consistently below levels found predicted for 1982. Converting from the conventionally fueled, Base Case, to similar emitting methanol fueled cars decreased HCHO along all three trajectories. Relatively small increases in ambient HCHO are noted when direct emissions of formaldehyde increase. In all cases, the predicted

---

[1] As in chapter 4, "advanced" does not imply that a different, more exacting technology is assumed to exist for these simulations. Instead, all the vehicles have emissions corresponding to the in-use vehicle standard for the year 2000 (see appendices to chapter 4). Thus the technology is the same as for new vehicles in the "standard" scenarios where newer vehicles meet more stringent levels and vehicle emissions are deteriorated over time. In this case, the older vehicles are responsible for a large proportion of the mobile source emissions. Advanced technology scenarios simulate the entire fleet meeting the in-use standard, not the new car emission rate, which is seen to be significantly less than the standard. The advanced technology simulations show the long term impact of the more stringent standards, and the standard cases show the shorter term impacts as MFVs are rolled in with emission levels that lower with vehicle model year.

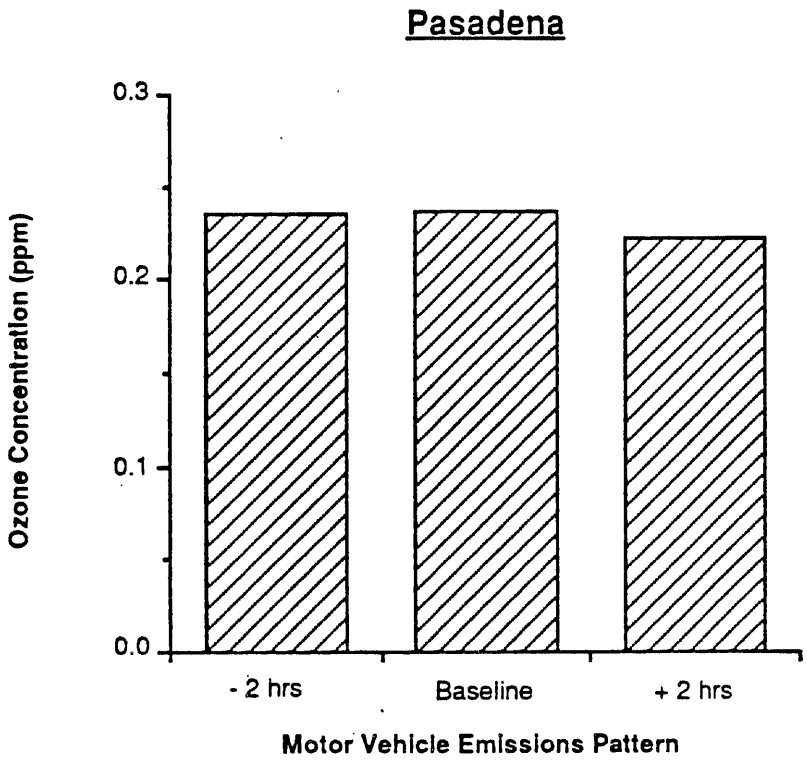

Figure 5.8 Effect of changing vehicle emission timing on ozone in Pasadena

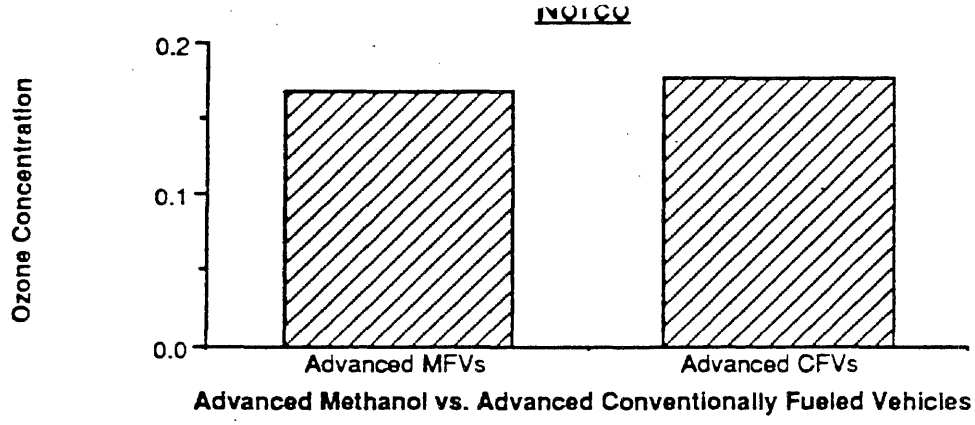

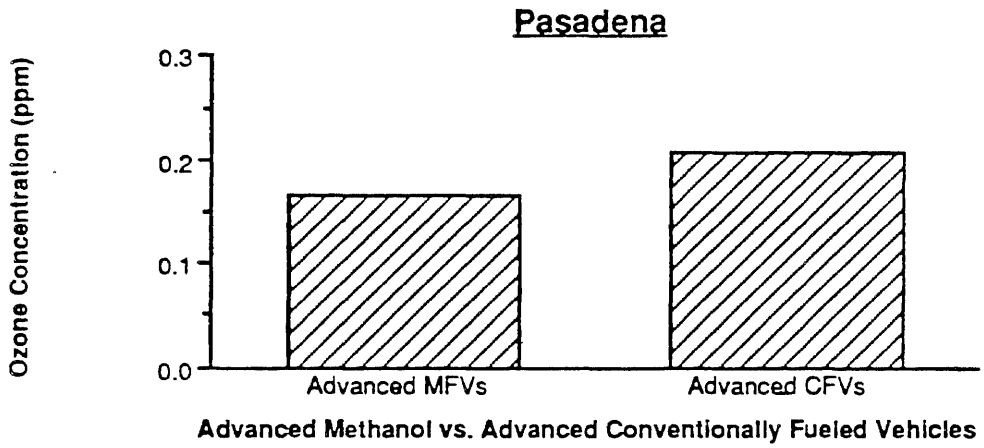

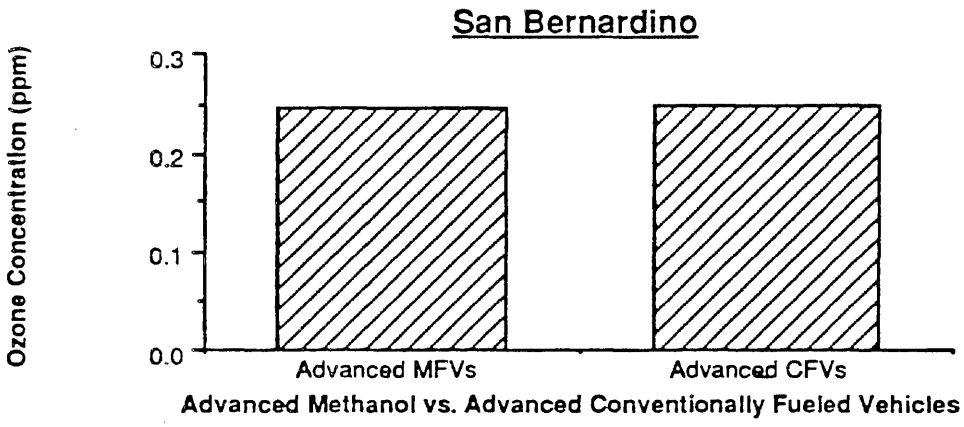

Figure 5.9 Ozone Concentration Prediction for advanced MFV and CFV Fleets

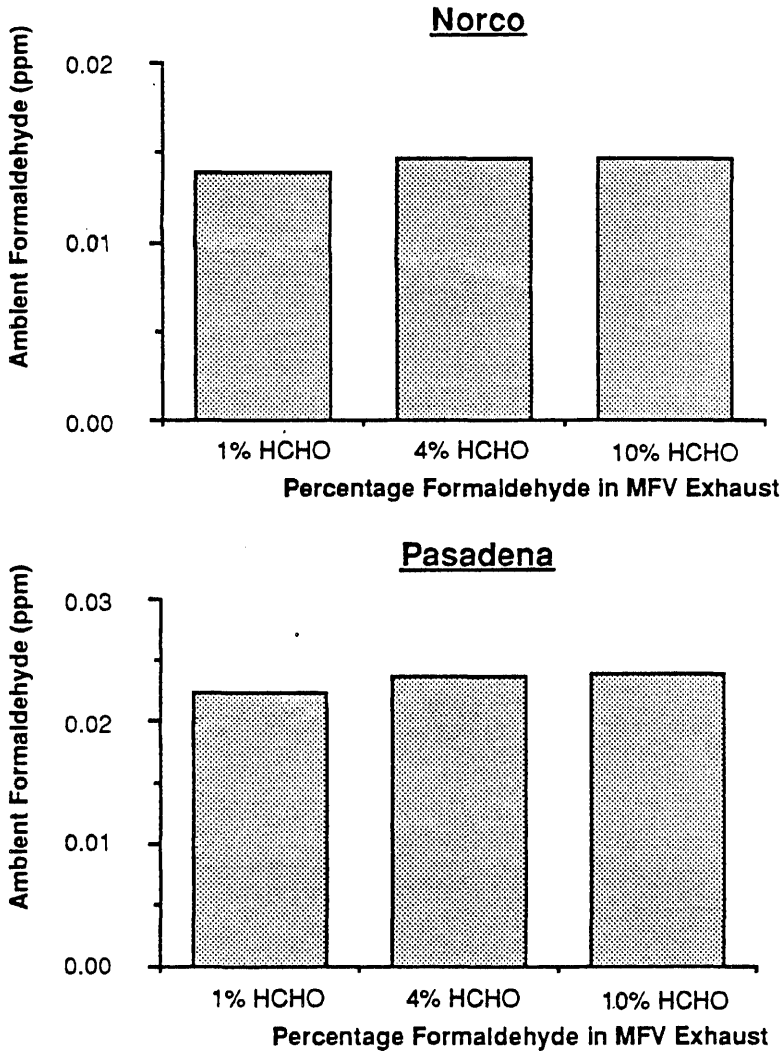

Figure 5.10 Ambient Formaldehyde Concentrations with Varying Formaldehyde Fraction of M100 MFV Exhaust

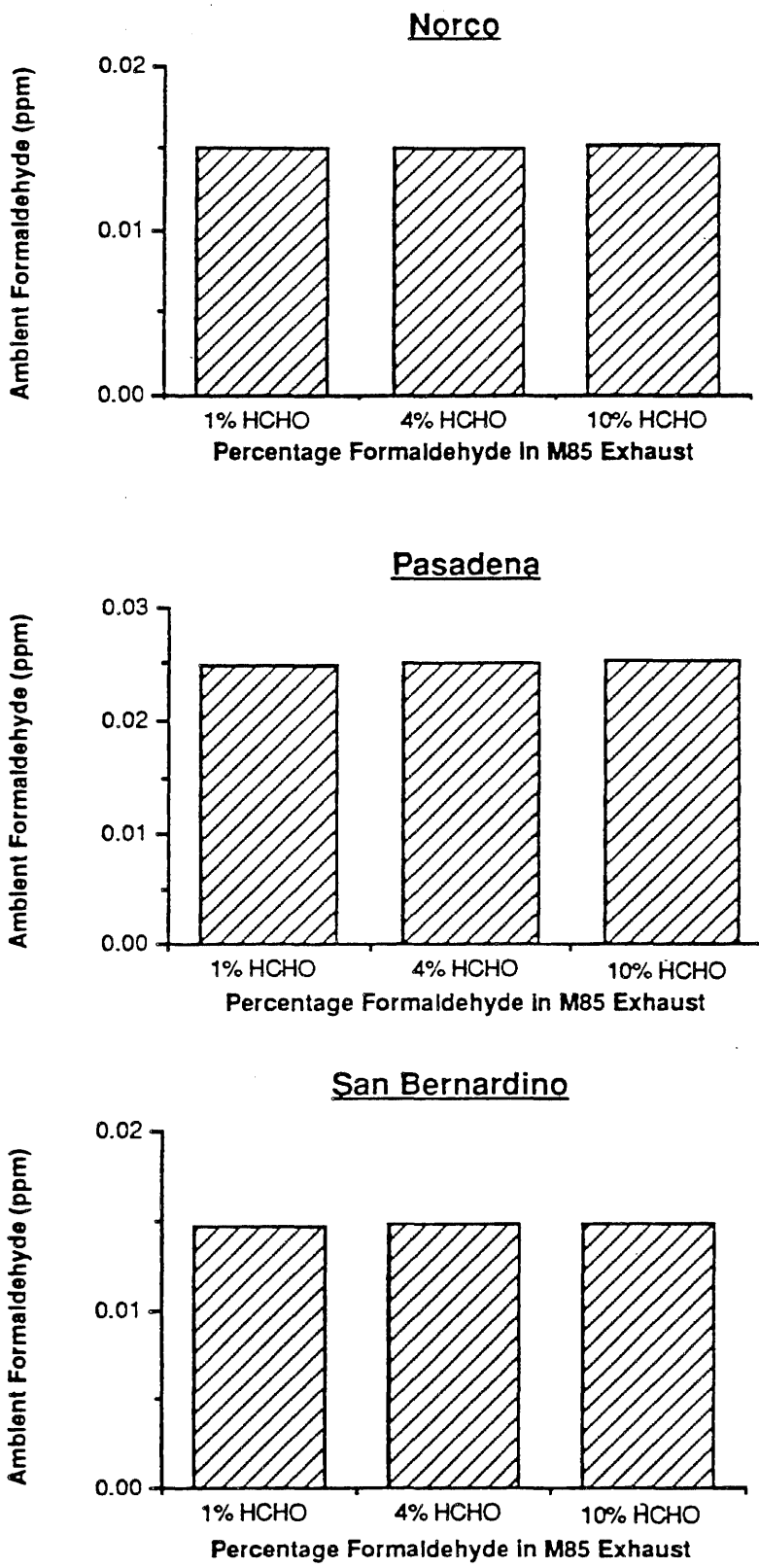

Figure 5.11 Ambient Formaldehyde Concentrations with Varying Formaldehyde Fraction of M85 MFV Exhaust

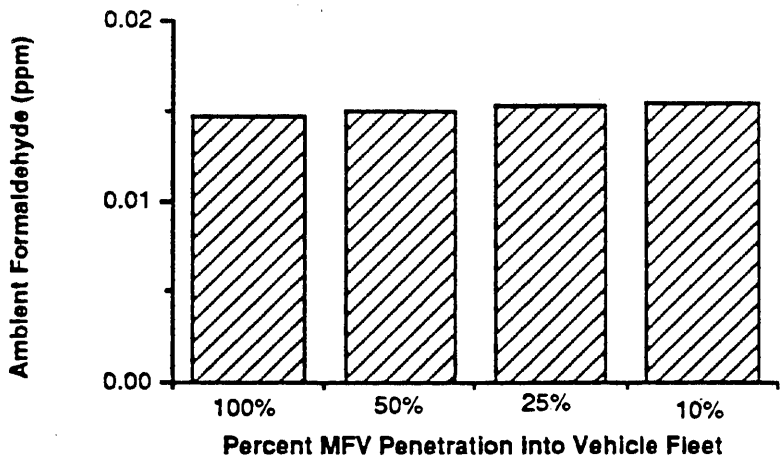

Pasadena

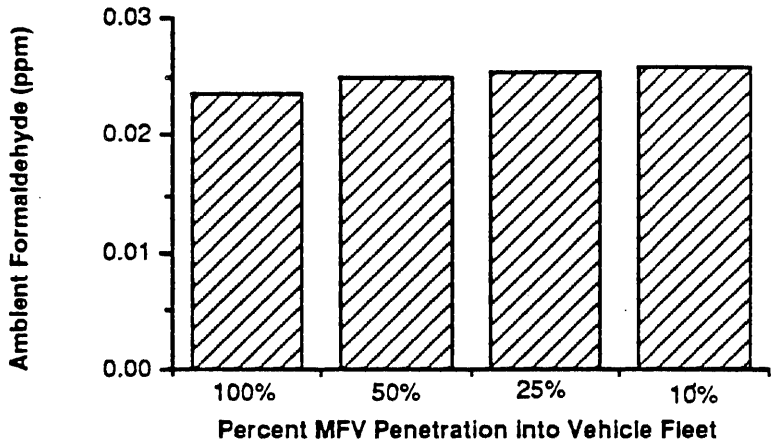

San Bernardino

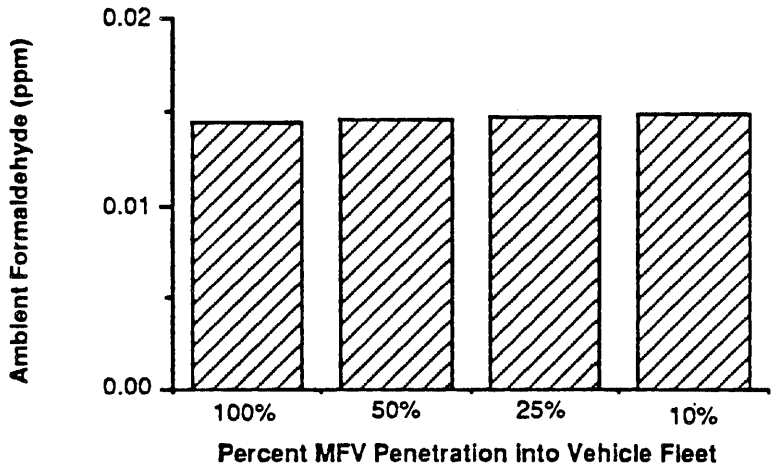

Figure 5.12 Ambient Formaldehyde Concentrations with Varying Percent of M100 MFV Penetration into the Vehicle Fleet

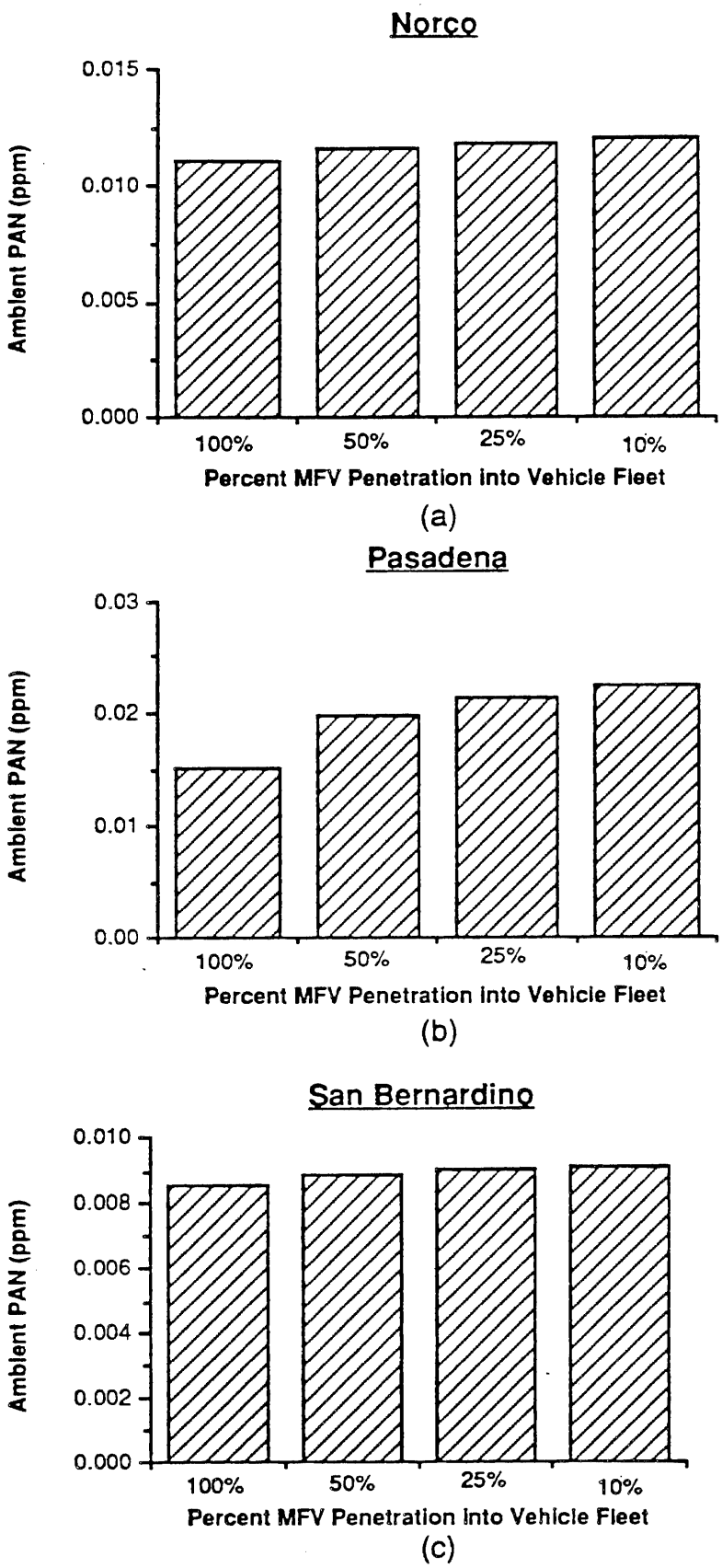

Figure 5.13 Ambient PAN Concentration with Varying Percentage of M100 MFV Penetration into the Vehicle Fleet a) Norco, b) Pasadena, and c) San Bernardino

HCHO for the Year 2000 methanol cases is less than that predicted for 1982. This indicates that an HCHO problem will not arise due to switching to methanol if direct emissions can be maintained at levels below about 10% of the ROG mass.

The reason that an increase in direct HCHO emissions does not lead to an increase in afternoon[2] ambient HCHO is that the secondary formation of HCHO is reduced. About 80-90% of the HCHO in the SoCAB atmosphere is formed by the photo-oxidation of reactive organics. Methanol reacts much more slowly to form the secondary HCHO than other components of CFV exhaust and evaporative emissions. This decrease in atmospherically produced HCHO more than offsets the increase in direct emissions.

Methanol and formaldehyde are not precursors of peroxyacetyl nitrate (PAN) formation. Switching to methanol will, as shown in Tables 5.2, 5.3 and 5.4, be reduced markedly. PAN levels at Pasadena are decreased up to about half of Base Case levels.

This analysis indicates that conversion to methanol should not increase HCHO levels, and could in fact decrease ambient concentrations. Furthermore, PAN levels should decrease markedly. These trends will be investigated further with airshed modeling.

5.6 Summary of Trajectory Modeling

Trajectory modeling, the second tier of the project, was used to further identify and quantify uncertainties, develop preliminary estimates of methanol fuel use - air quality relationships and to suggest particular calculations for further study using the grid-based airshed model. Trajectory model results also can be used to extend the results of airshed modeling, acting as a guide for interpolating and extrapolating airshed model results. The trajectory model has an advantage over the larger airshed model (the third tier), in that it is much faster computationally. However, the speed is accompanied by limitations in the model formulations. The speed makes it ideal for sensitivity analysis and preliminary investigation of air quality control impacts.

Three trajectories were identified to test the impact of methanol use in different areas of the SoCAB. Starting over the Pacific Ocean, the trajectories ended in San Bernardino, Norco and Pasadena. Calculations showed that conversion to methanol would lower ozone and PAN at all three sites, and that formaldehyde concentrations would be changed slightly. The extent of ozone reduction was highly dependent on location in the Basin.

Eastern Basin sites, i.e., Norco and San Bernardino, were found to be NO_X-limited in respect to ozone formation. In this case, ozone production is limited by the availability of NO_X rather than ROG, though methanol substitution did lower ozone. At Pasadena, the predicted ozone decreased markedly when simulating the methanol fuel use case. The extent of improvement in air quality increased more than linearly with the fraction of the vehicle fleet being replaced by MFVs. Results here indicated that the unburned methanol emissions contributed little to the predicted formation of ozone.

---

[2] Reference is made to afternoon HCHO levels because these trajectories terminate in the afternoon. Measurements show that there are two diurnal peaks, one occurring in the morning and one in the afternoon. These calculations are not appropriate for determining the impact on the morning peak. Airshed model calculations (chapter 6) and non-photochemical calculations (chapter 8) can be better used to determine the impact on the morning peak.

Sensitivity tests showed that the assumed deposition rate of HCHO does not affect ozone predictions markedly. Conversely, not including the deposition of ozone raised ozone predictions 40%. However, the relative benefits of methanol use would not be altered, just the absolute value of predictions. If ROG emissions are significantly higher than assumed for the evaluation, for example, if they are twice the inventoried amount, predicted ozone levels in the Central Basin would increase dramatically, though the downwind differences are smaller.

A test was done to see to what degree changing chemical mechanisms would change the results. Results of this test showed the same trends whether the SAPRC/ERT Mechanism were used or if the extended Caltech Mechanism was employed. Very satisfactory agreement has been found between the predictions of the two mechanisms.

Trajectory analysis suggested a number of calculations and trends to be further investigated using the airshed model. The primary result is the low sensitivity of ozone formation in the Eastern SoCAB to ROG replacement with methanol, i.e., switching to MFVs with the same NO_X emissions. Likewise, the ozone formation in the Eastern SoCAB is NO_X-limited. Similarly, ozone in the Central Basin can be reduced effectively by switching to methanol fuel use. MFV use should be compared to no mobile source emissions, no mobile source ROG, or NO_X emissions, and a fleet of more stringently controlled CFVs. The role of HCHO emissions was also found to be important. Likewise, use of methanol for reducing NO_X could be a potential strategy for reducing ozone in the Eastern SoCAB. These results suggest that methanol use would improve air quality. This will be studied further using the airshed model which has fewer limitations than the trajectory model.

6.0 Airshed Modeling of Ozone, PAN and Formaldehyde

6.1 Introduction

The third tier of the photochemical modeling portion of this study was the application of the grid-based, Eulerian airshed model to determine the response of air pollutants to widespread use of methanol. The grid model has a number of distinct advantages over the models employed in the first two tiers. Most importantly, the formulation of the airshed model has minimal limitations. It is the most complete description of atmospheric physics and chemistry available for studying the dynamics of pollutants in an urban basin. A second advantage of the airshed model over the trajectory model is that it provides the basin-wide air quality impacts resulting from control strategy implementation. The primary disadvantage is the greatly increased computer time required to test a single strategy, limiting the number of simulations possible. This disadvantage has been circumvented by using the three-tiered approach, and a complete picture of the impact of methanol use is developed using the available resources most advantageously.

Thirty-six airshed calculations were conducted for the three day modeling period. First, the model's ability to accurately simulate an actual smog event was demonstrated. Three calculations showed how air quality will evolve between the 1982 evaluation period and the future modeling years, 2000 and 2010. These base cases do not consider the use of alternative fuels or extraordinary emission controls. The next eleven scenarios investigated the models sensitivity to specification of the initial and boundary conditions. The remaining 22 scenarios simulated the impact that various controls would have on air quality in the years 2000 and 2010 corresponding to conversion to methanol fuel and more stringent conventional controls. These scenarios cover the range of likely emission levels and establish bounds on likely air quality levels.

The airshed model calculates the concentrations of photochemically active pollutants throughout the basin. This chapter focuses primarily on ozone, formaldehyde, NO_2 and PAN changes resulting from emission controls. (Aerosol nitrate concentrations, also calculated by the airshed model, are discussed in the next chapter.) The model results can be used to determine peak concentrations, the exposure of an area over a certain pollutant level, the spatial and temporal duration above that level and population exposure measures.

First, a brief description of the airshed model is presented along with the basic equations solved. This is followed by a section describing evaluation of the model performance. Next, the base case predictions of the air quality in the years 2000 and 2010 are described, followed by diagnostic calculations. Then, the series of emissions scenarios are characterized that will be used to evaluate the effectiveness of methanol to reduce photochemical smog. These scenarios cover the impact in the years 2000 and 2010. Predicted ozone, formaldehyde, PAN, NO_2, and HNO_3 levels are presented in the results section. Finally a discussion on the significance of these results is presented in the concluding section.

6.2 Airshed Model Description

The CIT (Carnegie/California Institute of Technology) airshed model used in this study is a descendent of the "Caltech" model (McRae et al. 1982,1983) and solves the

reaction-diffusion-advection (RDA) equation in an Eulerian, or control volume, reference frame. This equation describes the transport, diffusion, reaction and emission of compounds in the atmosphere. The general form of the RDA, in an Eulerian frame and for a pollutant species i with mean ensemble concentration $\langle c_i(x,t)\rangle$, is (Seinfeld, 1975):

$$\frac{\partial \langle c_i \rangle}{\partial t} + \nabla \cdot (\mathbf{u} \langle c_i \rangle) = \nabla \cdot (K \nabla \langle c_i \rangle) + R_i(\langle c_1 \rangle, \langle c_2 \rangle, \ldots, \langle c_n \rangle) + S_i(\langle c_i \rangle) \qquad (6.1)$$

subject to the initial conditions:

$$\langle c_i(\mathbf{x},0) \rangle = \langle c_i^0(\mathbf{x}) \rangle \qquad (6.2)$$

and boundary conditions, at the top of the modeling region (z=H) :

$$(K_{zz} \frac{\partial \langle c_i \rangle}{\partial t}) = 0 \qquad (6.3)$$

and at ground level (z=0):

$$\left[v_g^i \langle c_i \rangle - K_{zz} \frac{\partial \langle c_i \rangle}{\partial t} \right] = E_i \qquad (6.4)$$

where **u** is the wind velocity vector, **x** is the location vector, K is the atmospheric diffusivity tensor, R_i is the production of species i by chemical reaction, S_i is the upper level source rate of species i by direct emission, v_g^i is the deposition velocity of species i to the surface and E_i is the ground level emissions of species i. $\partial \langle c_i \rangle / \partial t$ is the rate of change of the concentration of species i with respect to time. The top boundary condition implies no vertical transport or diffusion through the top of the modeling region, as discussed in Chapter 5. The bottom boundary condition is a mass balance, stating that the net flux into the atmosphere is the difference of emissions into the atmosphere and deposition from the atmosphere. Boundary conditions along the horizontal boundary, Ω, $c_i^b(\Omega,t)$ are derived from the measured concentrations and vary throughout the modeling period. Initial conditions are as measured at the beginning of the 1982 episode.

Except for the diagnostic scenarios, all scenarios use the same initial conditions and side and top boundary conditions as are used in the model evaluation described below. The only difference between control scenarios are the emissions into the atmosphere, both from ground level and elevated sources. This is done so that the observed changes in pollutant concentrations are solely a function of basin-wide emissions, and not by re-specification of boundary and initial conditions. Separate calculations demonstrate the dependence on initial and boundary conditions.

6.3 Model Performance Evaluation

In previous studies, earlier versions of the CIT Airshed Model accurately predicted dynamics of ozone and NO_2 throughout the SoCAB (McRae and Seinfeld, 1983; Russell et al, 1988). Additional measurements were available for trace, nitrogen-containing pollutants for the evaluation described in Russell et al. (1988), including PAN, HNO_3 and aerosol nitrate levels. The model has undergone significant improvements since these studies. First, the chemical mechanism has been updated and methanol specific reactions have been included. Reaction rates reflect the conclusions of recent studies by Atkinson and Lloyd (1984), Carter et al. (1986ab) and Baulch et al. (1984). Photolytic rates are as specified by Carter et al. (1986b). The airshed model now uses spatially and temporally varying cloud cover, temperature and relative humidity when calculating reaction rates on a grid-by-grid basis. Additionally, photolytic rates are now calculated at the average elevation of the air mass, rather than at sea level.

In the previous evaluation of the model using data from the August 30-31, 1982 episode, predictions were compared against observations for those two days. This study has extended the modeling period to include the following day, September 1. Reasons for choosing this period are detailed in Chapter 4. Because of the increased time period, model enhancements and enlarged modeling region (see Figure 6.1), model performance was re-evaluated. However, the non-routine measurements of trace nitrogen-containing compounds was not continued to September 1, so only the model's ability to predict O_3 and NO_2 is analyzed for the three day period. Generally, performance measures improved: normalized bias and error in the ozone and NO_x predictions decreased. The models ability to track the evolution of the trace nitrogen-containing pollutants, such as nitric acid, PAN, aerosol nitrate and ammonia can be found in Russell et al. (1988), and are briefly described here for completeness.

Initial conditions for the model evaluation are the pollutant concentrations as measured at 0:00 August 30, 1982 and are detailed in Russell and Cass (1986). Horizontal boundary conditions were split into upper and lower level concentrations. The mixing height divides the upper and lower levels. Lower level boundary conditions come from field data of ground level pollutant concentrations, as measured over the three day period, and upper level concentrations come from measurements during a separate study (Blumenthal, 1988). A more detailed discussion of the specific data, their sources and preprocessing procedures used appears in Russell et al. (1988).

A summary of the model performance statistics for ozone and NO_2 is shown in Table 6.1. Representative plots of predicted and observed ozone are shown in Figures 6.2ab. (This evaluation was conducted by the staff of the Technical Services Division (TSD) of CARB. Their assistance in conducting the analysis and plotting the results is greatly appreciated.) The performance for predicting ozone is similar to, or better than previous model applications in the SoCAB (Wagner and Ranzieri, 1984; Wagner, 1984; Seinfeld, 1988). A previous multiday modeling study of a 1974 ozone episode in the SoCAB, performed by Caltech, had a bias of 3.4%. A study of the same period by SAI had a bias of 7.2%. Both are substantially higher than this study's 0.9%. The normalized error was 0.411 for the previous SAI study, 0.34 for the Caltech study and 0.368 for this study. Peak ratios were 0.7 for the SAI study, 0.8 for the Caltech study and 0.93 for this

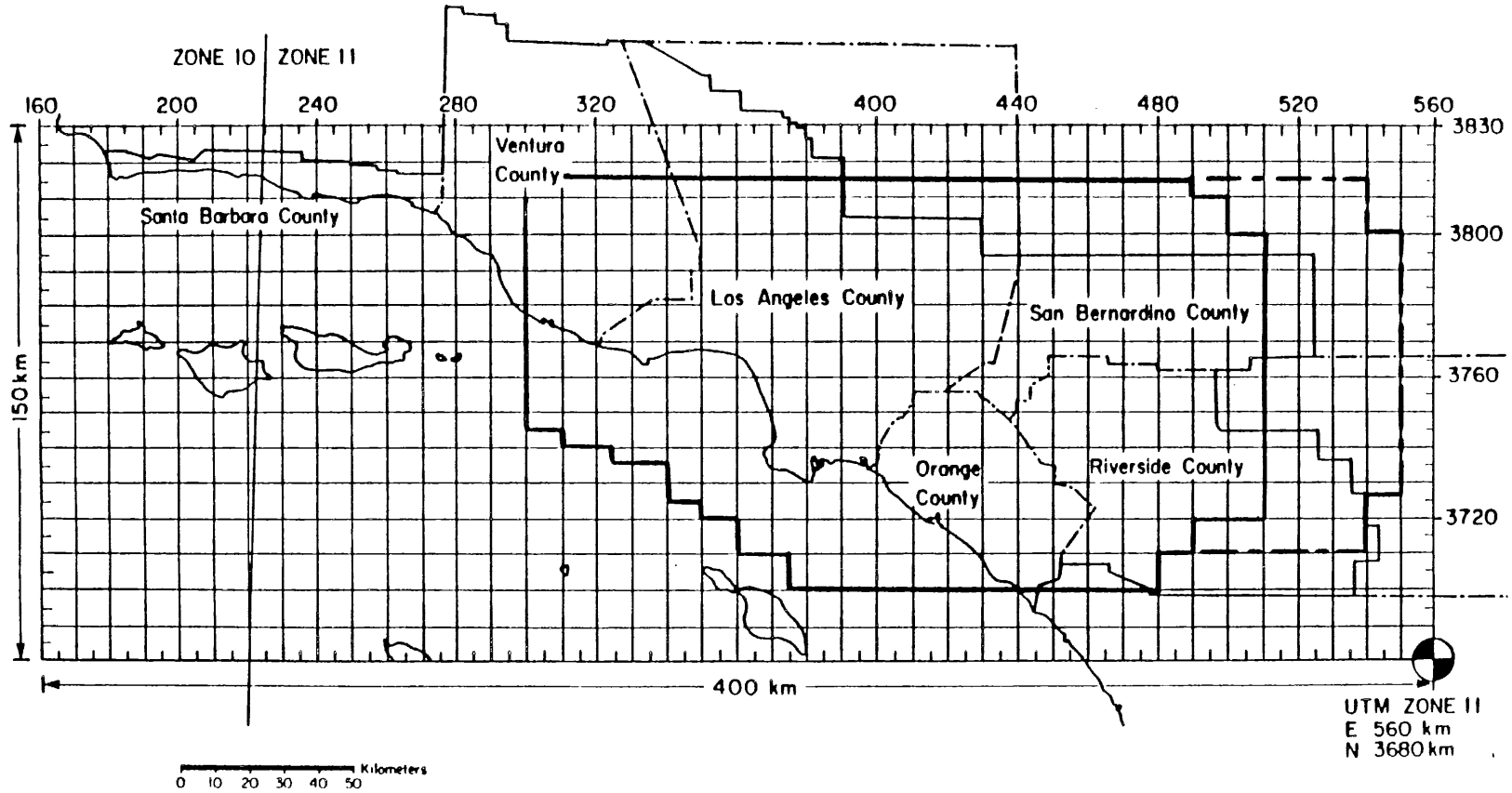

Figure 6.1 Gridded map of California's South Coast Air Basin (SoCAB), showing the region used for airshed modeling. The modeling region used for year 2000 calculations is outlined by the heavy, solid line (———). The expanded region in the eastern basin used for year 2010 calculations is shown with a heavy, intermittent line (— — —). The fine, solid line marks the boundary of the SoCAB.

Table 6.1 Statistical Evaluation of Model Performance, Aug 30-Sept 1, 1982

	Ozone	NO2
Normaliazed Bias	-0.90%	9%
Normalized Absolute Bias	0.37	0.35
Regression:		
Slope	0.75	0.46
Intercept	0.02 ppm	0.02 ppm
Correlation (r)	0.81	0.64
Average Error	37%	35%
Peak Ratio	0.84	1.3
Average Peak Ratio	0.79	0.91

*Performance over the two day period, August 30-31, 1982 for ozone, NO2, total nitrate, HNO3, aerosol nitrate and NH3 is contained in Russell et al. (1988)

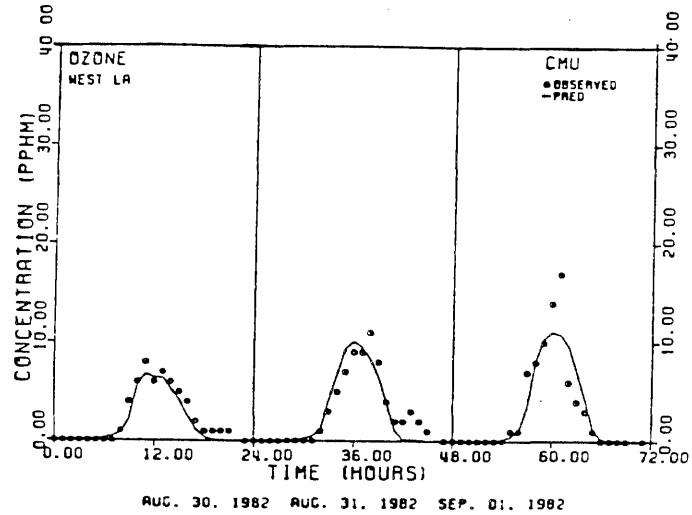

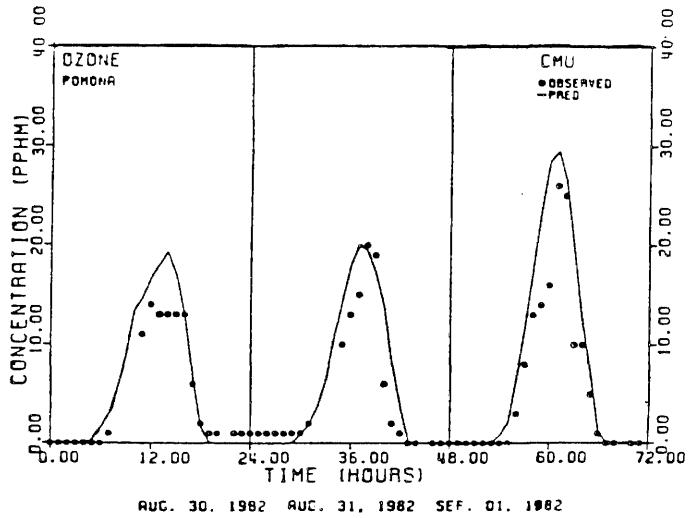

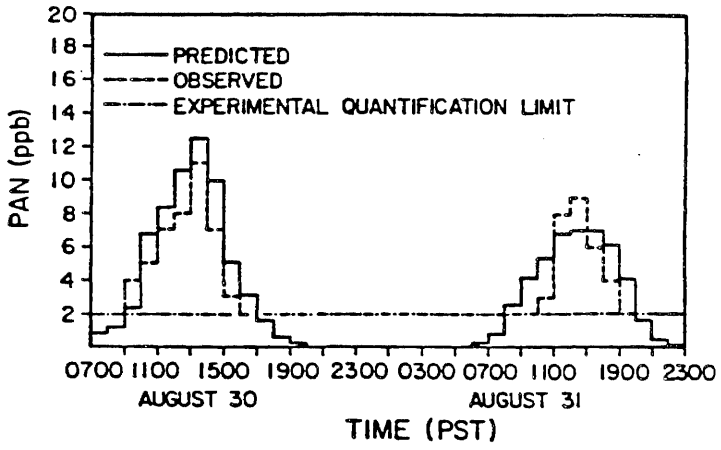

Figure 6.2 Comparison of predicted and observed ozone (a,b) and PAN (c) concentrations versus time for the 1982 period. (a) Ozone at West Los Angeles (b) Ozone at Pomona (c) PAN at Pasadena (for the first two days only).

study. The peak predicted ozone was 0.327 ppm, compared to the observed 0.35 ppm. The improvement in performance for NO_2 prediction is similar.

An extensive field experiment was conducted during the first two days of the three day modeling period. In addition to routine measurements of ozone, NO_2, CO and organics, trace species such as gaseous HNO_3, NH_3, PAN, aerosol ammonium, aerosol nitrate and aerosol sulfate concentrations were monitored (Russell and Cass, 1984). A comparison of the model results with these measurements is contained in Russell et al. (1988). That study represented the first time an airshed model was successfully employed to simulate the dynamics of these trace species. As an example of the agreement, predicted and observed PAN levels are shown in Figure 6.2c. PAN is an excellent species for testing model performance because it is very sensitive to radical production and NO_2 concentrations. As with ozone and NO_2, the agreement between predicted and observed PAN concentrations is very good. Predicted and observed nitrate and nitric acid for a variety of locations in the SoCAB is shown in Figure 6.3ab. The absolute difference is small.

Formaldehyde concentrations were not measured during the three day modeling period. A later measurement program (Lawson et al., 1988) monitored HCHO at Glendora during a period with slightly lower photochemical reactivity. During this field study, formaldehyde concentrations were found to be just below those predicted for the 1982 episode evaluation. The direction of the difference is expected given the decreased photochemical activity and lower emissions corresponding to the later measurement period. In general, the peak concentrations and timing of the model predictions and observations were very similar.

Very good agreement was found between the observed and predicted ozone, NO_2 and trace species such as HNO_3, NH_3, aerosol nitrate, HCHO and PAN. Performance criteria, such as ozone and NO_2 prediction bias and error, were comparable or better than similar studies of the SoCAB. Especially encouraging is the agreement between the measured and predicted concentrations of the trace, nitrogen-containing compounds such as inorganic nitrate, PAN and ammonia, as well as HCHO. The agreement is unique to this model, and demonstrates that the model is suitable for testing control strategies.

6.4 Description of Airshed Model Calculations for Future Years

Airshed model calculations of 3 baseline, 22 control strategy and 10 diagnostic scenarios were conducted to develop, quantitatively, the relationship between air quality, emissions and fuel type use in the years 2000 and 2010. These scenarios are listed in Tables 6.2abc and described in more detail below. Three runs are used to predict the baseline air quality corresponding to forecast emissions. Of the twenty-two control strategy scenarios, six consider continued full use of conventional fuels at different emissions levels for the two future years. Ten scenarios investigate the use of methanol fuel in on-road and, in some cases, off-road vehicles. Another scenario considers additional methanol fuel usage in certain stationary sources. Five scenarios repeat above scenarios but remove either all or some component of the mobile source pollutants (e.g. NO_x , CH_4O and/or ROG emissions) from mobile or stationary sources. This is done to determine how air quality responds to specific emissions and also to set upper bounds in

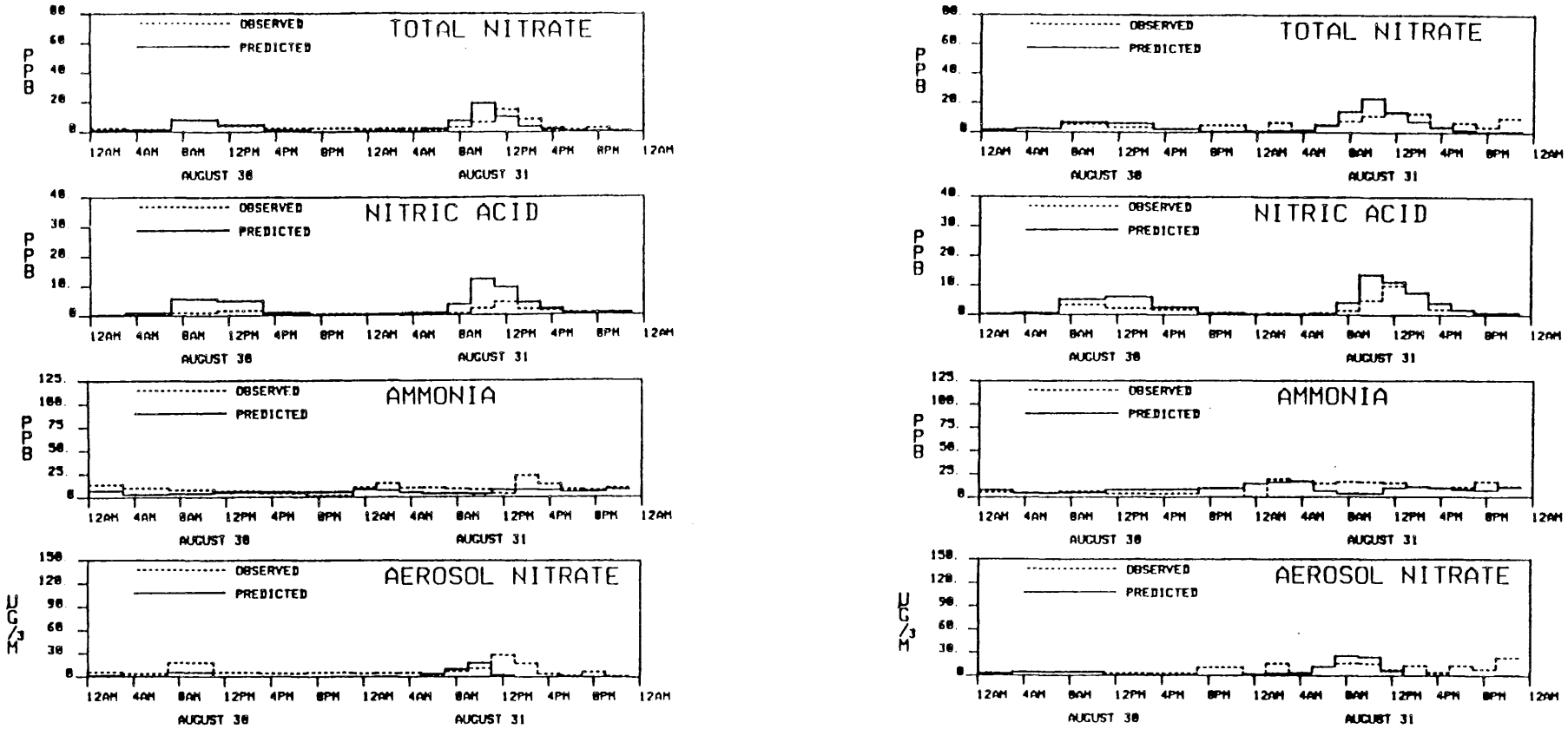

Figure 6.3 Comparison of predicted and observed concentrations of total nitrate, HNO_3, aerosol nitrate, and NH_3 on 30-31 August 1982. (a) Central Los Angeles (b) Anaheim.

Table 6.2a List of Emissions Scenarios, Year 2000

Scenario Name	Scenario Description*
BASE1A	Original projected year 2000 emissions inventory. (4.A-1)
BASE1	Base case emissions. Mobile emissions reduced from those in EMFAC7C Appendices. (4.A)
NO MOBILE	Base case emissions (BASE1) minus emissions from: petroleum refining operations, retail gasoline and diesel distribution, all on-road sources except motorcycles as well as mobile off-road farm equipment, construction equipment, locomotives, utility vehicles, and recreational vehicles except motorcycles.
ADV CONV	Full penetration of low emitting CFVs into on-road mobile sources. All others as per BASE1. These vehicles have emissions matching in-use for year 2000.(4.C)
ADV METH	Full penetration of low emitting MFVs into on-road mobile sources. Convertible off-road mobile sources (NO MOBILE) also switched to methanol fuel. Gasoline retailing converted to methanol. (4.D)
STD M100	100% penetration of MFVs into on road mobile sources from 1990 to 2000. Similar conversion for off-road mobile sources and retail gasoline operations as described in ADV METH. HCHO emissions from LDVs 15-27 mg/mi
FULL METH	Same as ADV METH plus conversion to methanol of utility boilers, stationary industrial IC Engines, and non--refinery industrial boilers.
BASE-ROG	Same as BASE1 minus ROG emissions of all sources listed in NO MOBILE.
BASE-NOx	Same as BASE1 minus NOx emissions of all sources listed in NO MOBILE. (4.A)
STD M85	Same as STD M100 except fuel used is M85 instead of M100.
METH 50	Same as STD M100 except only 50% penetration of on-road mobile sources from 1990 to 2000.
HIGH FORM	Same as STD M100 except nominal HCHO emissions are increased from 15 mg/mi to 55 mg/mi. (4.B)
ADV METH/NO ROG	Same as ADV METH minus methanol and HCHO emissions of all sources converted to methanol. (4.D)

*Letters in parentheses refer to Appendices describing emissions factors or emissions reductions.

Table 6.2b List of Emissions Scenarios, Year 2010

Scenario Name	Scenario Description
BASE 2010	Original projected year 2010 inventory.
ADV CONV 2010	Full penetration of low emitting CFVs into on-road mobile source's. See Appendix 4.C for emissions. (e. g. LDA 0.25 g/mi ROG, 0.2 g/mi NOx.) Other sources unperturbed.
ADV METH 2010	Full penetration of low emitting M100 MFVs into vehicle fleet. MFVs meet proposed year 2000 standard. Other sources unperturbed.(4.D)
STD M100 2010	100% penetration of standard technology M100 vehicles into light and medium duty vehicle fleet from 1990 on. Methanol emissions, on a carbon mass, set to same rate as used for CFVs in the base case. HCHO emissions from LDAs set to 15-23 mg/mi. Service station emissions adjusted; refinery, heavy, and medium duty vehicle emissions unaltered. (4.C)
STD M85 2010	Same as STD M100 2010, except that M85 vehicles are used. Exhaust emissions assumed to be 50% methanol, 50% gasoline components, with HCHO emissions at 15-23 mg/mi. (4.E)
NO MOBILE 2010	On-road mobile source emissions removed from base 2010 inventory.
NO MOBILE ROG 2010	BASE 2010 calculation with the ROG fraction of on-road emissions removed.
ADV LMD 2010	Advanced conventionally fueled vehicles, except heavy duty vehicle emissions are unaltered. (4.C)
ADV LMD NO ROG 2010	Similar as above, except ROG component of light and medium duty vehicles is removed. All other sources unaffected.
ADV CONV/LO IC 2010	Similar to ADV CONV 2010, except that initial and boundary conditions were lowered to clean background levels.
ADV METH/LO IC 2010	Similar to ADV METH 2010, except that initial and boundary conditions were set to clean, background levels.
M85 LO IC 2010	Similar to STD M85 2010, except that initial conditions and boundary conditions were set to clean, background levels.

	Table 6.2c Evaluative and Diagnostic Calculations
Scenario Name	Scenario Description
1982	Simulation using base 1982 emissions used for performance evaluation.
Year 2000	
LO IC	Low initial conditions - BASE1 calculation except initial conditions set to background values, all other inputs unaltered.
NO EM	No emissions - BASE1 calculation with emission inputs removed, all other inputs left unaltered.
NO EM/LO IC	BASE1 calculation with emission inputs removed, and initial conditions set to background levels.
NO ROG	BASE1 calculation with ROG and CO emissions removed from year 2000 inputs, NOx emisisons unaltered, all other inputs remain the same.
NO ROG/LO IC	BASE1 calculation with ROG and CO emissions removed, and initial conditions set to background values. All other inputs unaltered.
2000X	BASE1 calculation with expanded modeling region.
Year 2010	
NO ROG/LO IC 2010	Same as NO ROG/LO IC above, except that the 2010 inventory is used at the base.
LO IC 2010	Same as LO IC above, except that the base inventory is for 2010.
CLEAN BC 2010	Boundary conditions over Pacific Ocean set to very clean conditions. All other inputs unaltered.
LO BC/LO IC 2010	BASE 2010 conditions with initial conditions and western boundaries set to clean levels.

possible air quality benefits of methanol fuel utilization. Diagnostic calculations investigated the model's sensitivity to initial conditions, boundary conditions, and emissions. First the base inventories for the tests are briefly described. A detailed discussion of the baseline emissions estimates and treatment of emissions for control calculations is contained in Chapter 4. Emissions for the different scenarios vary widely, as shown in Figure 6.4.

6.4.1 Base Case Calculations for the Years 2000 and 2010

First, the airshed model was employed to provide an estimate of the baseline air quality in the years 2000 and 2010. These calculations use the best estimate of future emissions in the absence of alternative fuel use. Two base cases were used for the year 2000 because an improved inventory became available during the course of this project. **BASE1A** represents the initial emissions projections of basin-wide emissions. Emissions data used in this scenario come from the inventory for the SoCAB, as forecast by CARB in 1986 (Allen, 1986; Avlani, 1986), and were those used in the trajectory modeling described in Chapter 5. Emission factors for on-road vehicles are listed in appendix 4.A1 Emissions totals are contained in Table 6.3. This case uses only conventional fuels and controls. **BASE1** is the same as **BASE1A**, except that on-road mobile source emissions have been updated to reflect expected, more stringent, regulatory action (appendix 4.A). This reflects the belief that on-road emissions in future years will be lower than previously projected (EMFAC7D emissions factors as opposed to EMFAC7C). The total emissions for **BASE1** are given in Table 6.3, showing a 5% reduction in NMOG and NO_x emissions. **BASE1** is used as the baseline emissions scenario for the year 2000 diagnostic and control calculations.

Similarly, the best estimate of future emissions for the year 2010 was used to predict the air quality that would occur during a similar meteorological episode at that later date. These emissions estimates correspond to those being used in the SCAQMD's Air Quality Management Plan under development at this time. Total emissions within the modeling grid are given in Table 6.3. This base case calculation is referred to as **BASE 2010**, and serves as the baseline for the corresponding diagnostic tests and control evaluations.

6.4.2 Diagnostic Calculations

Any major air quality modeling effort should include tests of how the inputs affect predictions. Airshed model predictions can be sensitive to initial and boundary conditions, as well as emissions and reaction rates (McRae et al. 1982; Carmichael et al. 1988; Seigneur et al. 1987). A series of nine diagnostic calculations were conducted to determine to what degree the results depend on the specification of initial and boundary conditions. These are listed in Table 6.2c. The need for this exercise is that the boundary and initial conditions used in the evaluation correspond to the emission pattern in 1982, and would change as emission patterns evolve between then and the years 2000 and 2010. To what degree they would change is unknown *a priori*, and to evaluate the effect of emission controls it is necessary to develop a defensible method for treating boundary and initial conditions. Two methods are possible. One is to develop an algorithm for altering initial

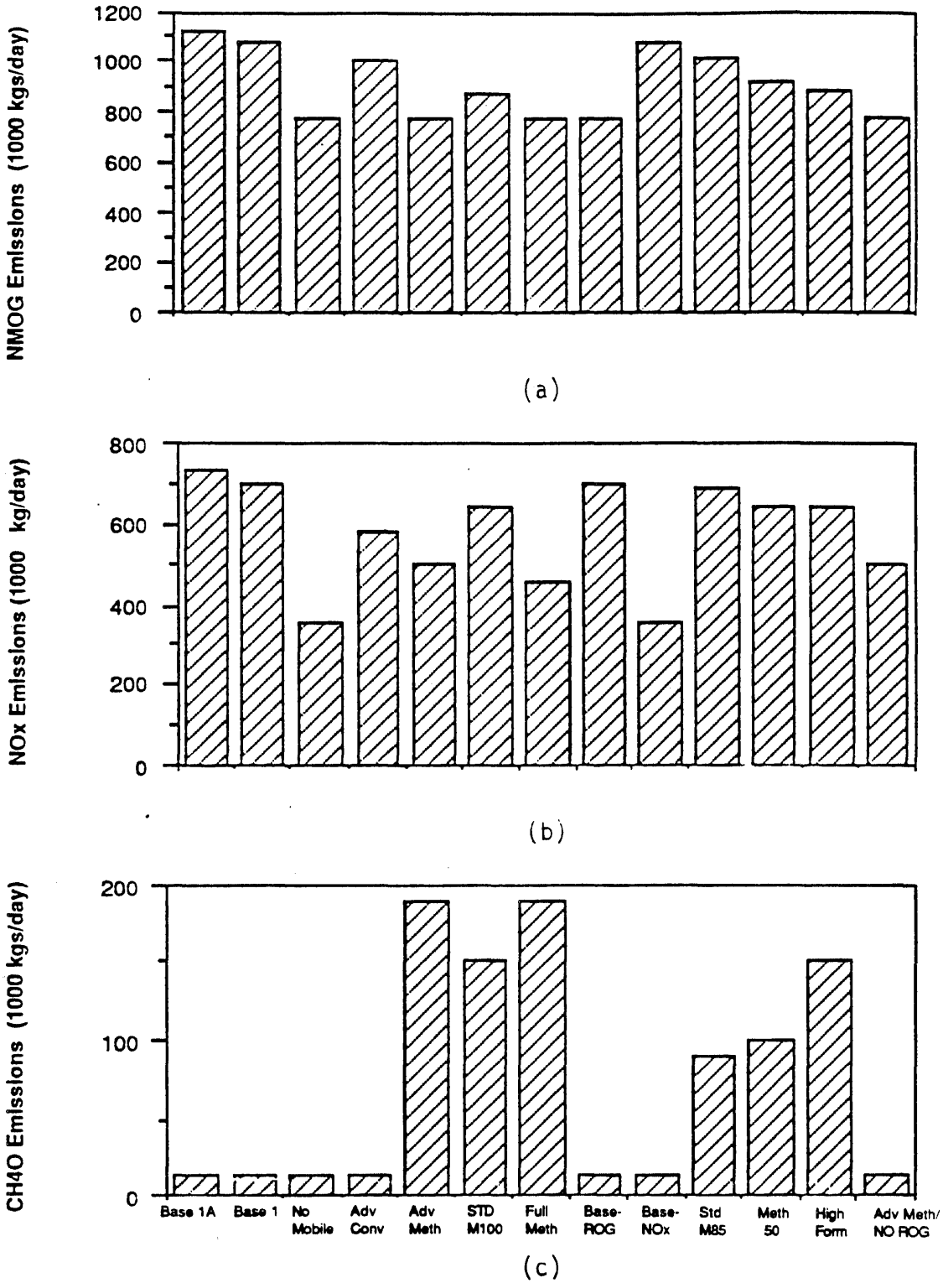

Figure 6.4a Emissions of pollutants for the year 2000 (in Kgs/day)
a) NMOG, b) NOx, and c) CH4O emissions (in grams C)

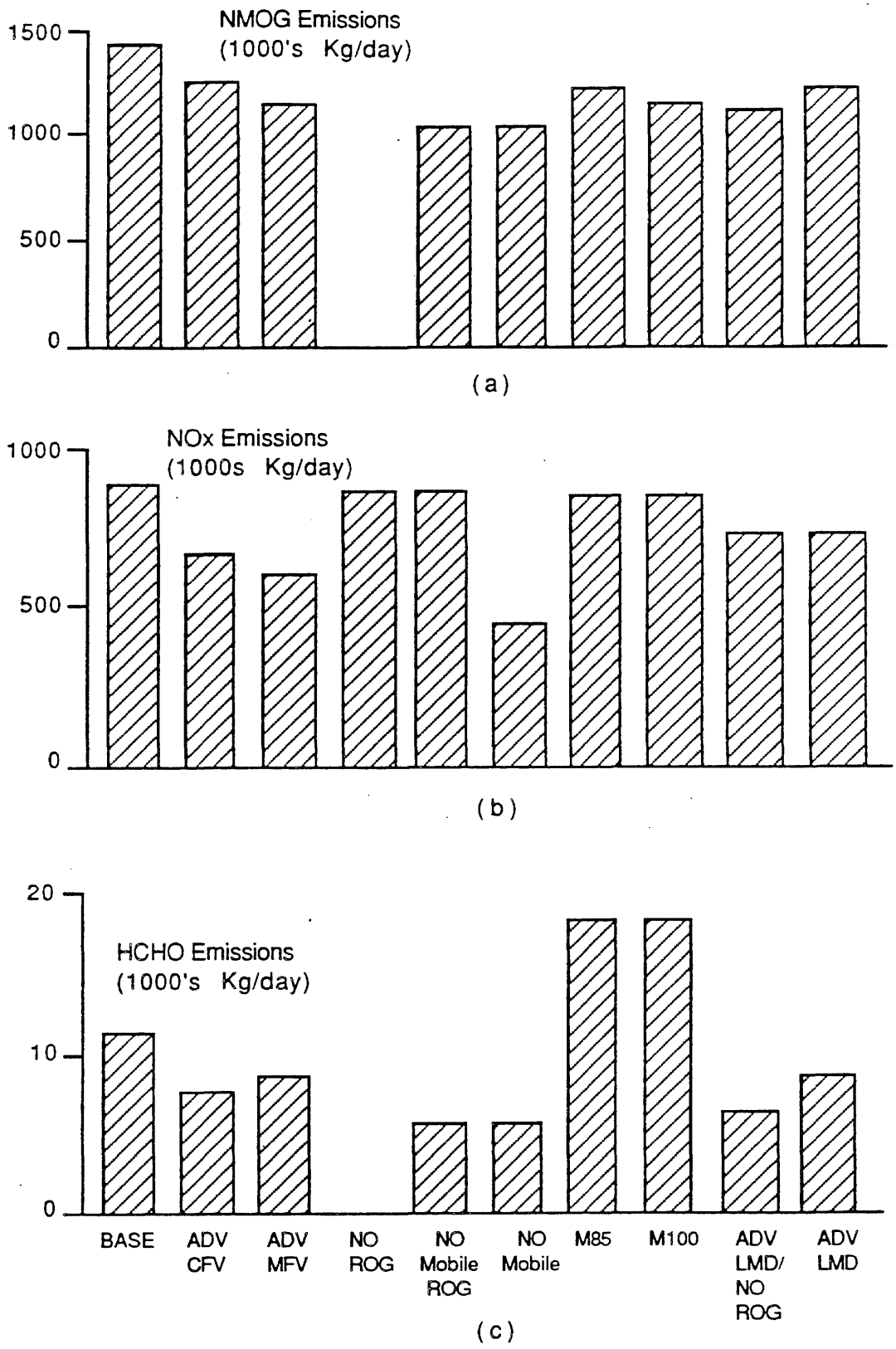

Figure 6.4b Emissions of pollutants for the year 2010 in 1000's Kg/day. a) NMOG, b) NOx, and c) HCHO.

Table 6.3 Emissions of NOx and TOG (1000 kg/day) [1]

	NOx	TOG	
BASE1			
ON-ROAD	283	251	
OFF-ROAD	67	27	
STATIONARY	350	1517	2
TOTAL	700	1795	
BASE1A			
ON-ROAD	327	311	
OFF-ROAD	67	27	
STATIONARY	350	1517	2
TOTAL	744	1855	
BASE 2010			
ON-ROAD	430	405	
STATIONARY & OFF-ROAD	436	1607	2
TOTAL	866	2012	

1 Includes emissions in SoCAB and surrounding basins in modeling region.

2 Approximately half of the stationary TOG is from landfill and other waste oriented operations, of which the primary emission is methane, and hence non-reactive for the purpose of urban photochemical modeling.

and boundary conditions in response to changing emissions. However, the system response is highly non-linear and this method can lead to artificially biasing the results to an unknown degree, and is open to criticism. This has been the problem with one day simulations when the initial and boundary conditions were assumed to respond linearly.

The second, more credible, tack is to elucidate the dependence of the calculations on initial and boundary value specification. Analysis of the control strategy calculations then account for this dependence. While the results need not, and should not, be totally independent, the role of boundary and initial conditions should be minimized and physically reasonable. This is the approach chosen in this study.

Reducing the effect of initial conditions is accomplished by starting the modeling period at a time with relatively low pollutant concentrations, and using multiple day calculations. However, as the modeling period increases, boundary conditions become more important. A period of three days was chosen as an optimal compromise. It should be noted that the calculations should not be absolutely independent of boundary conditions because pollutants, especially organics, are transported into the region. In the case of the SoCAB, inflow over the northern and the over land portions of the western boundary are responsible for non-negligible transport of organics into the basin.

Likewise, the results may depend on initial conditions. Even after two and one half days (from the start of the simulation to the time of the ozone peak on the third day), the pollutants originally in the basin have not totally dissipated, nor have they been transported out of the region. Trajectory analysis for the three day period being modeled showed that a portion of the initial pollutant cloud would still be in the eastern basin. Thus, even if the emissions input during the three day simulation are removed, one would not expect the pollutant concentrations to drop to background levels. In this case, the initial conditions represent the pollutants derived from emissions prior to the episode and will lead to further pollutant formation. The following tests were designed to elucidate the dependence of the airshed model on initial and boundary conditions.

Three tests are used to quantify the effects of initial conditions. First, **LO IC** is similar to the year 2000 base case (**BASE1**), except that the initial pollutant concentrations were reduced to background levels (0.04 ppm O_3, 0.0 ppm NO_x, 0.02 ppmC THC, or approximately 0.01 ppmC ROG). A similar calculation was repeated for the 2010 period, and is called **LO IC 2010**. A second test is to remove emissions without changing the initial conditions, called **NO EM**. The first test provides an estimate of the degree that initial condition specification effects predictions under normal emission conditions and the second shows the maximum effect when no emissions are present. Together, they can be used to map out the spatial pattern of how initial conditions will impact calculations across the range of emissions levels.

As the length of the modeling period is increased to minimize the role of initial conditions, the impact of boundary conditions increases. In the previous study of methanol use in Philadelphia (Whitten et al., 1987), boundary condition infiltration overwhelmed the role of emissions, making it impossible to deduce source-air quality relationships. This study has minimized the dependence on boundary conditions over the urban and suburban regions of the basin by setting the edge of the modeling region well away from the more densely populated areas, and, when possible, out over the Pacific Ocean. The atmosphere

over the Pacific Ocean has generally low pollutant concentrations, and is an advantageous boundary for that reason.

Five calculations were conducted to map the impacts of the boundary conditions on the calculations. A first calculation, **NO EM/LO IC**, showed the effect of removing emissions and lowering the initial conditions to background values. A second test of boundary condition impact is to eliminate the ROG emissions and retain the NO_x emissions. This was done with and without the base case initial conditions in cases **NO ROG** and **NO ROG/LO IC**, respectively. This tests the importance of the ROG flux across the boundary. These two runs can be compared with the base case (**BASE1**) and **LO IC** calculations. Setting the upper level boundary conditions for O_3, THC (or total organics), and NO_x to low, or clean ocean, levels, i.e. 0.04 ppm, 0.02 ppmC, and 0.001 ppm, respectively, was used to test for the impact of the boundary conditions. The THC value corresponds to about 0.01 ppmC reactive organic gas. This calculation is called **CLEAN BC 2010**. Though little difference is expected, the **NO ROG/LO IC** also was conducted using the year 2010 emissions as the base, and is called **NO ROG/LO IC 2010**.

6.4.3 Descriptions of Control Calculations

Twenty five control strategy evaluation simulations were run to assess the effectiveness of utilizing methanol as an alternative fuel in various applications. Calculations covered both the years 2000 and 2010. Detailed treatment of emissions and the methodology used to simulate future strategies are covered in Chapter 4. Mobile source emission factors are documented in appendices 4.A1 through 4.G. Year 2010 scenario descriptions follow those for the year 2000.

6.4.3.1 Year 2000 Calculations

In **NO MOBILE**, emissions of mobile sources potentially convertible to methanol are removed. These source types are: on-road vehicles except motorcycles, land-based off-road farm equipment, construction equipment, locomotives, utility vehicles and recreational vehicles (except motorcycles). Petroleum refining operations and gasoline and diesel retail distribution emissions are also set to zero, though retail distribution emissions are replaced by methanol evaporation. This case is used to establish the maximum possible impact derived from the conversion of mobile sources to a perfectly clean fuel, and sets the maximum expected benefit from switching to methanol. It is also used to calculate the effectiveness of controls on these sources. If a scenario were to achieve similar air quality as in **NO MOBILE**, then the controls in that scenario would be comparable to removing all mobile sources in the basin.

ADV CONV is an advanced[1] conventional fuel use scenario. All applicable on-road motor vehicles are replaced with advanced technology (low emitting) vehicles (appendix 4.C). Other source emissions remain the same as in the base scenario. By

[1] As discussed in chapters 4 and 5, advanced means that all the vehicles emit at the in use standard for the year 2000 (see appendices to chapter 4). The technology assumed for these simulations is not beyond that for the other cases, including the base case (BASE1), but simply means that the technology involved is comparable to the newest vehicles in the standard simulations.

comparing the results from this calculation to **BASE1** and **NO MOBILE**, it is possible to identify how effective are more stringent controls on conventionally fueled vehicles.

ADV METH simulates the full penetration of advanced technology methanol fueled vehicles (except motorcycles) into the on-road vehicle fleet (Appendix 4.D). Off road vehicles listed in **NO MOBILE** are also converted to methanol fuel. Gasoline and diesel retail emissions are converted to methanol emissions, on a mass basis, with an adjustment for a difference in vapor pressures. The vapor pressure adjustment is used on emissions that are due to evaporation in a fixed volume, such as tank displacement, but not on spillage.

In **STD M100**, all the on-road vehicles introduced from 1990 on (except motorcycles), and all the off-road vehicles listed in **NO MOBILE**, are conventional technology M100 fueled vehicles (appendix 4.B). (It is realized that 100% penetration of MFVs starting in 1990 is not practical. The purpose of this calculation is to show the impact over a 10 year period of MFV penetration. This comment also pertains to other scenarios described below, and is discussed further in chapter 4.) Emissions from retail sale of gasoline and diesel are converted to methanol emissions by the ratio that methanol fuel usage replaces conventional fuel usage. Again, methanol emissions are adjusted for the difference in vapor pressures.

FULL METH is the maximum methanol fuel utilization scenario. In addition to the emissions changes described in **ADV METH**, methanol is being used in stationary sources to reduce NO_x emissions (appendices 4.D,4.G). The extra sources affected are utility boilers, stationary internal combustion engines, and non-refinery industrial boilers.

BASE-ROG and **BASE-NOX** are used to analyze the effect of removing the ROG component and NO_x component, respectively, of the sources potentially convertible to methanol. Because oxidant formation requires both, changes in either component will affect ozone levels. The relative response, however, can be very different and may vary within the basin. The same sources are being controlled as in **NO MOBILE**. These two calculations can be compared to **NO MOBILE** to determine if NO_x or ROG control, or a combination, is more effective at improving air quality.

In **METH 50**, only 50% of the on road motor vehicles (except motorcycles) introduced after 1989 are methanol fueled vehicles. Off-road vehicles listed in **NO MOBILE** are converted to methanol and the emissions of retail fuel distribution are adjusted, on a fuel usage basis, accordingly. Other stationary sources are unaffected. This scenario analyzes the ability of a partial methanol fuel usage scenario to improve air quality and can be used for interpolating between full and partial penetration.

STD M85 considers methanol fuel usage in the same sources as in **STD M100**. In all other methanol scenarios, the fuel is considered to be 100% methanol, or M100. In this scenario the fuel used is 85% methanol, 15% gasoline, or M85. M85 has several practical advantages over M100, including superior cold starting performance, it has a visible flame and is not as explosive. This scenario investigates the sensitivity of air quality to changes in fuel type. Emission factors for this scenario are given in appendix 4.E.

HIGH FORM is also a variation of **STD M100,** but in this scenario formaldehyde emissions of on-road vehicles are increased by about a factor of three. One issue of concern is that MFVs could, especially without proper maintenance, emit more formaldehyde than was considered in the **STD M100** or **STD M85** calculation. Formaldehyde is more reactive than methanol, so this scenario investigates how much of the benefits of methanol fuel usage are lost with higher formaldehyde emissions. The scenario also investigates the effects of higher formaldehyde emissions on ambient formaldehyde levels. Emission factors are given in appendix 4.B, with HCHO emissions from light and medium duty vehicles increased to 55 mg mi^{-1}.

Finally, **ADV METH/NO ROG** investigates sensitivity of air quality specifically to methanol and formaldehyde emissions. This is done by repeating **ADV METH**, except emissions of mobile source methanol and formaldehyde are removed.

6.4.3.2 Year 2010 Calculations

Emissions from mobile and stationary sources are expected to increase between the year 2000 and 2010 (Table 6.3). This is due to the expected increase in the population of the SoCAB overwhelming new emission controls. Also the distribution of pollutant emissions are expected to shift eastward. The increase in total emissions, and redistribution between types of sources and locations will change the air quality response to a methanol based control strategy. To fully capture the redistribution of emissions, the modeling region was expanded eastward, (Fig. 6.1).

Nine emission control simulations, described below, quantify the impact of methanol and CFV controls in 2010. Two are similar to the advanced technology CFV and MFV calculations described above for the year 2000. These are **ADV CONV 2010** and **ADV METH 2010**, corresponding to low emitting conventionally fueled and M100 vehicles, respectively. The same emission factors for mobile and stationary sources have been used as above (Appendices 4.C and 4.D) including the effects of vapor pressure changes.

Air quality benefits from converting on-road, light and medium duty vehicles to M100 and M85 fuel was simulated in **STD M100 2010** and **STD M85 2010.** Again, the conversion is assumed to start in 1990. Heavy-duty and off-road vehicles, and stationary sources were unchanged from the base case, except for evaporative emissions from refueling stations. Emission factors from light and medium duty vehicles are listed in Appendices 4.B and 4.E, respectively, and are for "standard" technology vehicles. These calculations can be compared to the calculation modeling stringent controls (e.g. 0.25 g/mi ROG and 0.20 g/mi NO_x on light duty vehicles) on conventionally fueled light and medium duty vehicles, called **ADV LMD 2010** (detailed emission factors shown in appendix 4.C). Heavy duty and off-road vehicle, and stationary source emissions were unchanged from the base case. As a base line for judging the ozone forming potential of the organic fraction of the vehicle emissions, a similar calculation, **ADV LMD/NO ROG 2010** was run. It is similar to **ADV LMD 2010**, except that the light and medium duty vehicle ROG emissions were removed. Comparing the results from **STD M100 2010, STD M85 2010, ADV LMD 2010** and **ADV LMD/NO ROG 2010** can be used to show the relative benefits of using M100, M85 or more stringent controls in light and medium duty vehicles.

As discussed below, increased emissions in the eastern basin, combined with the initial pollutant cloud, leads to a predicted peak about 50 km east of San Bernardino. It is difficult to prescribe how initial conditions will adjust to emission controls, so to quantify the effect of initial conditions on the perceived benefits of emission changes, four simulations were rerun using clean (0.04 ppm O_3, 0.0 ppm NO_x, and 0.01 ppmC ROG) initial conditions and boundary conditions in the western basin. The base case, advanced technology CFV, advanced technology MFV and the M85 simulations where rerun using clean conditions, and are called **LO BC/LO IC 2010**, **ADV CONV/LO IC 2010**, **ADV M100/LO IC 2010** and **STD M85/LO IC 2010**, respectively. These calculation tend to accentuate the benefits in the central and western, more densely populated regions.

6.5 Effect of Fuel Conversion

Results of the thirty-three airshed model runs show that methanol can be used to reduce photochemical air pollution in Los Angeles. A broad range of measures of air quality, as shown in Tables 6.4 through 6.14 and Figures 6.5 through 6.13, demonstrate the spatial and temporal response of air pollutants to changing emission patterns and composition. First the predicted air quality measures for the base emissions are presented. Then the diagnostic calculations are compared to these, and the implications of their results discussed. Finally, the results of the control simulations are presented.

6.5.1 Measures of Pollutants Levels

Use of an airshed model allows for developing a wide range of measures of pollutant levels over multiple days. This analysis focuses, primarily, on the predicted impact of emissions on air pollutants on the third day of the simulation. This was because the third day recorded significantly higher predicted and observed pollutant concentrations than the first two days, and the role of initial conditions decreases with time. Interest has been expressed in how the air quality on the second day responds to the controls being tested. This interest can be a result of wanting to delineate how photochemical pollutants might be affected under less severe conditions. For this reason, the corresponding statistics are supplied for the second day. It should be remembered that results on the second day are more sensitive to initial conditions than those for the third day, and less sensitive to emissions controls.

While much of the attention in the past has been concentrated on extreme statistical measures, such as the peak 1-hr average, there is little question that many of the harmful effects can be attributed to longer term exposure. Also, the peak value is not necessarily representative of basin-wide levels and the bulk of the populace may be exposed to very different levels. Of equal, or greater, concern for health and materials related impacts, are measures of exposure and the related dose. For this reason several measures of O_3, HCHO, NO_2 and PAN concentrations are given.

In addition to peak levels of the five species, Tables 6.4 through 6.14 contain measures of time-, area-, and population-weighted exposure. Basin-wide ozone exposure is reported as the time and area (in number of grids times hours) where the ozone concentration is greater than 0.12 ppm (the NAAQS), 0.20 (Stage I level) and 0.30 ppm.

Each grid is 5 km square. The spatial distribution of ozone at 1 PM on the third day is presented graphically for each scenario in Figures 6.5 and 6.13. This corresponds to the time of the peak ozone in both the evaluation and year 2000 base case calculations. Additionally area exposure is tabulated in Table 6.8 and 6.13 showing the number of grids where ozone exceeds 0.10, 0.12 and 0.20 ppm at any time during the third day. Also, peak 8-hr average ozone is given as a measure of longer term high concentrations.

Forecast, spatially resolved, population data for the years 2000 and 2010 (Liu, 1988) have been used to develop population-weighted exposure to ozone, NO_2, HCHO, HNO_3 and, when applicable, methanol. In Tables 6.4 through 6.14,"exposure", defined as:

$$E_i = \int_A \int_T P(x) C_i(x,t)\, dx\, dt \qquad (6.5)$$

weights the predicted concentrations by the collocated population. Here E_i is the exposure to pollutant i, P(x) is the population at location x, and $C_i(x,t)$ is the time varying concentration at x. This is integrated over the modeling region, A, and over a 24 hour time period,T (either the second or third day of the simulations). While this is not the definition of exposure used by many scientists, and does not take into account daily personal activity patterns, it is indicative of the relative exposure resulting from varying control alternatives. The population data base is only for areas within the SoCAB. Similar to the above area weighted measures, exposure to high ozone concentrations are shown using population-weighting. Two similar measures shown for comparing predicted ozone air quality are 1) the person-ppm-hours greater than C^0, defined as:

$$E(C^0) = \int_A \int_T P(x) C(x,t) H(C_{O3} - C^0)\, dt\, dx \qquad (6.6)$$

and 2) person hours greater than C^0, defined as:

$$E(C^0) = \int_T \int_A P(x) H(C_{O3} - C^0)\, dx\, dt \qquad (6.7)$$

Both of these measure the exposure above a cutoff level C^0. Here $H(C_{O3} - C^0)$ is the Heaviside step function, which is 1 if $C_{O3} - C^0$ is positive, and zero otherwise. Cutoff concentrations, C^0, used were 0.0, 0.12, 0.20, and 0.30 ppm ozone.

Peak formaldehyde levels are shown for the Downtown Los Angeles monitoring station. This location was chosen because formaldehyde levels there are particularly sensitive to direct emissions. If methanol fuel utilization significantly increased formaldehyde levels, this would show up at Downtown Los Angeles. Basin-wide average formaldehyde levels are averaged over the modeling region on the third day of the simulation. Peak and average PAN, HNO_3, and NO_2 concentrations are also listed in the tables. Exposure to HNO_3 could be used as an indication of materials damage.

Table 6.4 Ozone Concentrations and Exposures in the Year 2000

SCENARIO	CONCENTRATIONS		EXPOSURES						
			Person ppm hours[3] ([O3] > x)				Person hours[4] ([O3] > x)		
	MAX.[1] (ppm)	AVG.[2] (ppm)	x = 0.00 (1000s)	x = 0.12 (1000s)	x = 0.20 (1000s)	x = 0.30 (1000s)	x = 0.12 (1000s)	x = 0.20 (1000s)	x = 0.30 (1000s)
BASE1A	0.26979	0.04504	12,568	7,314	2,586	0	41,348	11,690	0
BASE1	0.26114	0.04444	12,459	7,080	2,171	0	40,683	9,902	0
NO MOBILE	0.20631	0.04081	12,486	5,384	58	0	35,391	284	0
ADV CONV	0.24565	0.04346	12,506	6,655	1,392	0	39,647	6,509	0
ADV METH	0.22317	0.04053	11,707	5,655	352	0	35,769	1,688	0
STD M100	0.22343	0.04055	11,725	5,673	364	0	35,848	1,747	0
FULL METH	0.21907	0.04042	11,805	5,626	241	0	35,948	1,163	0
BASE-ROG	0.22760	0.03833	9,819	4,449	462	0	27,878	2,236	0
BASE-NOx	0.21532	0.04234	14,432	6,837	131	0	44,598	636	0
METH 50	0.25025	0.04280	12,015	6,530	1,483	0	38,935	6,902	0
STD M85	0.24479	0.04174	11,649	6,167	1,260	0	37,007	5,909	0
HIGH FORM	0.24199	0.04149	11,579	6,070	1,108	0	36,660	5,202	0
ADV METH/NO ROG	0.21501	0.03962	11,192	5,153	217	0	33,091	1,047	0
SC1982	0.32709	0.05713	14,615	9,520	4,545	175	50,757	19,328	575
DIAGNOSTIC SCENARIOS									
NO EM	0.18483	0.02552	7,836	368	0	0	2,621	0	0
NO ROG	0.19081	0.02694	6,295	1,140	0	0	7,955	0	0
NO ROG/LO IC	0.16609	0.02106	4,990	244	0	0	1,843	0	0
LO IC	0.25428	0.04129	12,582	6,680	697	0	41,135	3,266	0
NO EM/LO IC	0.13919	0.02186	6,955	17	0	0	129	0	0

1 Maximum species concentration predicted within the modeling region.
2 Average species concentration throughout the modeling region for the day.
3 Exposure above cutoff, see Eqn. 6.6 (population x concentration x hours)
4 Exposure above cutoff, see Eqn. 6.7 (population x hours)

Table 6.5 Concentrations and Exposures of Pollutant Species in the Year 2000

	NO2			HCHO			PAN			HNO3		
SCENARIO	MAX.[1]	AVG.[2]	EXP.[3]	MAX.	AVG.	EXP.	MAX.	AVG.	EXP.	MAX.	AVG.	EXP.
	(ppm)	(ppm)	(1000s)	(ppb)	(ppb)	(1000s)	(ppb)	(ppb)	(1000s)	(ppb)	(ppb)	(1000s)
BASE1A	0.206	0.021	13,959	27.6	5.5	2,439	16.8	2.6	748	26.4	3.3	1,370
BASE1	0.192	0.020	13,201	29.7	5.8	2,779	15.2	2.5	722	24.5	3.1	1,317
NO MOBILE	0.090	0.010	7,005	23.7	3.9	1,578	14.0	2.0	689	16.9	2.0	895
ADV CONV	0.153	0.016	11,124	27.1	4.8	2,073	15.0	2.4	736	21.5	2.7	1,168
ADV METH	0.114	0.014	9,684	29.2	4.9	2,320	11.1	1.8	559	18.5	2.3	938
STD M100	0.125	0.014	9,687	28.9	5.0	2,326	11.1	1.8	562	18.5	2.3	938
FULL METH	0.111	0.014	9,239	28.7	4.9	2,257	11.5	1.8	565	18.1	2.2	896
BASE-ROG	0.155	0.019	11,964	30.9	4.3	1,752	11.2	1.7	447	23.3	2.9	1,117
BASE-NOx	0.092	0.009	6,828	29.5	5.1	2,550	15.9	2.0	863	15.9	1.7	715
METH 50	0.152	0.019	12,753	26.7	5.6	2,656	12.0	2.1	632	22.8	2.9	1,156
STD M85	0.164	0.019	12,411	27.7	5.4	2,551	11.8	2.0	590	22.6	2.9	1,134
HIGH FORM	0.170	0.018	12,142	35.0	6.1	3,203	11.5	1.9	564	22.3	2.8	1,118
ADV METH/NO ROG	0.107	0.014	9,588	30.4	4.1	1,750	10.3	1.7	530	18.2	2.3	928
SC1982	0.338	0.031	20,175	50.6	8.4	4,062	28.4	3.9	1,033	69.5	5.0	2,045
DIAGNOSTIC SCENARIOS												
NO EM	0.013	0.001	140	8.0	1.9	537	8.7	0.6	146	7.3	0.6	185
NO ROG	0.087	0.017	9,103	10.7	2.6	824	8.5	0.9	173	25.2	2.7	933
NO ROG/LO IC	0.088	0.017	8,888	10.6	2.3	747	8.5	0.6	123	25.9	2.6	905
LO IC	0.181	0.021	11,630	38.0	6.0	2,490	16.9	2.2	728	31.5	3.0	1,137
NO EM/LO IC	0.013	0.001	124	6.8	1.6	475	8.5	0.4	107	4.3	0.5	161

1 Maximum species concentration predicted within the modeling region.
2 Average species concentration throughout the modeling region for the day.
3 Population exposure within the SoCAB as defined in Eqn. 6.5 (population x concentration x hours)

Table 6.6 Ozone Concentrations and Exposures in the Year 2000, Day 2

SCENARIO	CONCENTRATIONS	EXPOSURES						
		Person ppm hours[2] ([O3] > x)				Person hours[3] ([O3] > x)		
	MAX.[1] (ppm)	x = 0.00 (1000s)	x = 0.12 (1000s)	x = 0.20 (1000s)	x = 0.30 (1000s)	x = 0.12 (1000s)	x = 0.20 (1000s)	x = 0.30 (1000s)
BASE1A	0.23872	11,657	4,330	779	0	26,631	3,612	0
BASE1	0.23715	11,628	4,186	660	0	26,085	3,086	0
NO MOBILE	0.19126	11,649	2,741	0	0	19,079	0	0
ADV CONV	0.22063	11,674	3,813	320	0	24,536	1,532	0
ADV METH	0.20731	11,151	3,169	96	0	21,147	469	0
STD M100	0.20795	11,164	3,178	98	0	21,201	478	0
FULL METH	0.20352	11,162	3,091	44	0	20,864	218	0
BASE-ROG	0.21642	9,874	2,657	251	0	16,888	1,204	0
BASE-NOx	0.18784	12,929	3,241	0	0	22,935	0	0
METH 50	0.22385	11,343	3,773	390	0	23,889	1,854	0
STD M85	0.22227	11,076	3,567	351	0	22,680	1,677	0
HIGH FORM	0.22056	11,065	3,503	320	0	22,350	1,530	0
ADV METH/NO ROG	0.20617	10,807	2,864	81	0	19,101	397	0
SC1982	0.25032	12,676	5,578	1,534	0	33,850	6,974	0
DIAGNOSTIC SCENARIOS								
NO EM	0.12912	8,061	136	0	0	1,102	0	0
NO ROG	0.17595	7,070	953	0	0	6,530	0	0
NO ROG/LO IC	0.13938	4,525	2	0	0	16	0	0
LO IC	0.20844	10,161	1,833	0	0	13,687	2	0
NO EM/LO IC	0.10192	6,237	0	0	0	0	0	0

1 Maximum species concentration predicted within the modeling region.
2 Exposure above cutoff, see Eqn 6.6 (population x concentration x hours)
3 Exposure above cutoff, see Eqn. 6.7 (population x hours)

Table 6.7 Concentrations and Exposures of Pollutant Species in the Year 2000, Day 2

	NO2		HCHO		PAN		HNO3	
SCENARIO	MAX.[1] (ppm)	EXP.[2] (1000s)	MAX. (ppb)	EXP. (1000s)	MAX. (ppb)	EXP. (1000s)	MAX. (ppb)	EXP. (1000s)
BASE1A	0.176	8,548	20.0	1,911	15.9	683	15.9	807
BASE1	0.159	8,103	19.8	2,137	15.6	668	15.0	782
NO MOBILE	0.061	4,508	19.1	1,356	12.0	625	9.7	576
ADV CONV	0.122	6,857	19.4	1,676	14.9	668	12.7	710
ADV METH	0.101	5,957	19.6	1,908	11.5	550	10.8	575
STD M100	0.101	5,961	19.6	1,912	11.7	551	10.8	575
FULL METH	0.100	5,690	19.3	1,842	11.3	546	10.1	550
BASE-ROG	0.146	7,529	19.9	1,559	12.9	494	13.9	669
BASE-NOx	0.059	4,356	20.0	2,042	11.2	706	8.0	462
METH 50	0.151	7,872	20.2	2,133	13.1	606	13.2	683
STD M85	0.148	7,581	20.3	2,060	13.1	578	12.8	672
HIGH FORM	0.145	7,413	22.1	2,484	12.8	565	12.6	665
ADV METH/NO ROG	0.099	5,919	19.4	1,540	11.7	532	10.8	572
SC1982	0.254	11,807	35.6	2,930	17.9	823	25.6	1,088
DIAGNOSTIC SCENARIOS								
NO EM	0.059	149	9.3	596	8.1	189	4.9	186
NO ROG	0.087	6,457	10.5	883	8.7	250	14.8	653
NO ROG/LO IC	0.088	5,963	10.4	659	8.1	136	13.8	548
LO IC	0.130	7,315	29.4	1,839	9.4	511	14.7	746
NO EM/LO IC	0.059	125	6.1	451	8.1	111	4.9	144

1 Maximum species concentration predicted within the modeling region.
2 Population exposure within the SoCAB as defined by Eqn. 6.5 (population x concentration x hours)

Table 6.8 Basinwide ozone concentrations calculated in the emissions scenarios.

Scenario	Grid*hr*ppm $[O_3]$>.12 ppm	Grids*hrs $[O_3]$ >.12 ppm	Grids*hrs $[O_3]$ >.20 ppm	Grids with $[O_3]$ >.10 ppm	Grids with $[O_3]$ >.12 ppm	Grids with $[O_3]$>.20 ppm
BASE1A	430	2502	603	510	468	215
BASE1	410	2420	510	504	460	198
NO MOBILE	263	1747	12	466	393	10
ADV CONV	364	2224	296	493	443	138
ADV METH	301	1927	73	471	398	45
STD M100	302	2028	140	483	428	74
FULL METH	294	1901	50	471	399	36
BASE-ROG	299	1893	122	476	419	72
BASE-NOx	286	1891	12	481	419	12
METH 50	377	2290	344	492	453	156
STD M85	358	2186	286	488	439	137
HIGH FORM	351	2152	251	486	438	126
ADV METH/NO ROG	284	1839	51	467	394	37
1982	617	3410	1068	634	579	303
LO IC	343	2103	182	491	417	87
NO-EM/ LO-IC	5	37	0	50	24	0
NO EM	33	239	0	107	77	0
NO ROG	98	680	0	375	218	0
NO ROG/LO IC	34	246	0	228	86	0
2000X	504	2825	844	601	542	263

Table 6.9 Ozone concentrations and Exposures in the Year 2010

SCENARIO	CONCENTRATIONS		EXPOSURES						
			Person ppm hours[3] ([O3] > x)				Person hours[4] ([O3] > x)		
	MAX.[1] (ppm)	AVG.[2] (ppm)	x = 0.00 (1000s)	x = 0.12 (1000s)	x = 0.20 (1000s)	x = 0.30 (1000s)	x = 0.12 (1000s)	x = 0.20 (1000s)	x = 0.30 (1000s)
BASE 2010	0.32149	0.05159	15,264	9,840	5,159	108	50,989	21,473	353
NO MOBILE 2010	0.28045	0.04644	15,154	7,804	1,950	0	46,412	8,860	0
NO MOBILE ROG 2010	0.32188	0.04804	13,082	7,782	3,609	83	42,043	15,242	272
ADV CONV 2010	0.30265	0.04927	15,111	8,906	3,668	1	48,650	15,884	4
ADV METH 2010	0.28506	0.04611	14,019	7,651	2,365	0	43,947	10,568	0
STD M100 2010	0.30788	0.04799	13,470	7,976	3,823	9	43,101	16,389	29
STD M85 2010	0.30853	0.04928	14,266	8,700	4,234	9	46,482	17,964	29
ADV LMD 2010	0.29846	0.04891	14,703	8,656	3,807	0	47,176	16,481	0
ADV LMD NO ROG 2010	0.30849	0.04676	12,770	7,303	3,259	9	40,356	14,086	29
ADV CFV/LO IC 2010	0.26578	0.04267	13,014	6,985	1,202	0	41,970	5,485	0
ADV MFV/LO IC 2010	0.25600	0.04133	12,924	6,683	844	0	40,920	3,888	0
M85 LO IC 2010	0.28312	0.04223	12,176	6,613	1,653	0	38,795	7,495	0
DIAGNOSTIC SCENARIOS									
CLEAN BC 2010	0.32201	0.04925	13,885	8,373	4,392	78	43,513	18,091	257
LO BC/LO IC 2010	0.30553	0.04785	13,604	8,093	4,040	9	42,834	16,991	29
NO ROG/LO IC 2010	0.19049	0.01527	2,498	14	0	0	107	0	0
LO IC 2010	0.31258	0.04617	14,051	8,836	3,471	37	48,757	15,331	120

1 Maximum species concentration predicted within the modeling region.
2 Average species concentration throughout the modeling region for the day.
3 Exposure above cutoff, see Eqn. 6.6 (population x concentration x hours)
4 Exposure above cutoff, see Eqn. 6.7 (population x hours)

Table 6.10 Concentrations and Exposures of Pollutants Species in the Year 2010

SCENARIO	NO2 MAX.[1] (ppm)	NO2 AVG.[2] (ppm)	NO2 EXP.[3] (1000s)	HCHO MAX. (ppb)	HCHO AVG. (ppb)	HCHO EXP. (1000s)	PAN MAX. (ppb)	PAN AVG. (ppb)	PAN EXP. (1000s)	HNO3 MAX. (ppb)	HNO3 AVG. (ppb)	HNO3 EXP. (1000s)
BASE 2010	0.222	0.022	17,485	27.2	6.0	3,071	21.1	3.1	952	31.3	3.7	1,747
NO MOBILE 2010	0.122	0.011	9,511	23.0	4.5	2,082	18.7	2.4	898	18.1	2.3	1,163
NO MOBILE ROG 2010	0.191	0.021	16,461	40.0	4.9	2,232	19.9	2.6	688	31.5	3.7	1,691
ADV CONV 2010	0.177	0.017	13,828	24.0	5.3	2,582	19.6	2.8	924	23.8	3.0	1,467
ADV METH 2010	0.158	0.015	12,476	25.4	5.3	2,588	15.8	2.2	713	21.0	2.7	1,219
STD M100 2010	0.180	0.021	16,338	29.5	6.6	3,478	16.4	2.3	643	30.0	3.6	1,557
STD M85 2010	0.184	0.021	16,775	28.8	6.4	3,328	17.0	2.5	755	29.5	3.6	1,572
ADV LMD 2010	0.193	0.019	15,096	24.8	5.5	2,726	16.3	2.5	802	25.6	3.2	1,419
ADV LMD NO ROG 2010	0.199	0.021	16,171	41.3	5.1	2,322	16.7	2.3	617	29.9	3.6	1,530
ADV CFV/LO IC 2010	0.146	0.016	13,240	23.8	4.5	2,274	15.7	2.0	670	24.4	3.0	1,460
ADV MFV/LO IC 2010	0.157	0.015	12,209	27.8	4.7	2,441	13.7	1.7	607	20.9	2.6	1,204
M85 LO IC 2010	0.174	0.021	15,971	29.0	5.5	2,982	13.8	1.8	539	29.9	3.6	1,545
DIAGNOSTIC SCENARIOS												
CLEAN BC 2010	0.197	0.021	16,623	27.1	5.6	2,770	20.6	2.8	787	31.0	3.7	1,727
LO BC/LO IC 2010	0.185	0.021	16,561	27.1	5.5	2,747	18.5	2.6	753	30.7	3.7	1,721
NO ROG/LO IC 2010	0.088	0.017	11,117	8.0	1.4	467	8.5	0.4	36	24.0	2.4	896
LO IC 2010	0.225	0.022	17,147	27.8	5.4	2,903	19.4	2.4	805	30.8	3.7	1,737

1 Maximum species concentration predicted within the modeling region.
2 Average species concentration throughout the modeling region for the day.
3 Population exposure within the SoCAB as defined in Eqn. 6.5 (population x concentration x hours)

Table 6.11 Ozone Concentrations and Exposures in the Year 2010, Day 2

SCENARIO	CONCENTRATIONS	EXPOSURES						
		Person ppm hours[2] ([O3] > x)				Person hours[3] ([O3] > x)		
	MAX.[1] (ppm)	x = 0.00 (1000s)	x = 0.12 (1000s)	x = 0.20 (1000s)	x = 0.30 (1000s)	x = 0.12 (1000s)	x = 0.20 (1000s)	x = 0.30 (1000s)
BASE 2010	0.26304	13,540	5,803	2,208	0	33,224	9,808	0
NO MOBILE 2010	0.22237	13,566	4,232	394	0	27,477	1,870	0
NO MOBILE ROG 2010	0.25807	12,068	4,520	1,610	0	25,787	7,144	0
ADV CONV 2010	0.24412	13,510	5,159	1,134	0	31,131	5,184	0
ADV METH 2010	0.23053	12,778	4,315	657	0	26,799	3,083	0
STD M100 2010	0.25155	12,377	4,711	1,538	0	27,203	6,907	0
STD M85 2010	0.25399	12,876	5,084	1,685	0	29,394	7,572	0
ADV LMD 2010	0.24554	13,216	5,060	1,268	0	30,116	5,784	0
ADV LMD NO ROG 2010	0.24840	11,891	4,271	1,325	0	24,844	5,977	0
ADV CFV/LO IC 2010	0.17368	10,944	2,720	0	0	19,124	0	0
ADV MFV/LO IC 2010	0.16094	10,906	2,324	0	0	16,966	0	0
M85 LO IC 2010	0.17771	10,267	2,532	0	0	17,211	0	0
DIAGNOSTIC SCENARIOS								
CLEAN BC 2010	0.26357	12,974	5,371	2,180	0	30,172	9,679	0
LO BC/LO IC 2010	0.24339	12,312	4,692	1,450	0	27,375	6,663	0
NO ROG/LO IC 2010	0.11259	2,878	0	0	0	0	0	0
LO IC 2010	0.18802	11,503	3,619	0	0	24,072	0	0

1 Maximum species concentration predicted within the modeling region.
2 Exposure above cutoff, see Eqn. 6.6 (population x concentration x hours)
3 Exposure above cutoff, see Eqn. 6.7 (population x hours)

Table 6.12 Concentrations and Exposures of Pollutant Species in the Year 2010, Day 2

	NO2		HCHO		PAN		HNO3	
SCENARIO	MAX.[1] (ppm)	EXP.[2] (1000s)	MAX. (ppb)	EXP. (1000s)	MAX. (ppb)	EXP. (1000s)	MAX. (ppb)	EXP. (1000s)
BASE 2010	0.157	10,833	27.2	2,374	18.3	824	18.0	991
NO MOBILE 2010	0.095	6,090	25.6	1,732	15.1	768	11.3	710
NO MOBILE ROG 2010	0.150	10,394	23.6	1,834	17.5	667	18.7	962
ADV CONV 2010	0.119	8,612	28.9	2,055	17.0	799	13.8	857
ADV METH 2010	0.109	7,725	27.1	2,128	13.5	660	13.0	713
STD M100 2010	0.169	10,193	26.4	2,687	15.0	631	17.0	877
STD M85 2010	0.160	10,383	27.4	2,580	15.4	698	16.7	884
ADV LMD 2010	0.137	9,317	24.8	2,181	15.1	721	14.5	811
ADV LMD NO ROG 2010	0.158	10,118	26.2	1,927	15.0	613	17.0	865
ADV CFV/LO IC 2010	0.109	8,163	24.0	1,714	7.4	531	14.9	843
ADV MFV/LO IC 2010	0.109	7,401	22.1	1,906	7.8	491	13.2	695
M85 LO IC 2010	0.139	9,786	24.7	2,199	7.3	450	17.7	854
DIAGNOSTIC SCENARIOS								
CLEAN BC 2010	0.142	10,635	24.7	2,238	18.3	764	17.9	994
LO BC/LO IC 2010	0.137	10,491	25.6	2,169	16.3	703	17.9	975
NO ROG/LO IC 2010	0.083	7,020	6.3	379	4.9	61	11.8	507
LO IC 2010	0.162	10,431	23.7	2,134	9.8	603	20.0	959

1 Maximum species concentration predicted within the modeling region.

2 Population exposure as defined by Eqn. 6.5 within the SoCAB (populations x concentration x hours)

Table 6.13 Basinwide ozone concentrations calculated in the emissions scenarios.

Scenario	Grid*hr*ppm [O3]>.12ppm	Grids*hrs [O3]>.12ppm	Grids*hrs [O3]>.20ppm	Grids*hrs [O3]>.30ppm	Grids with [O3]>.12ppm	Grids with [O3]>.20ppm	Grids with [O3]>.30ppm
BASE 2010	615	3226	1282	33	570	340	22
ADV CONV 2010	525	2898	942	1	547	271	1
ADV METH 2010	457	2632	646	0	521	217	0
STD M85 2010	565	3033	1112	3	558	309	3
STD M100 2010	538	2920	1029	3	550	286	3
NO ROG 2010	24	174	0	0	74	0	0
NO MOBILE ROG-2010	543	2940	1013	26	548	291	16
DV METH/LO IC-2010	372	2325	152	0	493	68	0
LO IC 2010	519	2930	831	6	553	276	6
NO MOBILE 2010	420	2488	518	0	501	181	0
CLEAN BC 2010	558	2922	1148	29	546	301	16
ADV LMD 2010	534	2923	990	0	550	278	0
DV LMD NO ROG-2010	514	2832	926	3	546	273	3
M85 LO IC 2010	430	2552	445	0	523	172	0
DV CONV/LO IC-2010	403	2459	269	0	502	122	0
LO BC/LO IC-2010	533	2848	1053	3	544	293	3

Table 6.14 2000x Scenario Results vs. BASE1 Results

	Exposure (person ppm hours)							
					([O3] > x)			
	NO2 (1000s)	HCHO (1000s)	PAN (1000s)	HNO3 (1000s)	x = 0.00 (1000s)	x = 0.12 (1000s)	x = 0.20 (1000s)	x = 0.30 (1000s)
SC2000X	13,112	2,790	736	1,340	12,751	7,287	2,671	0
BASE1	13,201	2,779	722	1,317	12,459	7,080	2,171	0
Day 2								
SC2000X	8,111	2,149	658	779	11,553	4,014	704	0
BASE1	8,103	2,137	668	782	11,628	4,186	660	0

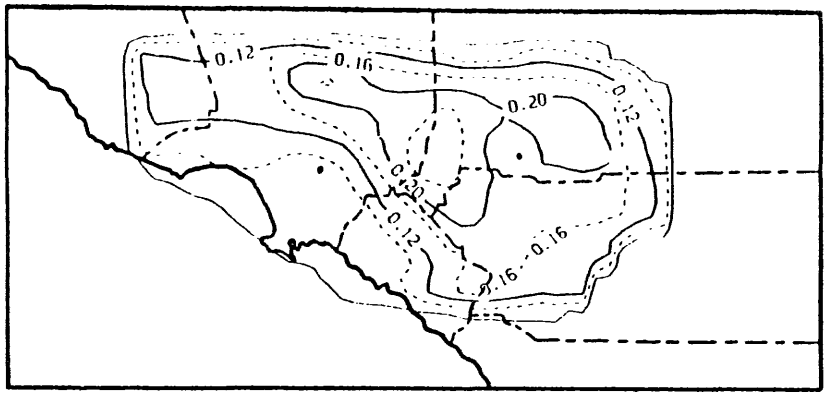

a) BASE1A

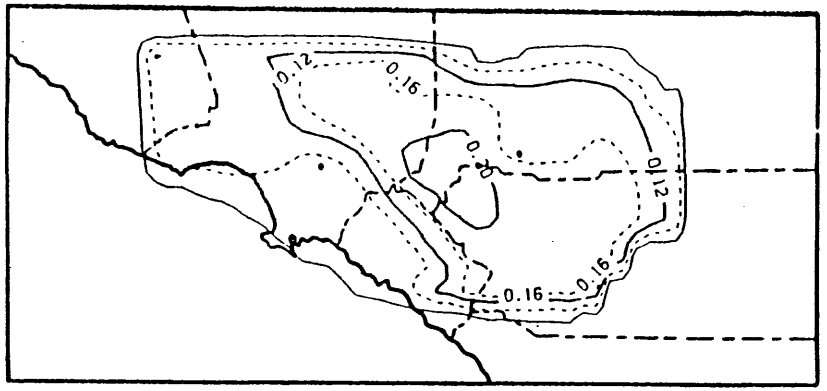

c) LO IC

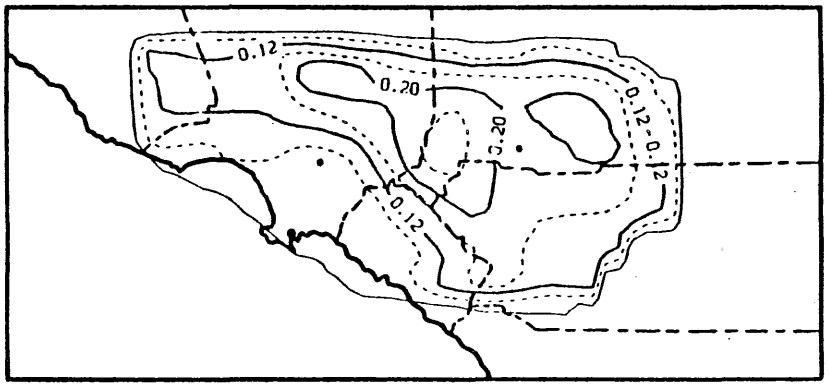

b) BASE1

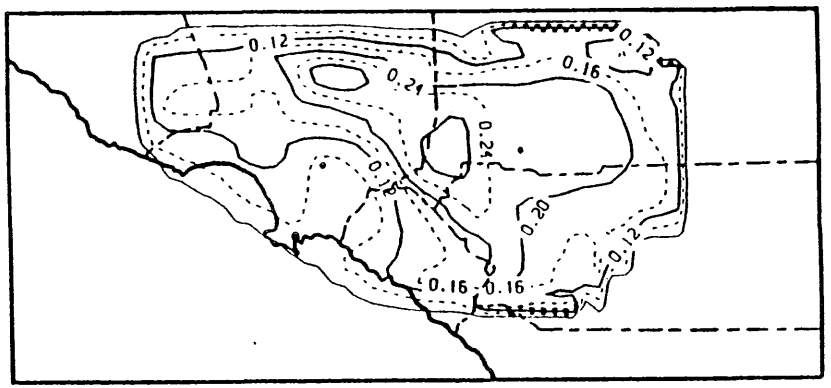

d) 1982

Figure 6.5 Spatial Distribution of Ozone at 1:00 pm on the Third Day of the Simulation. Ozone isopleths are shown at 4 pphm intervals. a) BASE1A; b) BASE1; c) LO IC: d) 1982.

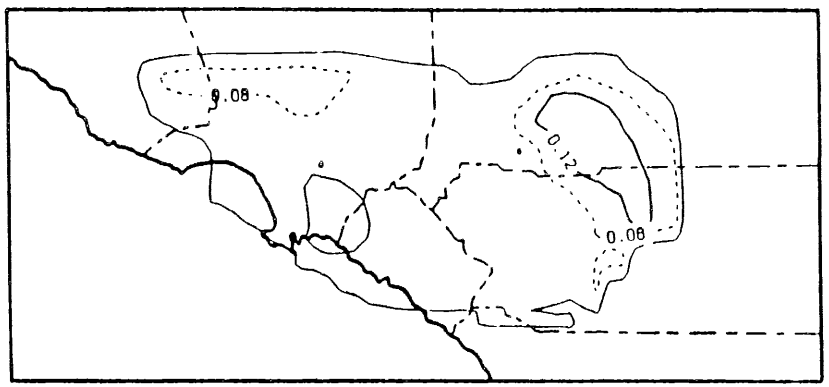

(a)

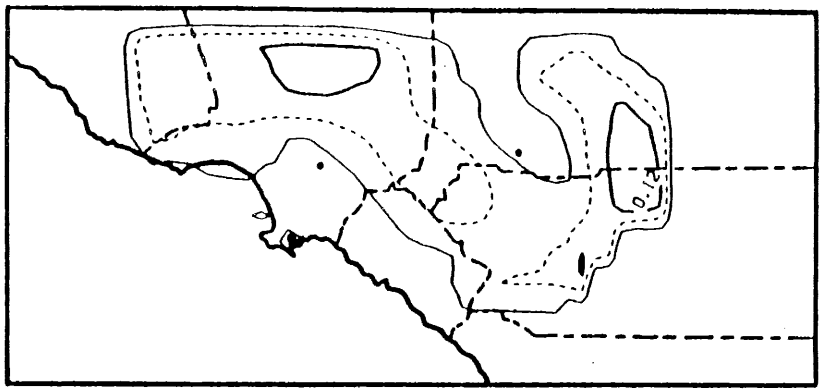

(c)

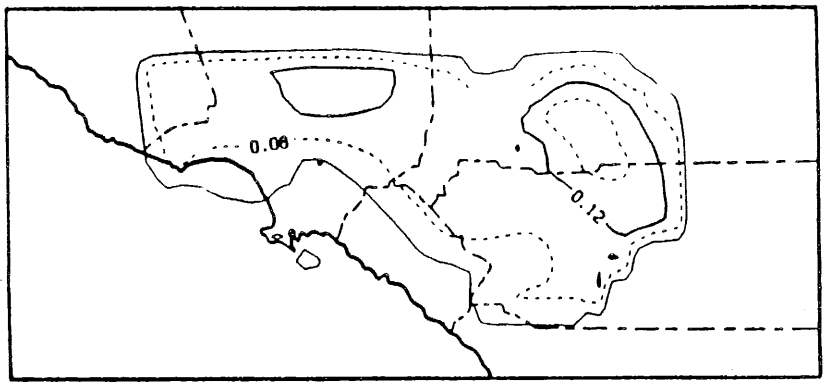

(b)

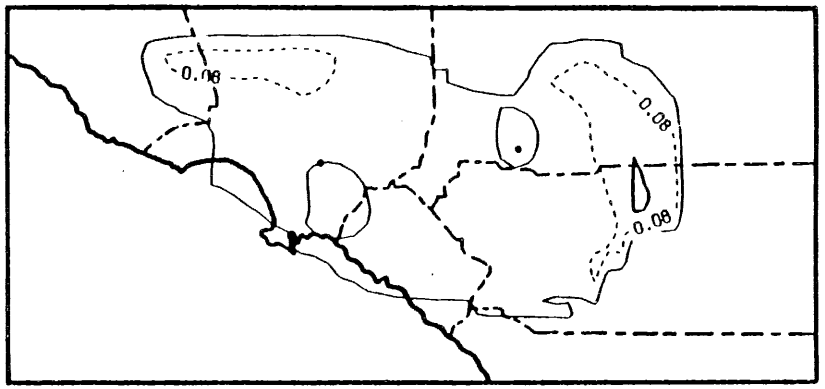

(d)

Figure 6.6 Spatial Distribution of Ozone at 1:00 pm on the Third Day of the Simulation. Ozone isopleths are shown at 4 pphm intervals. a) NO EM: b) NO ROG; c) NO ROG/LO IC; d) NO EM/LO IC.

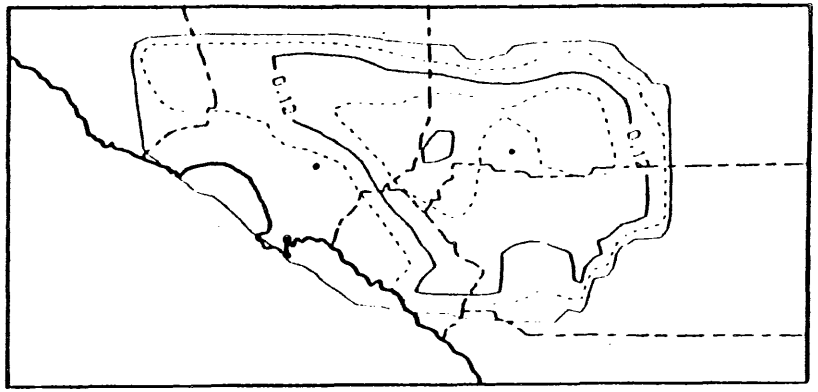

(a)

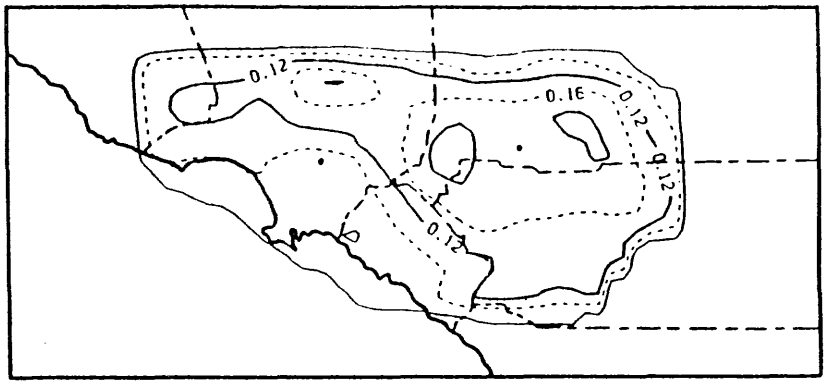

(b)

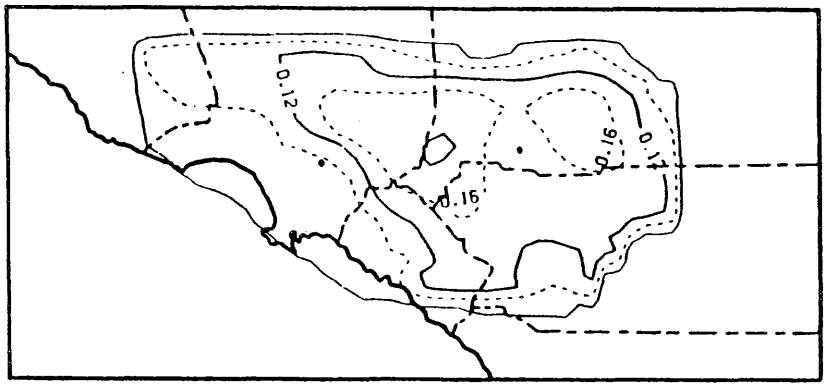

(c)

Figure 6.7 Spatial Distribution of Ozone at 1:00 pm on the Third Day of the Simulation. Ozone isopleths are shown at 4 pphm intervals. a) NO MOBILE; b) BASE-ROG; c) BASE-NOX.

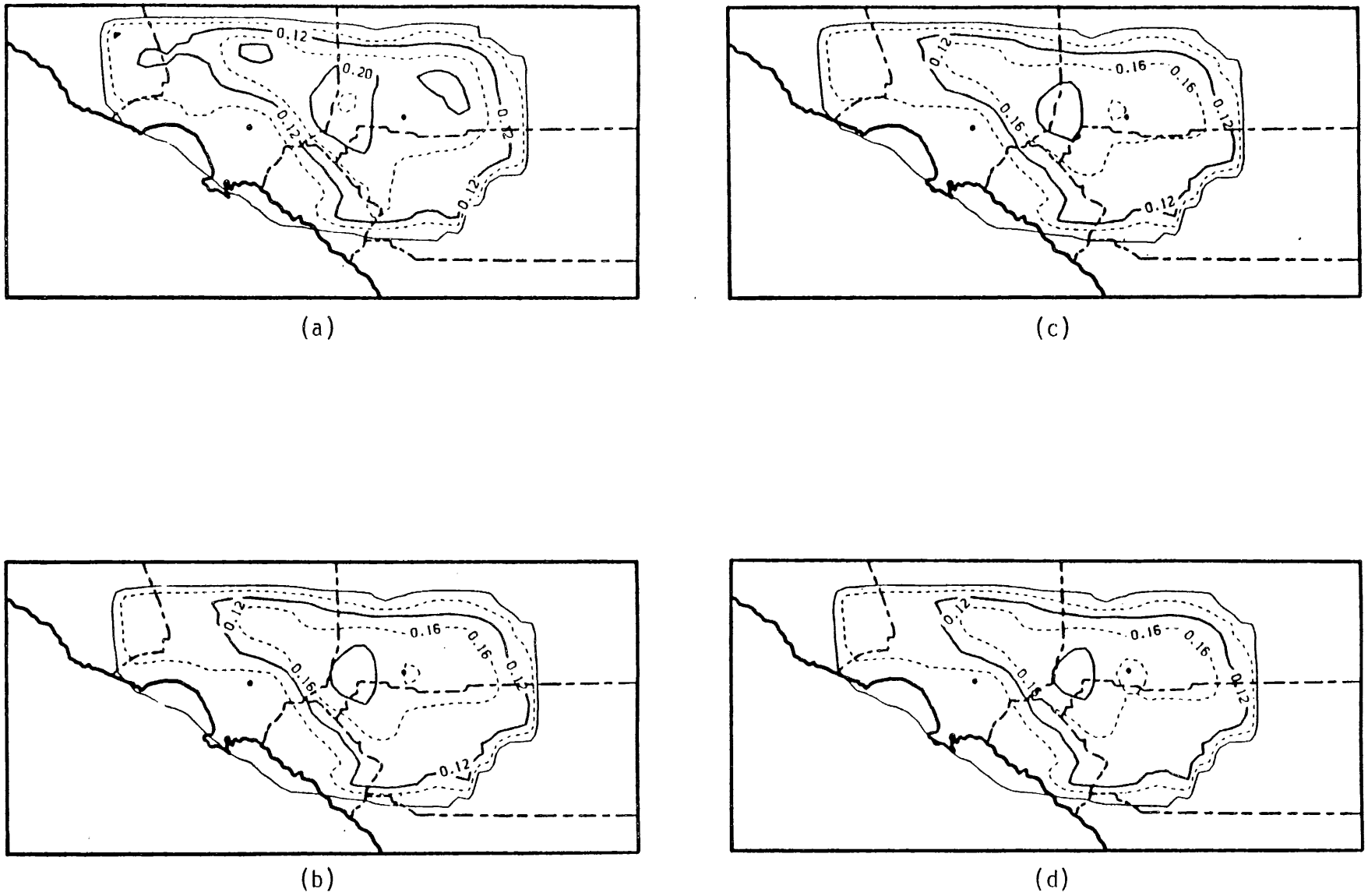

Figure 6.8 Spatial Distribution of Ozone at 1:00 pm on the Third Day of the Simulation. Ozone isopleths are shown at 4 pphm intervals. a) ADV CONV; b) ADV METH; c) STD M100; d) FULL METH.

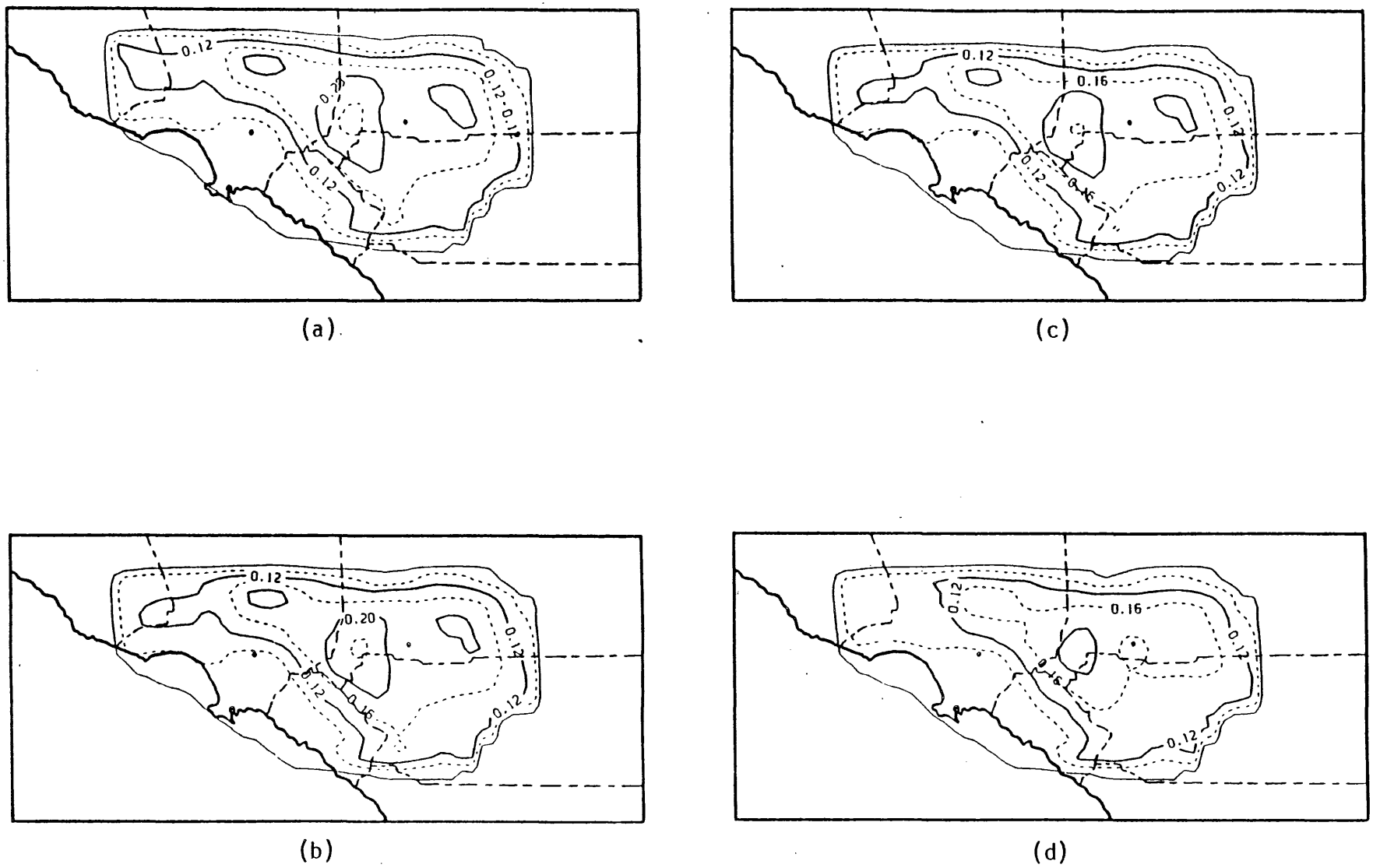

Figure 6.9 Spatial Distribution of Ozone at 1:00 pm on the Third Day of the Simulation. Ozone isopleths are shown at 4 pphm intervals. a) METH 50; b) STD M85; c) HIGH FORM; d) ADV METH/NO ROG.

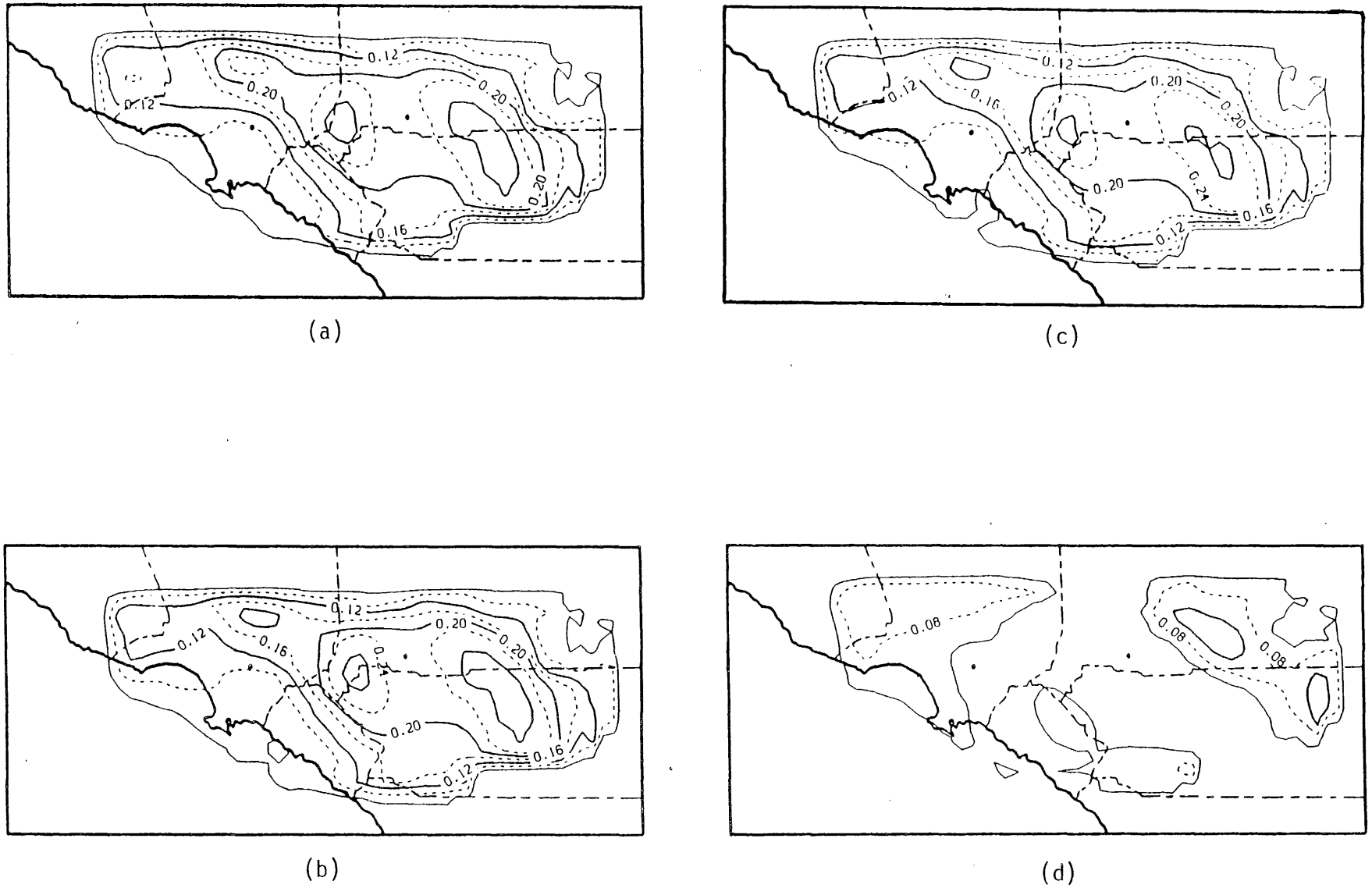

Figure 6.10 Spatial Distribution of Ozone at 1:00 pm on the Third Day of the Simulation. Ozone isopleths are shown at 4 pphm intervals. a) BASE 2010; b) CLEAN BC 2010; c) LO BC/LO IC 2010; d)NO ROG/LO IC 2010.

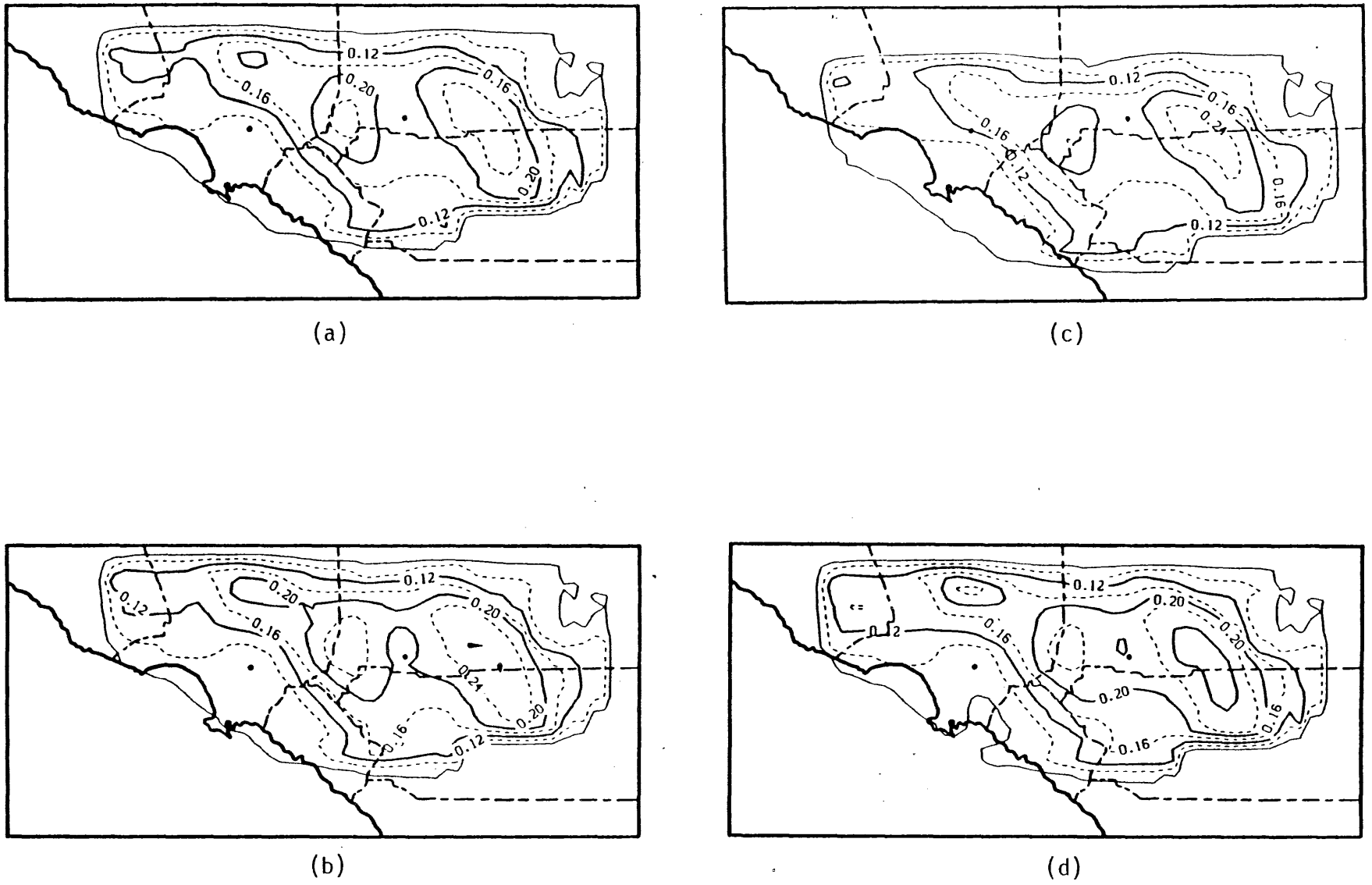

Figure 6.11 Spatial Distribution of Ozone at 1:00 pm on the Third Day of the Simulation. Ozone isopleths are shown at 4 pphm intervals. a) ADV METH 2010; b) ADV CONV 2010; c) NO MOBILE 2010; d) NO MOBILE ROG 2010.

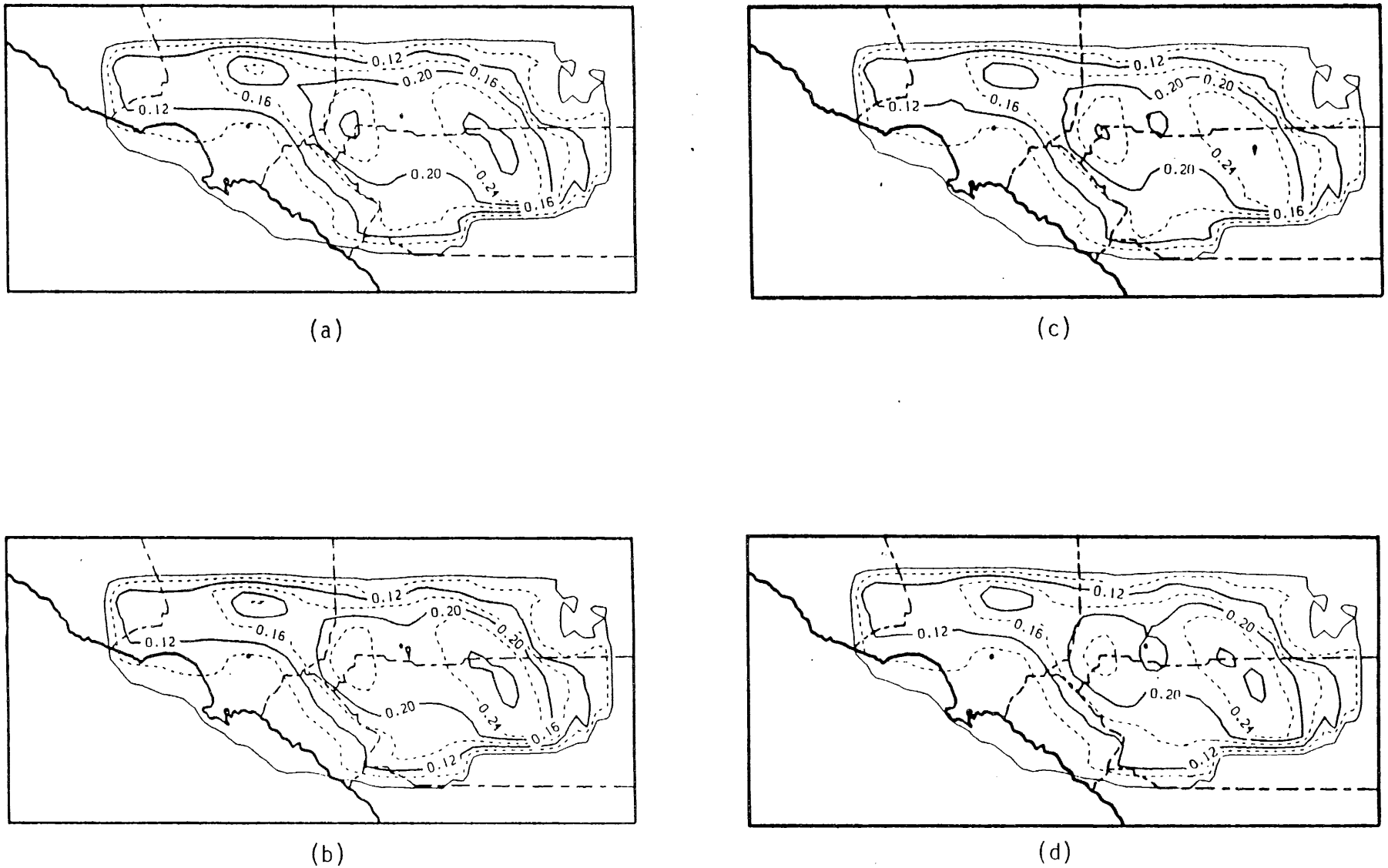

Figure 6.12 Spatial Distribution of Ozone at 1:00 pm on the Third Day of the Simulation. Ozone isopleths are shown at 4 pphm intervals. a) STD M85 2010; b) STD M100 2010; c) ADV LMD 2010; d) ADV LMD/NO ROG 2010.

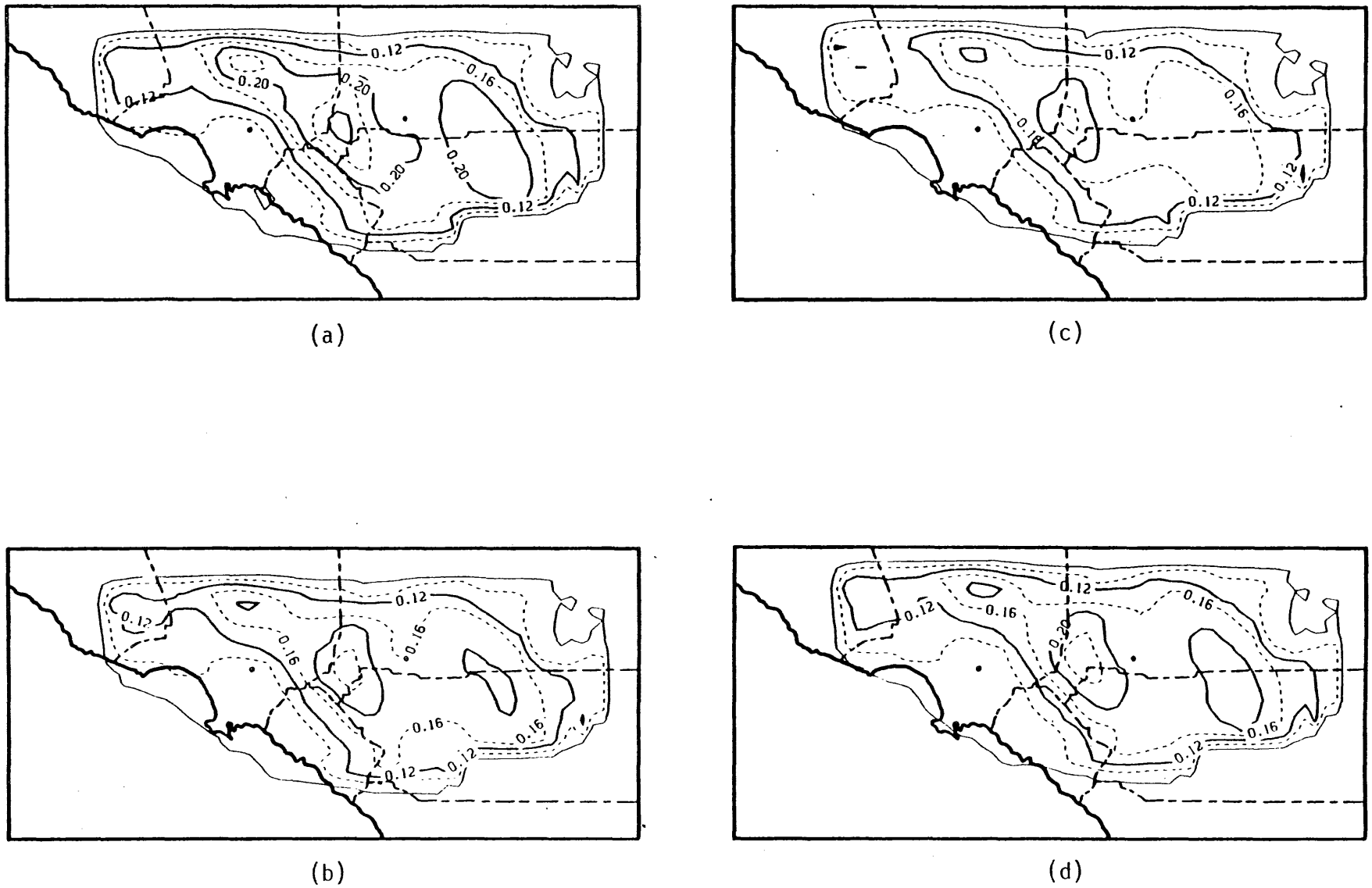

Figure 6.13 Spatial Distribution of Ozone at 1:00 pm on the Third Day of the Simulation. Ozone isopleths are shown at 4 pphm intervals. a) LO IC 2010; b) ADV CONV/LO IC 2010; c) ADV METH/LO IC 2010; d) STD M85/LO IC 2010.

Presenting the wide range of air quality measures, both numerically and graphically, gives a detailed view of the spatial and temporal air quality response to emissions changes. Also, they are used to quantify the function of initial and boundary conditions. These measures provide the foundation for evaluating the effectiveness of utilizing methanol fuel as compared to other controls.

6.5.2 Baseline Air Quality Predictions

If emissions continue to decrease from 1982 levels, as indicated by using either the **BASE1A** or **BASE1** inventories, there will be a substantial improvement in ozone air quality. The peak ozone drops from the 1982 prediction of 0.327 ppm to 0.27 ppm (17% less) for **BASE1A** and 0.261 (20% less) for **BASE1** (Table 6.6). The difference in the peak ozone predictions of the two base cases is small, only 3%, as is the spatial distribution (Figs. 6.5a vs. 6.5b). The difference between the two is that **BASE1** assumes considerably cleaner vehicles in the late 1990's. However, those vehicles comprise, on an emissions weighted basis, a rather small portion of the inventory. The population, time and area weighted calculations, especially the population exposure and number of grids times hours greater than 0.2 ppm ozone (first stage levels), change more dramatically when emissions are reduced from **BASE1A** to **BASE1** levels. In this case there is a 15% difference. Formaldehyde and PAN levels are nearly the same in the two calculations. Both are well below the 1982 levels.

Increased economic activity and population growth in the eastern basin between 2000 and 2010 are expected to alter the spatial distribution of pollutants towards the east. The modeling region was extended eastward to capture the impact of the shift when conducting 2010 calculations. To show the impact of increasing the modeling region between that used for year 2000 calculations and the larger region used for 2010, the base case year 2000 (BASE1) calculation was run using the larger region. As seen in Table 6.14, the size of the modeling region had little impact on the exposure to the different pollutants. The large difference between the exposures and concentrations between the year 2000 and 2010 calculations seen below is due to the increased emissions and population.

While the results for the year 2000 calculations show significant improvement from 1982 levels, it is lost by 2010. If emissions in the year 2010 are similar to the forecast inventory used here, the peak ozone rises back up to 0.321 ppm. The location of the predicted peak is much farther east, downwind of San Bernardino as opposed to the Pomona area. This is a result of the increasing population and activity in the eastern basin. A second, slightly lower peak (about 0.31 ppm), occurs around the Pomona area in the central portion of the SoCAB (Fig. 6.10a). Concentrations of other photochemical pollutants, such as HCHO and NO_2, also increase between the two modeling years, leading to increased exposure, especially to higher concentrations of ozone.